Research project : Taking into account electronic interactions with Hartree-Fock method in regular lattices, graphene and carbon nanotubes

Robert Benda, Ecole Polytechnique, X2013

February 17, 2016

Contents

Introduction

This project aims at estimating the effects of interactions between electrons in simple atom lattices as well as in graphene and carbon nanotubes. Few ab initio calculations have been made so far to compute the correction of the band structures of solids by taking into account electron-electron correlations. Band structures describe quite accurately the properties of numerous solids and are widely used to know some useful information about materials at the Fermi level for instance. Band structures can be obtained thanks to experiments, which aren't always easy. Photo-emissions methods are quite accurate to estimate the band structure of the **occupied states** of a solid, below the Fermi energy. The most common method is the Angle Resolved Photo Emission Spectroscopy (ARPES) which uses the photoelectric effect : by focusing a light beam on the solid, valence electrons are ejected. By detecting the direction in which the electrons are ejected, this method enables to compute both their momentum and their energy. Therefore it is possible to reconstruct the band structure of the solid. In three dimensions, what is known thanks to the experiment if how the energy evolves along a given direction of the Fermi sea. Deducing the entire Fermi sea and Fermi surface implies to use specific techniques, similar to tomography in optics.

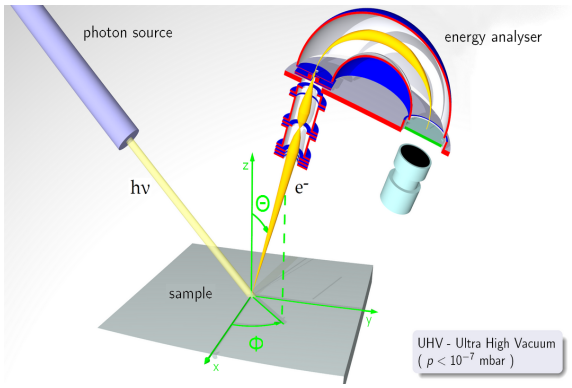

Figure 1: Experimental Setup of Angle-Resolved Photoemission Spectroscopy (Wikipedia)

However, the bands corresponding to **empty states**, above the Fermi level, turn out to be more difficult to compute. Inverse photo-emission is a way to obtain them : by focusing an electron beam on a sample of the solid, the electrons of the beam will have a given probability to occupy an empty state of the conduction band. When an electron in this excited level decays to an unnocupied state, a photon is emitted. By measuring its energy and the energy of the new state in the valence state, we can deduce the energy of the state in the conduction band. Knowing the momentum of the conduction electron implies to focus the electron beam in a given direction with a lot of precision. This kind of experiment turns out to be difficult and is not fully mastered yet.

We have explained the importance of band structures ab initio calculations, in particular to describe the conduction band. The bandwidth of the energy structure is also a very important quantity, useful when estimating several physical properties. One must often compare the bandwidth, which accounts for a kinetic energy, with the exchange energy, for instance to guess whether a system will have a magnetic behavior or not. We will study how bandwidth evolves when we include Coulomb interaction in the model.

Let's delve into the calculations I have done during this numerical project. I have used a very general method : the **mean-field approximation**, also called Hartree-Fock method in this context. My goal was to estimate the influence of electron-electron interaction *ab initio*. Hartree-Fock equations can be derived from a variational principle : we look for eigen states among the states making the means value of the hamiltonian stationary. This gives a set of one-electron wave functions coupled equations : all the wave functions of the electrons in the system play a role in the Schrödinger equation satisfied by any electron. The i^{th} electron wave-function satisfies the following Schrödinger equation :

$$-\frac{h^2}{2m}\Delta\psi_i(\vec{r}) + U_{ion}(\vec{r})\psi_i(\vec{r}) + \int d\vec{r'}\frac{e^2\sum_j|\psi_j(\vec{r'})|^2}{|\vec{r}-\vec{r'}|}\psi_i(r) - \sum_{jocc.}\delta_{\sigma_i,\sigma_j}\int d\vec{r'}\frac{e^2\psi_j^*(\vec{r'})\psi_i(\vec{r'})}{|\vec{r}-\vec{r'}|}\psi_j(\vec{r}) = \epsilon_i\psi_i(\vec{r}) \tag{1}$$

In the equation, we denote $e^2 = \frac{q_e^2}{4\pi\epsilon_0}$. This equation has a physical meaning. Hartree's term (the third term in the expression above) accounts for electron-electron Coulomb interaction : it is the integral of the Coulomb potential created at position $\vec{r}$ by the distribution of charges of all the others electrons. This is the reason why the total electronic density $n(\vec{r}) = \sum_j|\psi_j(\vec{r'})|^2$ appears, as it sums up this charge distribution. Because the i^{th} electron itself appears in this sum on occupied states, there is a **self-interaction error** : the electron is influenced by the potential it creates itself !

Fock's term (the last term in the member on the left) takes Pauli principle into account, and corrects the self-interaction error made in Hartree's term (thanks to the term for $j = i$).
Fock's term involves a non-local potential, being of the following form :

$$\int V(\vec{r},\vec{r'})\psi_i(\vec{r'})d\vec{r'} \tag{2}$$

and is more difficult to understand thoroughly. It is an exchange term, that is to say a contribution due to Pauli principle. Hence the contributions to that term only for occupied states having an electron with same spin as the i^{th} electron.

A rigorous proof of Hartree-Fock equations can be easily found in litterature, for instance in Ashcroft and Mermin *Solid state physics* book (page 332). The idea is to assume that the groud-state wave function can be written as a Slater determinant of one-electron wave functions (in order to be compatible with Pauli principle). However, this is already an assumption because nothing prooves that the total wave-function for a system of N electrons can be decomposed thanks to N one-electron wave-functions. By minimizing the means value of the hamiltonian in this state, and using Lagrange multiplicators to satisfy the constraints of one electron normalized wave functions, we obtain a set of equations on the individual wave functions. The hamiltonian changes, as two new terms appear : Hartree and Fock's terms. Therefore the previous wave functions aren't eigen vectors anymore. The approach I undertook is pertubative : assuming that Hartree-Fock's term only induces a slight modification of the eigen function, I computed the correction to the eigen value ; the energy, thanks to **first order perturbation theory**. Let's denote $W = H^{Hartree} + H^{Fock}$ the perturbation to the hamiltonian.

$$\Delta E_{k_i} = <\psi_{k_i}|W|\psi_{k_i}> = \Delta E_{k_i}^{Hartree} + \Delta E_{k_i}^{Fock} \tag{3}$$

$$\Delta E_{k_i,\sigma_i} = \sum\int d\vec{r}d\vec{r'}\frac{e^2|\psi_i(r)|^2|\psi_j(\vec{r'})|^2}{|\vec{r}-\vec{r'}|} - \sum_{jocc.}\delta_{\sigma_i,\sigma_j}\int d\vec{r}\int d\vec{r'}\frac{e^2\psi_i^*(\vec{r})\psi_j^*(\vec{r'})\psi_i(\vec{r'})\psi_j(\vec{r})}{|\vec{r}-\vec{r'}|} \tag{4}$$

The second term $\Delta E_{k_i}^{Fock}$ is always negative. Indeed, Hartree's term takes into account Coulomb interaction of an electron with respect to all the others electrons, leading to an overestimation of these interactions. The term of Fock corrects this by lessening the repulsive Coulomb interaction for two electrons having same spins. It is a way to apply Pauli principle, which tends to make electrons with same spin far from each other (in a classical view), thereby reducing the Coulomb energy which goes in $\frac{1}{r}$.

The above expression will be used in Chapter 2 to compute the corrections of the band structure due to this specific treatment of Coulomb interaction. We notice that this expression is valid not only for occupied states (k_i, σ_i), but also for empty states, which is crucial to derive the whole corrected band

structure. In the case k_i is occupied, the self-interaction term in Hartree's term cancels out with the corresponding one in Fock's term. Because of Fock's term, which involves different contributions when the distribution of spins σ_j changes, Hartree-Fock approximation can lead to **spin-polarized** band structure corrections, with possible magnetic behaviors at low temperatures. We will see in chapter 2, section 2.2.4, how taking Hartree-Fock's term into account leads to a phase transition in a one dimensionnal lattice.

The final goal of the project is to apply these numerical methods to compute the correction to the tight-binding energy spectrum of real materials, like graphene or carbon nanotubes (well described by the tight-binding approximation results). However, it is very useful to start applying these calculations to free electrons, or to low dimensional atom lattices. In the first section, I will study some properties like the density of states of such regular lattices, in the tight-binding approximation. These results will be useful to gain intuition on the future results. I will also present some caracteristic results obtained as we increase the dimension. Then, I will compute thoroughly the correction of the energy spectrum obtained with Hartree-Fock method for a free electron gas, before doing it for the one and two dimensionnal lattices.

Although it wasn't planned at the beginning of the project, my work also allows to estimate *ab initio* the screening length in regular lattices of atoms. I will explain this in further detail, and display corresponding graphs, in chapter 2, section 2.2.3. The code I developed allows to replace very easily the usual Coulomb potential in $\frac{1}{r}$ by a screened Coulomb potential, also called Yukawa potential, proportionnal to $\frac{e^{-\lambda r}}{r}$. The screening length only depends on the density of states at the Fermi level. I did an autocoherent method to find the value of λ that better describes the *real* electronic effective potential in the material. This screened Hartree-Fock method consists to compute the correction to the band structure for a Yukawa potential with an arbitrary initial value λ_{in}, then to update λ thanks to the new corrected band structure, etc. The successive values of λ tend towards a limit value, which is the real screening length in my model.

Chapter 1

Density of states calculations

1.1 One dimensional lattice

Let's consider a one dimensionnal lattice ; a chain of **N** aligned atoms separated from a distance a one from each other. The energy spectrum computed in the tight binding approximation is :

$$E_k = E_0 - t_0 - 2tcos(ka), k \in [-\frac{\pi}{a}, \frac{\pi}{a}[= 1Z.B. \tag{1.1}$$

where the quasi-momentum k spans the First Brillouin Zone. E_0 is the energy of the atomic orbital level. t is the coupling between two neighbouring sites, and t_0 is the coupling in a given site. The chain of N atoms repeats periodically. This periodicity quantifies k, because of the Periodic Boundary Conditions (PBC).

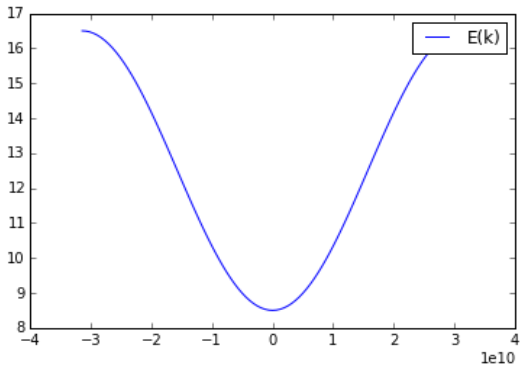

Figure 1.1: Energy spectrum in a one-dimensional lattice under LCAO approximation, for $a = 10^{-10}$ m

Let's do a reminder about the tight-binding approximation. This method assumes that the eigen wave-functions of the hamiltonian have the following form :

$$\psi_k(x) = \frac{1}{\sqrt{N}} \sum_{m=1}^{N} e^{ikma} \chi_m(x) \tag{1.2}$$

where $\chi_m(.)$ is the atomic orbital wave-function of the m^{th} site of the lattice. We assume that either all atoms are of the same type, or that they energy levels are such that **only one energy level per atom plays a role**. Otherwise, the form of the wave-function would be more complicated, including hybridisation between different atomic levels. Several atomic orbital wave-functions $(\chi_m^n)_n$ would be needed (see **Annex 14**).

With these notations :

$$t =< \chi_{m-1}|V_{at}|\chi_m >, t_0 =< \chi_m|V_{at}|\chi_m > \tag{1.3}$$

where V_{at} is the ionic effective potential.

The form of the wave-function derives from Bloch's theorem, and makes the probability amplitude of presence maximal in the neighborhood of the sites of the lattice. An electron having this wave-function is delocalised all over the lattice, but only close to the sites, and not in-between. If we measured the position of the electron, we would find it with very high probability very close to one of the site of the lattice. This is why this method is called "tight-binding", or "Linear Combination of Atomic Orbitals" (LCAO).

In the lattices we have studied, this approximation is well-suited. The opposite approximation, namely "weak-binding", works for solids whose electrons behave nearly like free electrons (plane waves) ; their probability of presence being as important between two atoms than close to an atom. The band structure obtained is the correction computed by a perturbative approach, to the set of free-electrons parabola describing the energy spectrum of these electrons. Each Fourier mode opens a gap at a given node of the spectrum, which gives the final band structure. We assume that electrons in regular lattices, graphene and carbon nanotubes are bound enough to the atoms. Therefore, we won't use this method in the project.

The calculation of the density of states for the one-dimensionnal lattice gives :

$$D(E) = (\frac{dN_<}{dE})(E) = \frac{N}{2\pi t} \frac{1}{\sqrt{1 - (\frac{E-(E_0-t_0)}{2t})^2}} \tag{1.4}$$

where $N_<(E)$ is the total number of states having an energy less than E :

$$N_<(E) = N - \frac{N}{\pi} Arccos(\frac{E - (E_0 - t_0)}{2t}) \tag{1.5}$$

As I will present the calculation in two dimensions, I don't proove these formula in this simple case.

In the following graphs and throughout the whole report, we will use the values $E_0 = 13eV$, $t_0 = 0.5eV$, $t = 2eV$ and $a = 10^{-10}m$, to plot the functions.

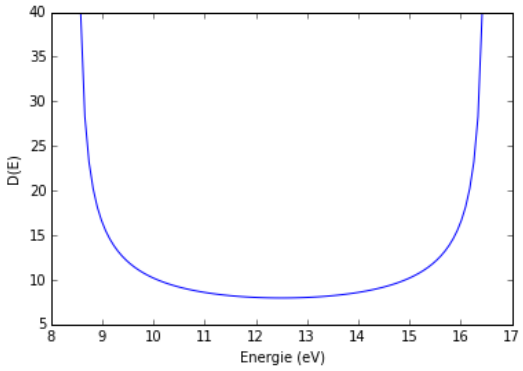

Figure 1.2: Density of energy states $D(E)$ in a one-dimensional lattice under LCAO approximation

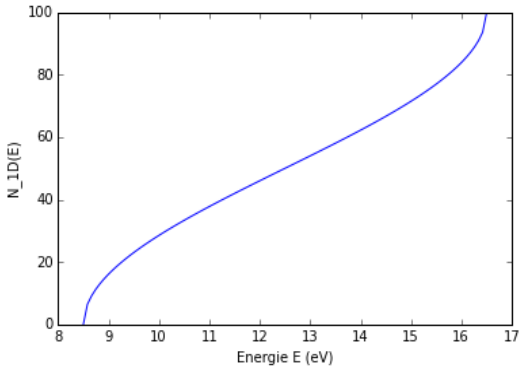

Figure 1.3: Number of energy states $N_<(E)$ in a one-dimensional lattice under LCAO approximation (N=100)

1.2 Two dimensional lattice

The energy spectrum of electrons in a two dimensional lattice in the tight-binding approximation is :

$$E(k_x, k_y) = E_0 - t_0 - 2t(cos(k_x a) + cos(k_y a)) \in [E_0 - t_0 - 4t, E_0 - t_0 + 4t] \tag{1.6}$$

where $\vec{k} = \begin{pmatrix} k_x \\ k_y \end{pmatrix}$ is the quasi-momemtum of the electron.

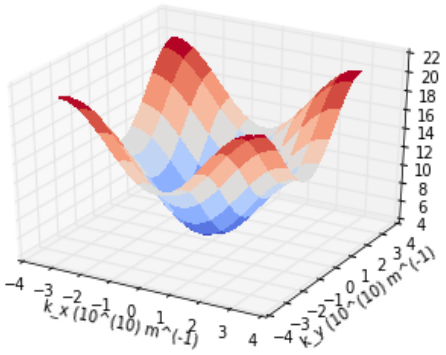

Figure 1.4: Energy spectrum in a square lattice under LCAO approximation

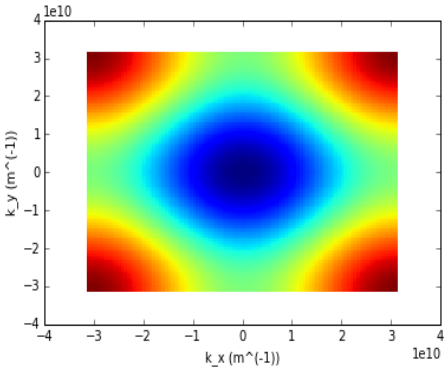

Figure 1.5: Projection of the energy spectrum of a square lattice in the quasi-momentum space

We suppose Periodic Boundary Conditions, such that $k_x = \frac{2\pi m_1}{Na}$, $k_y = \frac{2\pi m_2}{Na}$ with m_1 and m_2 integers. The first Brillouin zone is described by $(k_x, k_y) \in [-\frac{\pi}{a}, \frac{\pi}{a}[^2$.

The number of electronic possible states whose energy is smaller than or equal to E is :

$$N_<^{2D}(E) = \int\int dm_1 dm_2 = \frac{(Na)^2}{(2\pi)^2} \int\int_{\{\vec{k}\in 1.B.Z. | E_{\vec{k}} \leq E\}} dk_x dk_y \tag{1.7}$$

$$= \frac{N^2}{(2\pi)^2} \int\int_{\{\begin{pmatrix} x \\ y \end{pmatrix} \in [-\pi,\pi[^2 | cos(x)+cos(y) \geq \alpha(E)\}} dxdy \tag{1.8}$$

where $\alpha(E) = \frac{E_0 - t_0 - E}{2t} \in [-2, 2]$. This expression of $N_<^{2D}(E)$ as the area of a specific region in the square $[-\pi, \pi]^2$ of the plane is remarkable. We will use it to compute some similar quantities in three dimensions.

$$N_<^{2D}(E) = (\frac{N}{2\pi})^2 \int_{-\pi}^{\pi} (\int_{\{z | cos(z) \geq \alpha(E) - cos(y)\}} dz) dy \tag{1.9}$$

At that stage, as $\alpha(E) - cos(y) = \alpha(E + 2tcos(y))$, we could use for some values of E the expression of the number of states computed in a one dimensional lattice :

$$E + 2tcos(y) \in [E_0 - t_0 - 2t, E_0 - t_0 + 2t] \Rightarrow \int_{\{z | cos(z) \geq \alpha(E) - cos(y)\}} dz = \frac{2\pi}{N} N_<^{1D}(E + 2tcos(y)) \tag{1.10}$$

However it is not mandatory to use to the lower dimension calculations here. After some rewriting and calculations (see **Annex 1**), we find :

$$E \geq E_0 - t_0 \Rightarrow \alpha(E) \leq 0 \Rightarrow N_<^{2D}(E) = \frac{N^2}{\pi^2} (\pi Arccos(\alpha(E) + 1) + \int_{-1}^{\alpha(E)+1} \frac{Arccos(\alpha(E) - z)}{\sqrt{1 - z^2}} dz) \tag{1.11}$$

$$E \leq E_0 - t_0 \Rightarrow \alpha(E) \geq 0 \Rightarrow N_<^{2D}(E) = \frac{N^2}{2\pi^2} \int_{\alpha(E)-1}^{1} \frac{Arccos(\alpha(E) - z)}{\sqrt{1 - z^2}} dz \tag{1.12}$$

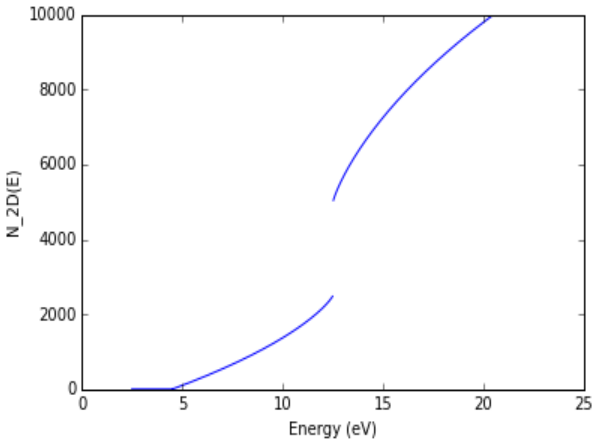

Figure 1.6: Number of energy states in a square lattice under LCAO approximation

We never see the infinite slope of $N_<^{2D}(E)$ in the neighbouring of $E_0 - t_0$, whatever close we look. $N_<^{2D}(E)$ has a square root behavior close to this point.

We notice that $N_<^{2D}(E)$ has a discontinuity in $E_0 - t_0$:

$$lim_{E \longrightarrow (E_0 - t_0)^-} N_<^{2D}(E) = \frac{1}{2} lim_{E \longrightarrow (E_0 - t_0)^+} N_<^{2D}(E) = \frac{N^2}{2\pi^2} \int_{-1}^{1} \frac{Arccos(-z)}{\sqrt{1 - z^2}} dz \tag{1.13}$$

as $\alpha(E) \longrightarrow_{E \longrightarrow E_0 - t_0} 0$.

Moreover, the slope of $N_<^{2D}(E)$ has a discontinuity at $E_0 - t_0 - 4t$:

$$lim_{E \longrightarrow (E_0 - t_0 - 4t)^-}(\frac{dN_<^{2D}}{dE})(E) = 0 \neq lim_{E \longrightarrow (E_0 - t_0 - 4t)^+}(\frac{dN_<^{2D}}{dE})(E) > 0 \tag{1.14}$$

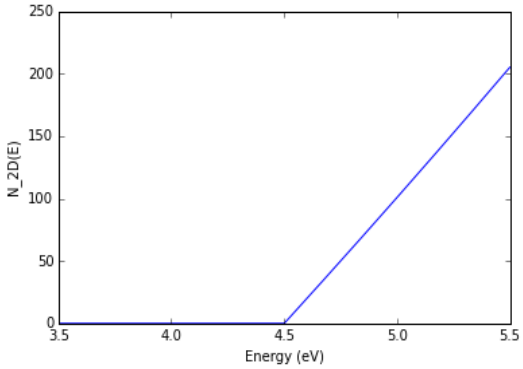

Figure 1.7: Discontinuity of the slope of the number of energy states in a square lattice at the minimal energy $E_0 - t_0 - 4t$

Identically :

$$lim_{E \longrightarrow (E_0 - t_0 + 4t)^+}(\frac{dN_<^{2D}}{dE})(E) = 0 \neq lim_{E \longrightarrow (E_0 - t_0 + 4t)^-}(\frac{dN_<^{2D}}{dE})(E) > 0 \tag{1.15}$$

These discontinuities will be seen directly in the function $E \longmapsto D^{2D}(E)$.

By taking the derivatives of the previous expressions of $N_<^{2D}(E)$, we derive the density of energy states in a square lattice :

$$E > E_0 - t_0 \Rightarrow D^{2D}(E) = \frac{N^2}{2t\pi^2} \int_{-1}^{\frac{E_0 - t_0 + 2t - E}{2t}} \frac{dz}{\sqrt{(1-z^2)(1-(\frac{E_0 - t_0 - 2tz - E}{2t})^2)}} \tag{1.16}$$

$$E < E_0 - t_0 \Rightarrow D^{2D}(E) = \frac{N^2}{2t\pi^2} \int_{\frac{E_0 - t_0 - 2t - E}{2t}}^{1} \frac{dz}{\sqrt{(1-z^2)(1-(\frac{E_0 - t_0 - 2tz - E}{2t})^2)}} \tag{1.17}$$

We could also directly compute the density of states with the following formula :

$$D_{2D}(E) = \int_{1Z.B.} \frac{d^2k}{V_{BZ}} \delta(\epsilon - \epsilon(\vec{k})) \tag{1.18}$$

but we will see that our method enables to deduce the density from the calculations in lower dimensions.

The function $E \longmapsto D(E)$ is a **Bessel function**. A computation of an equivalent of $D^{2D}(E)$ when $E \longrightarrow E_0 - t_0$ gives the following result :

$$D^{2D}(E_0 - t_0 + \epsilon) =_{\epsilon \to 0} O(\frac{1}{\sqrt{|\epsilon|}}) \tag{1.19}$$

Thus,

$$N_<^{2D}(E_0 - t_0 + \epsilon) =_{\epsilon \to 0^+} N_<^{2D}((E_0 - t_0)^-) + K\sqrt{\epsilon} \tag{1.20}$$

where K is a constant.

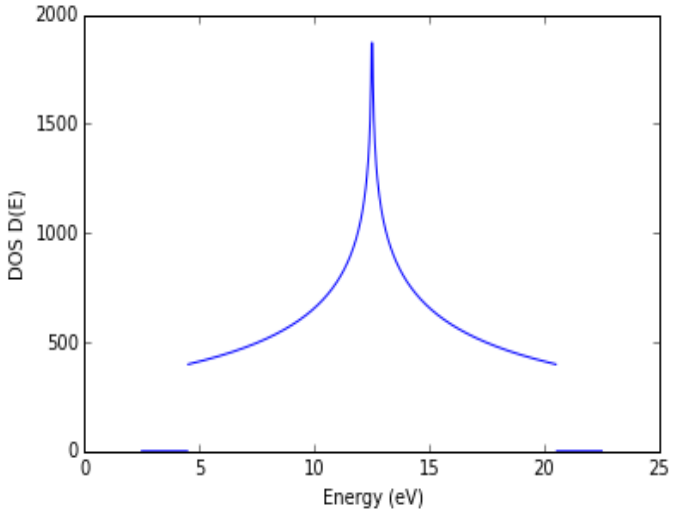

Figure 1.8: Density of energy states in a square lattice under LCAO approximation

Because of the limited resolution in energy, we can't properly see the divergence of $D^{2D}(E)$. We can guess that $D^{2D}(E) \longrightarrow +\infty$ when $E \longrightarrow E_0 - t_0$ thanks to the expression of $D^{2D}(E)$. Indeed both expressions of $D^{2D}(E)$ (for $E \geq E_0 - t_0$ and $E \geq E_0 - t_0$) tend towards :

$$\frac{N^2}{2t\pi^2} \int_{-1}^{1} \frac{dz}{(1-z^2)} = +\infty \tag{1.21}$$

We can also explain this divergence thanks to the saddle points that appear in the energy spectrum, which make the number of possible energy states increase.

1.3 Three dimensional lattice

Similarly to the lower dimensions, the energy spectrum of electrons in a three dimensional lattice in the tight-binding approximation is :

$$E(k_x, k_y, k_z) = E_0 - t_0 - 2t(cos(k_x a) + cos(k_y a) + cos(k_z a)) \in [E_0 - t_0 - 6t, E_0 - t_0 + 6t] \tag{1.22}$$

We suppose Periodic Boundary Conditions, with a cubical lattice of side length Na repeating periodically, such that $k_x = \frac{2\pi m_1}{Na}$, $k_y = \frac{2\pi m_2}{Na}$ and $k_z = \frac{2\pi m_3}{Na}$. The first Brillouin Zone is described by $(k_x, k_y, k_z) \in [-\frac{\pi}{a}, \frac{\pi}{a}[^3$.

Let's perform a similar calculations as in two dimensions. The number of electronic possible states whose energy is smaller or equal to E is :

$$N_<^{3D}(E) = \int\int\int dm_1 dm_2 dm_3 = \frac{(Na)^3}{(2\pi)^3} \int\int\int_{\{\vec{k} \in 1.B.Z. | E_{\vec{k}} \leq E\}} dk_x dk_y dk_z \tag{1.23}$$

$$= (\frac{N}{2\pi})^3 \int\int\int_{\{\begin{pmatrix} x \\ y \\ z \end{pmatrix} \in [-\pi,\pi[^3 | cos(x)+cos(y)+cos(z) \geq \alpha(E)\}} dxdydz \tag{1.24}$$

where $\alpha(E) = \frac{E_0 - t_0 - E}{2t} \in [-3, 3]$.

$$N_<^{3D}(E) = (\frac{N}{2\pi})^3 \int_{-\pi}^{\pi} (\int\int_{cos(y)+cos(z) \geq \alpha(E) - cos(x)} dydz)dx \tag{1.25}$$

Let denote :

$$I_x = \int\int_{cos(y)+cos(z) \geq \alpha(E) - cos(x)} dydz \tag{1.26}$$

We notice that

$$\alpha(E) - cos(x) = \frac{E_0 - t_0 - (E + 2tcos(x))}{2t} = \alpha(E + 2tcos(x)) \tag{1.27}$$

Let's now compute I_x according to the values of E and x :

$$\alpha(E) - cos(x) \geq 2 \Rightarrow I_x = 0 \tag{1.28}$$

$$\alpha(E) - cos(x) \leq -2 \Rightarrow I_x = \int_{-\pi}^{\pi}\int_{-\pi}^{\pi} dydz = (2\pi)^2 \tag{1.29}$$

If $\alpha(E) - cos(x) \in [-2, 2]$, it means that $\alpha(E + 2tcos(x)) \in [-2, 2]$, which implies that $E + 2tcos(x)$ is in the interval $[E_0 - t_0 - 4t, E_0 - t_0 + 4t]$. **We can therefore use the computations of the two-dimensional case to get the results in higher dimension** !
$N_<^{2D}(.)$ is indeed defined on the interval $[E_0 - t_0 - 4t, E_0 - t_0 + 4t]$:

$$\alpha(E) - cos(x) \in [-2, 2] \Rightarrow I_x = \int\int_{cos(y)+cos(z) \geq \alpha(E+2tcos(x))} dydz = (\frac{2\pi}{N})^2 N_<^{2D}(E + 2tcos(x)) \tag{1.30}$$

thanks to the previous expression 1.8.

After some further calculations (see **Annex 2**), we find :

$$\alpha(E) \leq -1 \Rightarrow N_<^{3D}(E) = \frac{N^3}{\pi} Arccos(\alpha(E) + 2) + \frac{N}{\pi} \int_{Arccos(\alpha(E)+2)}^{\pi} N_<^{2D}(E + 2tcos(x))dx \tag{1.31}$$

$$\alpha(E) \in [-1, 1] \Rightarrow N_<^{3D}(E) = \frac{N}{\pi} \int_0^{\pi} N_<^{2D}(E + 2tcos(x))dx \tag{1.32}$$

$$N_<^{3D}(E) = \frac{N}{\pi} (\int_0^{Arccos(\alpha(E))} N_<^{2D}(E + 2tcos(x))dx + \int_{Arccos(\alpha(E))}^{\pi} N_<^{2D}(E + 2tcos(x))dx) \tag{1.33}$$

$$\alpha(E) \geq 1 \Rightarrow N_<^{3D}(E) = \frac{N}{\pi} \int_0^{Arccos(\alpha(E)-2)} N_<^{2D}(E + 2tcos(x))dx \tag{1.34}$$

The order of magnitude of $N_<^{3D}(E)$ is N^3, as we have seen that $N_<^{2D}(E)$ is proportionnal to N^2.

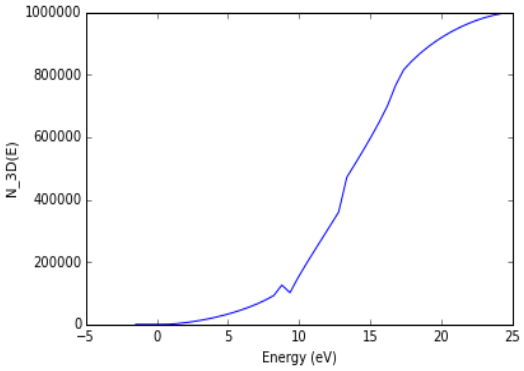

Figure 1.9: Number of energy states in a three dimensional lattice

It is worth to notice that the slope of $N_<^{3D}(E)$ is now continuous at the minimal and maximal energies $E_0 - t_0 - 6t$ and $E_0 - t_0 + 6t$, contrary to the two dimensional case.

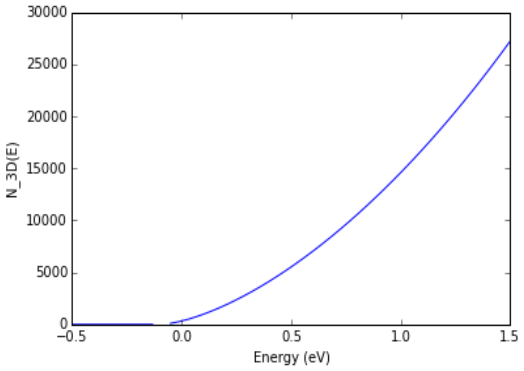

Figure 1.10: Continuity of slope of the number of energy states in a three dimensional lattice at the minimal energy $E_0 - t_0 - 6t$

We can take the derivative of the expression of $N^{3D}(E)$ for $E > E_0 - t_0 + 2t$ and $E < E_0 - t_0 - 2t$. Using that :

$$N_<^{2D}(E_0 - t_0 + 4t) = N^2 \tag{1.35}$$

and

$$N_<^{2D}(E_0 - t_0 - 4t) = 0 \tag{1.36}$$

we find the following :

$\forall E \geq E_0 - t_0 + 2t$,

$$D^{3D}(E) = \frac{N}{\pi} \int_{Arccos(\frac{E_0 - t_0 + 4t - E}{2t})}^{\pi} D^{2D}(E + 2tcos(x))dx \tag{1.37}$$

$\forall E \leq E_0 - t_0 - 2t$

$$D^{3D}(E) = \frac{N}{\pi} \int_{0}^{Arccos(\frac{E_0 - t_0 - 4t - E}{2t})} D^{2D}(E + 2tcos(x))dx \tag{1.38}$$

The density plot given by these analytical formula is dispayed in **Annex 3**. These formula seem to give the exact result only for $E \notin]E_0 - t_0 - 2t, E_0 - t_0 + 2t[$.

Let's now look at the density obtained with a probabilistic method, consisting of computing the energy for some random quasi-momentum values. This method will be further explained in the following section, for higher dimension lattices.

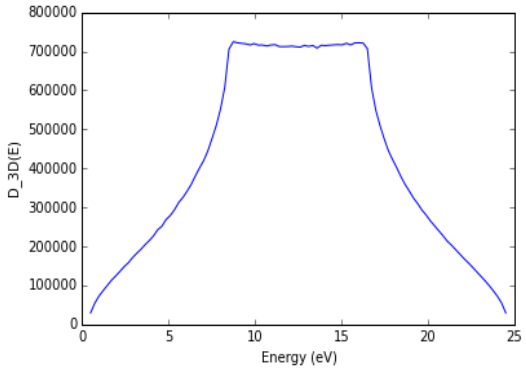

Figure 1.11: Density of states in a three dimensional lattice

This time, contrary to the one and two dimensionnal lattice, the density is continuous.

1.4 Regular lattice in higher dimension

It is interesting to look at the evolution of the density of states in higher dimensions and infinite dimension. Dimensions account for the number of closest neighbours, therefore increasing the dimension should be a way to describe real crystals better, where the atoms of the lattice may be coupled to a good deal of neighbors. Infinite dimension appears in many cases to give conclusions closer to the real three dimensional world than two-dimensional calculations.

To compute the density of states in dimension d, we could carry out the same trick as in 3D, using the results of D.O.S. calculations in lower dimension $d-1$. However a probabilistic method like the Monte-Carlo method is much simpler. Let's briefly explain how it works.

The energy spectrum in dimension d is given by :

$$E(k_1, k_2, .., k_d) = E_0 - t_0 - 2t \sum_{i=1}^{d} cos(k_i a) \tag{1.39}$$

the First Brillouin Zone being$[\frac{-\pi}{a}, \frac{\pi}{a}]^d$.

We consider random variables K_1, K_2,.., K_d, each uniform over $[-\frac{\pi}{a}, \frac{\pi}{a}]$. We choose a number n of random selections of $(K_1, K_2, .., K_d) \in [-\frac{\pi}{a}, \frac{\pi}{a}]^d$. Thus the random variable giving the energy, $E(K_1, K_2, .., K_d)$, is estimated n times.
We also choose the pace of discretization p of the possible interval for the energy, namely $[E_0 - t_0 - 2td, E_0 - t_0 + 2td]$, which is cut into p small intervals.
The distribution of the energy after the n random selections provides histograms telling how many times the random energy estimated was in the interval $[E_0 - t_0 + k\frac{4td}{p}, E_0 - t_0 + (k+1)\frac{4td}{p}]$ for $k \in [0, p-1]$. This histogram is therefore an approximation of the density of states. It would be interesting to be aware of the influence of the two discretizations, represented by n and p, on the precision of the density function computed. Intuitively, n is the most important parameter if p is large enough. (but p does not need to be too big)

Having fixed $E_0 = 13eV$, $t_0 = 0.5eV$, $t = 2eV$ and $a = 10^{-10}m$, we obtain the following results :

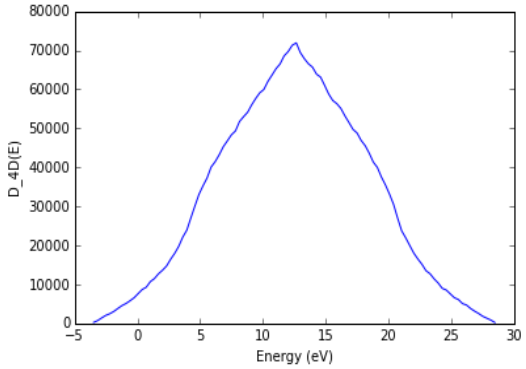

Figure 1.12: Density of states in a four dimensional lattice : n=1000000, p=100

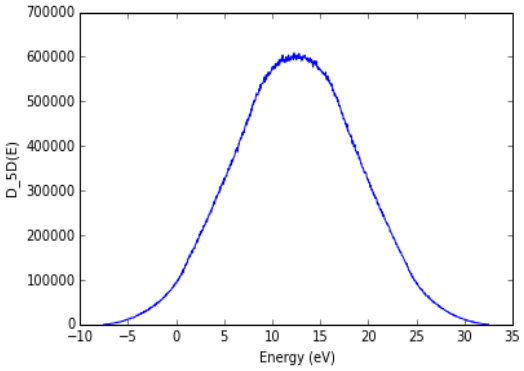

Figure 1.13: Density of states in a five dimensional lattice : n=1000000, p=100

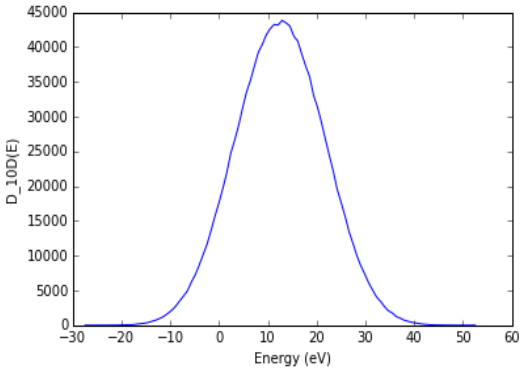

Figure 1.14: Density of states in a ten dimensional lattice : n=1000000, p=100

Each density is plotted over the whole possible interval for the energy : $[E_0 - t_0 - 2td, E_0 - t_0 + 2td]$.

The density of states looks increasingly like a gaussian when the dimension d increases. The standard deviation σ appears to increase in absolute value as the dimension increases, but the ratio $\frac{\sigma}{4dt}$ of the deviation to the width of the total interval appears to diminish. Let's try to justify this behaviour when d increases.

First, the mean value of the random variable E is $E_0 - t_0$:

$$< -2t \sum_{\nu=1}^{d} cos(K_\nu a) >= 0 \tag{1.40}$$

because

$$\int_{-\frac{\pi}{a}}^{\frac{\pi}{a}} cos(k_\nu a) dk_\nu = 0 \tag{1.41}$$

and the random variables K_1, .., K_d are independent.

Then, the standard deviation σ of the distribution of the energy in a d-dimensional lattice is given by:

$$\sigma^2 =< E^2 > - < E >^2 =< E^2 >= 4t^2 \sum_{\nu=1}^{d} \sum_{\nu'=1}^{d} \frac{1}{(\frac{2\pi}{a})^d} \int_{-\frac{\pi}{a}}^{\frac{\pi}{a}} .. \int_{-\frac{\pi}{a}}^{\frac{\pi}{a}} cos(k_\nu a) cos(k_{\nu'} a) dk_1 ... dk_d \tag{1.42}$$

Given that

$$\frac{1}{(\frac{2\pi}{a})^d} \int_{-\frac{\pi}{a}}^{\frac{\pi}{a}} .. \int_{-\frac{\pi}{a}}^{\frac{\pi}{a}} cos(k_\nu a) cos(k_{\nu'} a) dk_1 ... dk_d = \frac{1}{(\frac{2\pi}{a})^2} \int_{-\frac{\pi}{a}}^{\frac{\pi}{a}} cos^2(ka) dk = \frac{1}{2} \tag{1.43}$$

if $\nu = \nu'$, and 0 otherwise, we finally find :

$$\sigma = \sqrt{2d}t \tag{1.44}$$

In fact the hopping in dimension d should be slightly modified in the following way :

$$t = \frac{t}{\sqrt{d}} \tag{1.45}$$

Otherwise, as the standard variation becomes infinite when $d \longrightarrow \infty$, infinite energies could become possible which isn't possible. Under this normalization of the hopping :

$$\sigma = \sqrt{2} \tag{1.46}$$

For any dimension, the distribution of E is symmetric relatively to $E_0 - t_0$.

As $(K_\nu)_{\nu\in[1,d]}$ is a set of indepedent identically distributed random variables, it is also the case for $(X_\nu)_{\nu\in[1,d]} =^{def} (cos(K_\nu a))_{\nu\in[1,d]}$. The variance of X_ν is $\frac{1}{2}$ and its means 0. Therefore according to the Central Limit Theorem, $\frac{\sum_{\nu=1}^{d} cos(K_\nu a)}{d}$ tends to a normally distributed variable when $d \to \infty$. Hence :

$$E_{K_1,\ldots,K_d} \sim_{d\gg 1} -2\sqrt{d} * N(0, 1/2) \tag{1.47}$$

1.5 Graphene

Graphene is a well-known bi-dimensionnal structure which was discovered in 2004. It is made up of atoms of carbon forming a honeycomb lattice.

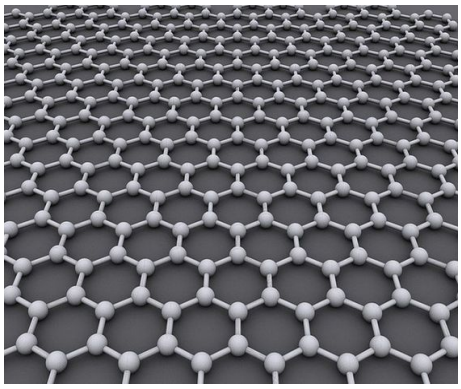

Figure 1.15: View of graphene direct lattice

The energy spectrum of graphene can be easily derived within the tight-binding approximation, thanks to Bloch's theorem. The calculation generalises the one-dimensionnal result, the only difference being that there are more couplings with neighbouring atoms to take into account, and that a unit cell of the direct lattice now contains two carbon atoms. Therefore, there are two possible energy states for each value of the quasi-momemtum, corresponding to two different wave functions $\psi^+_{k_x,k_y}$ and $\psi^-_{k_x,k_y}$. These fonctions have the following form :

$$\psi^+_{k_x,k_y}(\vec{r}) = \frac{1}{\sqrt{2N}} \sum_{\vec{R_n}} e^{i\vec{k}.\vec{R_n}} (\lambda^A_+ \chi^1(\vec{r} - \vec{R_n}) + \lambda^B_+ \chi^2(\vec{r} - \vec{R_n})) \tag{1.48}$$

and

$$\psi^-_{k_x,k_y}(\vec{r}) = \frac{1}{\sqrt{2N}} \sum_{\vec{R_n}} e^{i\vec{k}.\vec{R_n}} (\lambda^A_- \chi^1(\vec{r} - \vec{R_n}) + \lambda^B_- \chi^2(\vec{r} - \vec{R_n})) \tag{1.49}$$

where λ^+_A, λ^-_A and λ^+_B, λ^-_B are constant coefficients, and $\vec{R_n}$ spans all the cells of the direct lattice. We find that these functions are eigen wave-functions of the tight-binding hamiltonian, with good coefficients $\lambda^{+/-}_A$ and $\lambda^{+/-}_B$, and with the following eigen energies :

$$E^-_{k_x,k_y} = E_0 - t_0 - t\sqrt{3 + 2(2cos(\frac{3a}{2}k_x)cos(\frac{\sqrt{3}a}{2}k_y) + cos(\sqrt{3}ak_y))} \tag{1.50}$$

$$E^+_{k_x,k_y} = E_0 - t_0 + t\sqrt{3 + 2(2cos(\frac{3a}{2}k_x)cos(\frac{\sqrt{3}a}{2}k_y) + cos(\sqrt{3}ak_y))} \tag{1.51}$$

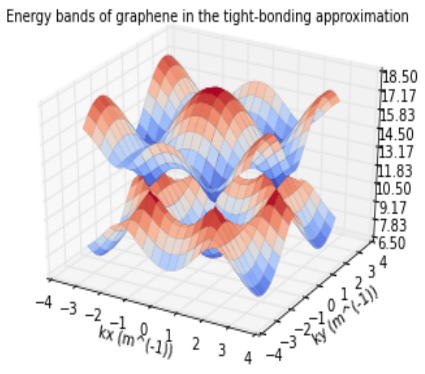

Figure 1.16: Energy spectrum of graphene under tight-binding approximation

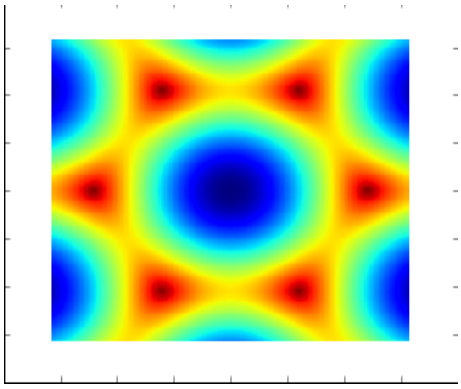

Figure 1.17: Projection of the energy spectrum of graphene in the quasi-momemtum space

As we did for regular lattices, we can estimate the density of states of graphene thanks to a Monte-Carlo method, by randomly choosing vectors $\vec{k}$ in the Brillouin Zone :

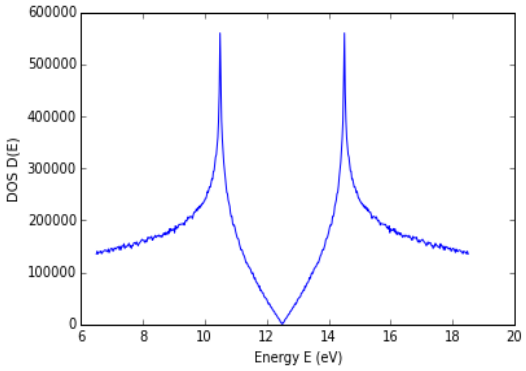

Figure 1.18: Density of states in graphene computed with the Monte-Carlo method with 1000000 random selections

We can see divergences of the density, which remind us of the behovior of the density in two dimensions, where the divergence was due to the saddle-points of the energy band at $E = E_0 - t_0$. For graphene, these singularities, called **Van Hove singularities**, appear at $E = E_0 - t_0 - t$ and $E = E_0 - t_0 + t$, also because of the saddle points, which make the number of states suddenly growing.

The particuliar shape of graphene energy spectrum at the Fermi energy, with a linear relation energy to wave-vector close to the so-called *Dirac points*, can lead to think that electron-electron interactions will have uncommon effects in graphene. For instance, as the density of states is equal to zero at the Fermi level, the screening length is in theory infinite, and there shouldn't be screening effects, which is quite surprising ! This is another motivation to understand the role of electronic interactions in graphene better.

Chapter 2

Taking into account Hartree-Fock

2.1 Free electrons in a box

Let's consider free electrons in a box of length L and volume $V = L^3$. The only objective of the calculations performed in this section is to have an idea of how Hartree's term and Fock's term could correct the band structures **qualitatively** in regular lattices of atoms. However, the free electron model may well be relevant for some type of electrons in metals, like conduction electrons, which are very delocalised and loosely bound to their respective atoms. We can therefore deal with the problem as if there were an underlying collection of ions, interacting only weakly with the electrons.

The number of electrons is denoted as N. The N electrons occupy N different quantum numbers α_i, each including both spin σ_i and momemtum $\vec{k}_i$:

$$\alpha_i = (\vec{k}_i, \sigma_i) \tag{2.1}$$

The energy spectrum of the electrons when we neglect the interactions is :

$$E_{\vec{k}} = \frac{h^2 k^2}{2m} \tag{2.2}$$

Let's denote

$$e^2 = \frac{q_e^2}{4\pi\epsilon_0} = 2.3.10^{-28} J.m \tag{2.3}$$

where q_e is the elementary charge of an electron.

If we consider an homogeneous ionic potential $v_0(\vec{r})$, Hartree's potential and $v_0(\vec{r})$ cancel out because of charge neutrality :

$$v_0(\vec{r}) + V_{Hartree}(\vec{r}) = \int d\vec{r'} \frac{\rho^+(\vec{r'}).(-e^2) + \rho^-(\vec{r'}).e^2}{|\vec{r} - \vec{r'}|} = 0 \tag{2.4}$$

$\rho^+(\vec{r})$ would be the density of positive charge while $\rho^+(\vec{r})$ would be the electronic density.

The wave function of an electron with quantum number $\alpha_n = (k_n, \sigma_n)$ is :

$$\psi_{\vec{k_n}}(\vec{r})|\sigma_n> = \frac{1}{\sqrt{V}} e^{i\vec{k_n}.\vec{r}}|\sigma_n> \tag{2.5}$$

The Fock term applied on $\psi_{\vec{k_n}}(\vec{r})$, knowing the wave-functions of the other occupied states, is :

$$(H_{Fock}\psi_{\vec{k_n}})(\vec{r}) = -\sum_{jocc.} \delta_{\sigma_j,\sigma_n} e^2 \int \frac{\psi^*_{\vec{k_j}}(\vec{r'})\psi_{\vec{k_n}}(\vec{r'})}{|\vec{r} - \vec{r'}|} \psi_{\vec{k_j}}(\vec{r}) \tag{2.6}$$

where the sum on j is a sum **over all occupied states**. This will turn out to be important when we will look at the correction of the energy due to Fock's term for occupied or non-occupied states. This term comes from Pauli principle and Fermi-Dirac statistics : it favors energetically situations with aligned spins of the electrons, because having the same spin implies that the two electrons won't be too close one

to each other.

As $\forall j$, $\psi_{\vec{k_j}}(\vec{r}) = \frac{1}{sqrt(V)} e^{i\vec{k_j}.\vec{r}}$:

$$(H_{Fock}\psi_{\vec{k_n}})(\vec{r}) = -\sum_j \delta_{\sigma_j,\sigma_n} e^2 \int \frac{e^{i(\vec{k_n}-\vec{k_j}).(\vec{r'}-\vec{r})}}{|\vec{r'}-\vec{r}|} \frac{1}{V} \frac{1}{\sqrt{V}} e^{i\vec{k_n}.\vec{r}} d\vec{r'} \tag{2.7}$$

$$= -\frac{e^2}{V} \frac{V}{(2\pi)^3} \int_{|\vec{k}|<k_F} (\int d\vec{u} \frac{e^{i(\vec{k_n}-\vec{k_j}).\vec{u}}}{|\vec{u}|}) d\vec{k} \psi_{\vec{k_n}}(\vec{r}) \tag{2.8}$$

where the integral deals with all states $\vec{k}$ occupied by one electron having the same spin as the n^{th} electron. We will deal in this section with a non-magnetic filling, where each occupied state k_n has two electrons with opposite spins.

Switching from the discrete sum over j to the integral over $\vec{k}$ is allowed insofar as the number of occupied states is big enough, so that the value of possible $\vec{k_j}$ vectors are very close one to each other. We notice that the self-interaction term doesn't count in the integral as the measure of Lebesgue of a point in three dimensions is 0.

The following term :

$$\int d\vec{u} \frac{e^{i(\vec{k_n}-\vec{k_j}).\vec{u}}}{|\vec{u}|} \tag{2.9}$$

turns out to be the Fourier transform of the funtion $\vec{u} \longmapsto \frac{1}{|\vec{u}|}$. Hence :

$$\int d\vec{u} \frac{e^{i(\vec{k_n}-\vec{k_j}).\vec{u}}}{|\vec{u}|} = \frac{4\pi}{|\vec{k_n}-\vec{k}|^2} \tag{2.10}$$

We conclude that

$$(H_{Fock}\psi_{\vec{k_n}})(\vec{r}) = (-\frac{4\pi e^2}{(2\pi)^3} \int_{|\vec{k}|<k_F} \frac{d\vec{k}}{|\vec{k_n}-\vec{k}|^2}) \psi_{\vec{k_n}}(\vec{r}) \tag{2.11}$$

As $\int |\psi_{\vec{k_n}}(\vec{r})|^2 = 1$, we find the following correction, thanks to the perturbative approach :

$$< \psi_{\vec{k_n}}(\vec{r}) | H_{Fock} | \psi_{\vec{k_n}}(\vec{r}) > = -\frac{4\pi e^2}{(2\pi)^3} \int_{|\vec{k}|<k_F} \frac{d\vec{k}}{|\vec{k_n}-\vec{k}|^2} \tag{2.12}$$

The energy of this electron now is :

$$E^{corr.}_{k_n} = \frac{h^2 k_n^2}{2m} - \frac{4\pi e^2}{(2\pi)^3} \int_{|\vec{k}|<k_F} \frac{d\vec{k}}{|\vec{k_n}-\vec{k}|^2} =^{def} \frac{h^2 k_n^2}{2m} - \Delta(\vec{k_n}) \tag{2.13}$$

The integral deals with all $\vec{k}$ vectors such that $|\vec{k}| < k_F$ only if the electronic states are occupied up to the Fermi energy. For instance in the half-filled case, the integral will adress fewer $\vec{k}$ states ($\vec{k} : |\vec{k}| < \alpha k_F$ where $\alpha < 1$).

Let's focus on this correction $\Delta(\vec{k})$ to the energy in the free electrons case :

$$\int\int\int_{|\vec{k'}|<k_F} \frac{d\vec{k'}}{|\vec{k}-\vec{k'}|^2} = \int\int\int_{|\vec{v}-\vec{k}|<k_F} \frac{d\vec{v}}{|\vec{v}|^2} \tag{2.14}$$

This integral appears difficult to compute in the general situation where the three components of $\vec{k}$ are different from 0. The expression in spherical coordinates is :

$$\Delta(\vec{k}) = \frac{4\pi e^2}{(2\pi)^3} \int_0^{k_F} \int_0^{\pi} \int_0^{2\pi} \frac{r'^2 sin(\theta')}{k^2 + r'^2 - 2r'[sin(\theta')(k_x cos(\phi') + k_y sin(\phi')) + k_z cos(\theta')]} dr' d\theta' d\phi' \tag{2.15}$$

We compute the integral in the simplified case $\vec{k} = k\vec{e_z}$. This will give us the trend of the correction in the direction $\vec{k} // \vec{e_z}$ in the reciprocal space, which is enough. The details of the calculations are given in

Annex 4. I didn't realize that such an easy calculation was possible, therefore I tried other probabilistic methods to estimate this integral. These are presented in **Annex 5**. We finally find :

$$\Delta(\vec{k}) = \frac{2e^2}{\pi} k_F G(x) \tag{2.16}$$

where $x = \frac{k}{k_F}$ and

$$G(x) = \frac{1}{2} + \frac{1-x^2}{4x} \ln|\frac{1+x}{1-x}| \tag{2.17}$$

The graph of the function $k \longmapsto G(\frac{k}{k_F})$ is given below (k_F being fixed at $10^8 m^{-1}$) :

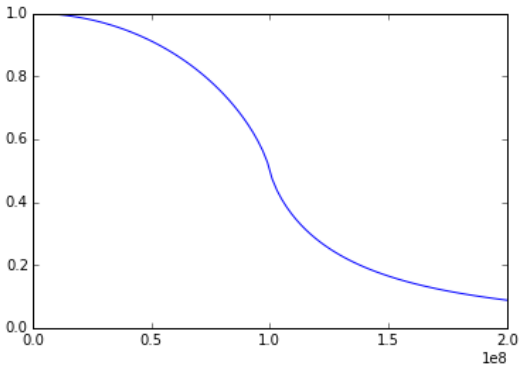

Figure 2.1: Function G

As $G(.)$ takes its values in $[0, 1]$, the correction to the energy of free electrons will be noticed if $e^2 k_F$ and $\frac{h^2 k^2}{2m}$ have the same order of magnitude (let's say 1 eV for instance). We find that :

$$e^2 k_F \sim \frac{h^2 k_F^2}{2m} \Longleftrightarrow k_F \sim 10^8 m^{-1} \tag{2.18}$$

We will therefore choose a Fermi vector of norm close to $10^8\ m^{-1}$ to plot the energies. This is associated with a Fermi velocity of 10^4 m/s approximately.

Let's plot on a same graph the energy of free independent electrons and the energy computed when taking into account Fock's term, namely :

$$E_{corrige}(k) = \frac{h^2 k^2}{2m} - \frac{q_e^2}{2\pi^2 \epsilon_0} k_F G(\frac{k}{k_F}) \tag{2.19}$$

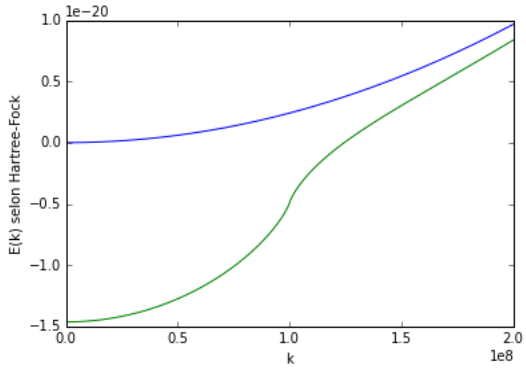

Figure 2.2: Correction of the energy (J) of free electrons by taking into account Hartree-Fock's term for $k_F = 10^8\ m^{-1}$

When k_F increases, the correction is slighter :

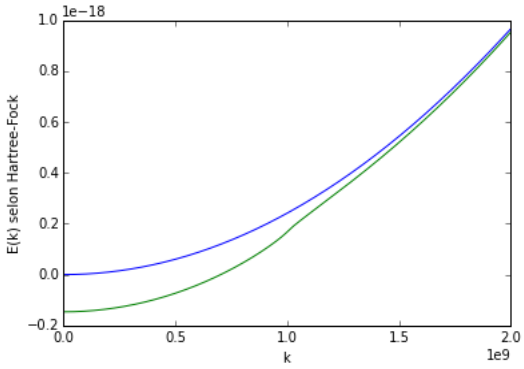

Figure 2.3: Correction of the energy (J) of free electrons by taking into account Hartree-Fock's term for $k_F = 10^9\ m^{-1}$

On the contrary when k_F decreases, **the variation** of the energy of free independent electrons becomes negligible in comparison with **the variation** of the Hartree-Fock energy.

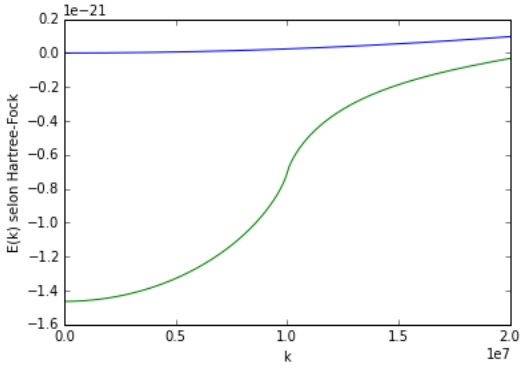

Figure 2.4: Correction of the energy (J) of free electrons by taking into account Hartree-Fock's term for $k_F = 10^7\ m^{-1}$

The behaviour at $k = k_F$ seems peculiar, let's zoom in on it :

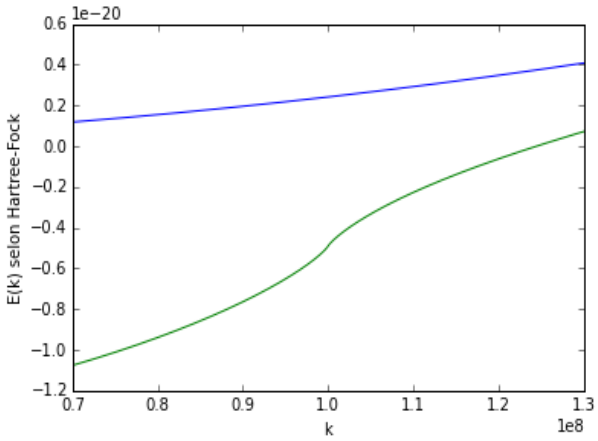

Figure 2.5: Correction of the energy (J) of free electrons by taking into account Hartree-Fock's term for $k_F = 10^8\ m^{-1}$, for k close to k_F

The derivative of the energy computed with Hartree-Fock's method is infinite at $k = k_F$. It tends logarithmically towards ∞ : when we zoom ten times more on the neighboourhood of k_F, the maximal value increases only twofold, which is typical of a logarithmic divergence :

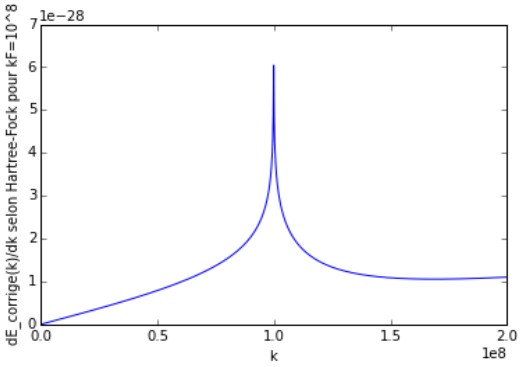

Figure 2.6: Derivative of the energy (J) of free electrons by taking into account Hartree-Fock's term for $k_F = 10^8\ m^{-1}$

Therefore **the Fermi velocity is infinite at** $k = k_F$, which is not physical. This will be corrected by taking screening into account. The two-fold derivative of this energy is also discontinuous, which is seen by the concavity which suddenly changes at $k = k_F$ (convex for $k < k_F$ and concave for $k > k_F$).

Computing the derivative of $G(.)$ and then the equivalent gives the following :

$$G'(x) \sim -\frac{1}{2}\ln(1-x) \Rightarrow (\frac{d\Delta}{dk})(k) \sim_{k\to k_F} -\frac{q_e^2}{4\pi^2\epsilon_0}\ln|k_F - k| \to \infty \tag{2.20}$$

We recognize the logarithmic divergence found by zooming on the peak of the derivative of $\Delta(k)$.

Analysis of the bandwidth :
Using that $G(0) = 1$ and $G(1) = \frac{1}{2}$, we find that :

$$E_{corrige}(k=0) = -\frac{q_e^2}{2\pi^2\epsilon_0}k_F =^{def} A \tag{2.21}$$

and

$$E_{corrige}(k=k_F) = \frac{h^2k_F^2}{2m} - \frac{q_e^2}{4\pi^2\epsilon_0}k_F = \frac{h^2k_F^2}{2m} - \frac{A}{2} \tag{2.22}$$

The bandwidth, namely the difference between the highest and the lowest energy of occupied states is in the filled case :

$$E_{corrige}(k_F) - E_{corrige}(0) = \frac{h^2k_F^2}{2m} + \frac{q_e^2}{4\pi^2\epsilon_0}k_F > \frac{h^2k_F^2}{2m} = E_{ind.electrons}(k_F) - E_{ind.electrons}(0) \tag{2.23}$$

We have :

$$\Delta E_{HF} = \Delta E_{free} + \frac{A}{2} \tag{2.24}$$

where ΔE_{free} is the bandwidth for the energy spectrum of free electrons. Therefore the Hartree-Fock's term makes the band-width increase compared with independent electrons, which is seen below :

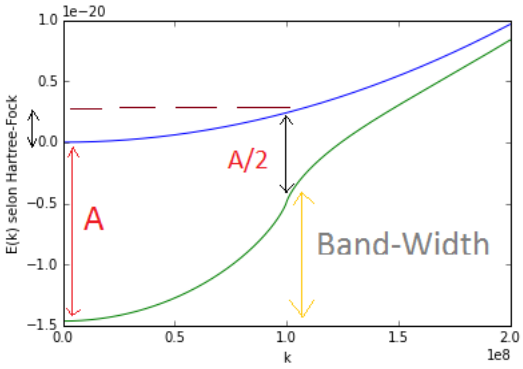

Figure 2.7: Correction of the energy (J) of free electrons by taking into account Hartree-Fock's term for $k_F = 10^8\ m^{-1}$

2.2 One dimensional lattice

Let's now perform similar calculations but in a more realistic system : a regular one-dimensionnal lattice, made up of N equally spaced atoms. Let k_n be a **possible** quantum state of an electron. We will make the distinction if the state is occupied or not. We denote the atomic orbital function of the n^{th} site as $\psi_n(.)$. The energy spectrum computed within the tight-binding approximation is :

$$E_k = E_0 - t_0 - 2tcos(ka) \tag{2.25}$$

where $k = \frac{2\pi m}{Na}$, $m \in Z$. We are now going to estimate the correction to the energy due to the terms of Fock and Hartree. The approach is identical as for free electrons, the only difference being the more complicated form of the wave-function.

$$(H_{Fock}\psi_{\vec{k_n}})(\vec{r}) = -\sum_{jocc.} \delta_{\sigma_j,\sigma_n} e^2 \int d\vec{r} \frac{\psi^*_{\vec{k_j}}(\vec{r'})\psi_{\vec{k_n}}(\vec{r'})}{|\vec{r}-\vec{r'}|}\psi_{\vec{k_j}}(\vec{r}) \tag{2.26}$$

As it was detailed in 1.1, the tight-binding wave-functions are :

$$\forall j, \psi_{k_j}(r) = \frac{1}{\sqrt{N}} \sum_n e^{ik_j na}\psi_n(r) \tag{2.27}$$

Hence :

$$\psi^*_{k_j}(r')\psi_{k_n}(r') = \frac{1}{N}\sum_n e^{i(k_n-k_j)na}|\psi_n(r')|^2 \tag{2.28}$$

because $\psi^*_{n_1}(r')\psi_{n_2}(r') = 0$ if $n_1 \neq n_2$. **We suppose that atomic orbitals don't overlap** : this is the main assumption which allows to simplify the following calculations.

$$(H_{Fock}\psi_{k_n})(r) = -\sum_{jocc.} \delta_{\sigma_j,\sigma_n}[\frac{e^2}{N}\sum_{m=1}^{N}(\int d\vec{r'}\frac{|\psi_m(r')|^2}{|\vec{r}-\vec{r'}|})e^{i(k_n-k_j)ma}]\psi_{k_j}(r) \tag{2.29}$$

Let denote :

$$\Gamma_{n,j}(r) = \frac{e^2}{N}\sum_{m=1}^{N}(\int d\vec{r'}\frac{|\psi_m(r')|^2}{|\vec{r}-\vec{r'}|})e^{i(k_n-k_j)ma} \tag{2.30}$$

so that:

$$(H_{Fock}\psi_{k_n})(r) = -\sum_{jocc.} \delta_{\sigma_j,\sigma_n}\Gamma_{n,j}(r)\psi_{k_j}(r) \tag{2.31}$$

If the state k_n is indeed occupied, the state labelled by the index n is reached in the sum over j. We thus distinguish two terms in the previous expression : the self-interaction term (for $j = n$) and the rest.

$$-\frac{e^2}{N}\int d\vec{r'}\frac{(\sum_{m=1}^{N}|\psi_m(r')|^2)}{|\vec{r}-\vec{r'}|}\psi_{k_n}(r) - \sum_{jocc.,j\neq n} \delta_{\sigma_j,\sigma_n}[\frac{e^2}{N}\sum_{m=1}^{N}(\int d\vec{r'}\frac{|\psi_m(r')|^2}{|\vec{r}-\vec{r'}|})e^{i(k_n-k_j)ma}]\psi_{k_j}(r) \tag{2.32}$$

$$(H^{Fock}_{auto-interaction}\psi_{k_n})(r) = -\frac{e^2}{N}\int d\vec{r'}\frac{(\sum_{m=1}^{N}|\psi_m(r')|^2)}{|\vec{r}-\vec{r'}|}\psi_{k_n}(r) \tag{2.33}$$

On the other side, we must consider Hartree's contribution :

$$(V_{Hartree}\psi_{k_n})(r) = e^2\int d\vec{r'}\frac{\rho(r')}{|r-r'|}\psi_{k_n}(r) \tag{2.34}$$

where $\rho(.)$ is the total electronic density :

$$\rho(r') = \sum_{jocc.}^{N}|\psi_{k_j}(r')|^2 \tag{2.35}$$

The equation 2.27 implies that

$$\forall j, |\psi_{k_j}(r')|^2 = \frac{1}{N}\sum_{m=1}^{N}|\psi_m(r')|^2 \tag{2.36}$$

which is the same for all occupied electronic states. We deduce that

$$\rho(r') = \frac{N_e}{N}\sum_{m=1}^{N}|\psi_m(r')|^2 \tag{2.37}$$

with N_e **the number of electrons** in the system, which differs from the number of occupied states N^{occ}, as we can have two electrons in each state. We thus have :

$$(V_{Hartree}\psi_{k_n})(r) = e^2\frac{N_e}{N}\int d\vec{r'}\frac{(\sum_{m=1}^{N}|\psi_m(r')|^2)}{|\vec{r}-\vec{r'}|}\psi_{k_n}(r) \tag{2.38}$$

We must not forget that this expression includes a self-interaction term if k_n is an occupied state (as $|\psi_{k_n}(r')|^2$ appears in the expression of $\rho(r')$ in this case):

$$(V^{Hartree}_{self-interaction}\psi_{k_n})(r) = e^2\int d\vec{r'}\frac{|\psi_{k_n}(r')|^2}{|r-r'|}\psi_{k_n}(r) \tag{2.39}$$

$$= -e^2\delta_{\sigma_n,\sigma_n}\int d\vec{r'}\frac{\psi^*_{k_n}(r')\psi_{k_n}(r')}{|r-r'|}\psi_{k_n}(r) \tag{2.40}$$

$$= -\frac{e^2}{N}\int d\vec{r'}\frac{(\sum_{m=1}^{N}|\psi_m(r')|^2)}{|\vec{r}-\vec{r'}|}\psi_{k_n}(r) \tag{2.41}$$

$$= -(H^{Fock}_{self-interaction}\psi_{k_n})(r) \tag{2.42}$$

if k_n is an occupied state.

We have proved that the Fock term allows to get rid of the self-interaction problem :

$$(V^{Hartree}_{self-interaction} + H^{Fock}_{self-interaction})\psi_{k_n}(r) = 0 \tag{2.43}$$

If k_n is not an occupied state, the self-interaction terms both in Hartree's potential and in Fock's term don't exist.

Among the four components of the Hartree-Fock perturbation term :
$H^{Fock}_{self-interaction}$, $H^{Fock}_{without-self-interaction}$, $V^{Hartree}_{self-interaction}$, $V^{Hartree}_{without-self-interaction}$, only two remain :

$$H^{Fock}_{without-self-interaction} + V^{Hartree}_{without-self-interaction} \tag{2.44}$$

At the first order, the variation of the energy of the electronic state k_n state **due to Fock's term** is

$$\Delta(E_{k_n})_{Fock} = < \psi_{k_n}|H^{Fock}_{without-self-interaction}|\psi_{k_n} > \tag{2.45}$$

$$\Delta(E_{k_n})_{Fock} = \int \psi^*_{k_n}(r)(H^{Fock}_{w.s.i.}\psi_{k_n})(r)d\vec{r} = -\sum_{j\neq n, jocc.} \delta_{\sigma_j,\sigma_n} \int \psi^*_{k_n}(r)\Gamma_{n,j}(r)\psi_{k_j}(r)d\vec{r} \tag{2.46}$$

thanks to 2.31.

Let's compute $\int \psi^*_{k_n}(r)\Gamma_{n,j}(r)\psi_{k_j}(r)d\vec{r}$:

$$\int \psi^*_{k_n}(r)\Gamma_{n,j}(r)\psi_{k_j}(r)d\vec{r} = \frac{1}{N}\sum_{l=1}^{N} e^{i(k_j-k_n)la} \int d\vec{r}|\psi_l(r)|^2\Gamma_{n,j}(r) \tag{2.47}$$

thanks to the non-overlapping assumption ($\psi^*_{l_1}(r)\psi_{l_2}(r) = 0$ if $l_1 \neq l_2$).

Therefore, using the expression 2.30 of $\Gamma_{n,j}(.)$:

$$\int \psi^*_{k_n}(r)\Gamma_{n,j}(r)\psi_{k_j}(r)d\vec{r} = \frac{e^2}{N^2}\sum_{l=1}^{N}\sum_{m=1}^{N}[\int d\vec{r}|\psi_l(\vec{r})|^2(\int d\vec{r'}\frac{|\psi_m(\vec{r'})|^2}{|r-r'|})]e^{i(k_n-k_j)(m-l)a} \tag{2.48}$$

We conclude that for a one dimensional lattice (seen in a three-dimensional space) :

$$\Delta(E_{k_n})_{Fock} = -\sum_{j\neq n, jocc.} \delta_{\sigma_j,\sigma_n}\frac{e^2}{N^2}\sum_{l=1}^{N}\sum_{m=1}^{N}[\int d\vec{r}|\psi_l(\vec{r})|^2(\int d\vec{r'}\frac{|\psi_m(\vec{r'})|^2}{|r-r'|})]e^{i(k_n-k_j)(m-l)a} \tag{2.49}$$

The knowledge of the orbital functions $\psi_l(.)$ appears necessary to estimate this correction to the energy.

We also have to consider the variation of the energy of the electronic state k_n state **due to Hartree's without-self-interaction term** :

$$\Delta(E_{k_n})_{Hartree} =< \psi_{k_n}|V^{Hartree}_{w.s.i.}|\psi_{k_n} >=^{def} < \psi_{k_n}|H^{Fock}_{s.i.} + V^{Hartree}|\psi_{k_n} > \tag{2.50}$$

$$\Rightarrow \Delta(E_{k_n})_{Hartree} = \int d\vec{r}\psi^*_{k_n}(\vec{r})(e^2\frac{N_e - \delta^{occ.}_{k_n}}{N}\int d\vec{r'}\frac{\sum_{m=1}^{N}|\psi_m(\vec{r'})|^2}{|\vec{r}-\vec{r'}|})\psi_{k_n}(\vec{r}) \tag{2.51}$$

where $\delta^{occ.}_{k_n} =^{def} 1$ iff k_n is an occupied state (and 0 otherwise). Therefore, using 2.36 :

$$\Delta(E_{k_n})_{Hartree} = e^2\frac{N_e - \delta^{occ.}_{k_n}}{N^2}\sum_{l=1}^{N}\sum_{m=1}^{N}\int d\vec{r}|\psi_l(\vec{r})|^2\int d\vec{r'}\frac{|\psi_m(\vec{r'})|^2}{|\vec{r}-\vec{r'}|} \tag{2.52}$$

To sum it all, the total correction to the energy at the first order is :

$$\Delta(E_{k_n}) = \Delta(E_{k_n})_{Hartree} + \Delta(E_{k_n})_{Fock} \tag{2.53}$$

namely :

$$e^2\frac{N_e - \delta^{occ}_{k_n}}{N^2}\sum_{l=1}^{N}\sum_{m=1}^{N}[\int d\vec{r}|\psi_l(\vec{r})|^2\int d\vec{r'}\frac{(|\psi_m(r')|^2)}{|\vec{r}-\vec{r'}|}] - \sum_{j\neq n, jocc.}\delta_{\sigma_j,\sigma_n}\frac{e^2}{N^2}\sum_{l=1}^{N}\sum_{m=1}^{N}[\int d\vec{r}|\psi_l(\vec{r})|^2(\int d\vec{r'}\frac{|\psi_m(\vec{r'})|^2}{|r-r'|})]e^{i(k_n-k_j)(m-l)a} \tag{2.54}$$

where $e^2 = \frac{q_e^2}{4\pi\epsilon_0}$. The correction to the energy due to Hartree's potential and Fock's term has'nt the same expression for free and occupied states.

Both terms coming from Hartree's term and from Fock's term have the same order of magnitude. Indeed for both, $\frac{e^2}{N^2}$ is a prefactor. The first term has a prefactor of order N_e, the number of occupied states, but the second term coming from Fock's term calculations involves a sum over the occupied states labeled by j, and there are $N^{occ} = \frac{N_e}{2}$ such non-zero terms (except in the case of a magnetic filling, where there can be N_e non-zero terms in the corrections for a given spin, and none for the other value of spin).

We also notice that the double integral involving the atomic orbital wave functions $\psi_m(.)$ and $\psi_l(.)$ appears in both term. An another expression of the energy correction would be :

$$\frac{e^2}{N^2}\sum_{l=1}^{N}\sum_{m=1}^{N}(\int d\vec{r}|\psi_l(\vec{r})|^2\int d\vec{r'}\frac{(|\psi_m(\vec{r'})|^2)}{|\vec{r}-\vec{r'}|})(N_e - \delta^{occ}_{k_n} - \sum_{j\neq n, jocc.}\delta_{\sigma_j,\sigma_n}e^{i(k_n-k_j)(m-l)a}) \tag{2.55}$$

Let's adopt the following notation :

$$I_{l,m} = \int d\vec{r} \int d\vec{r'} \frac{|\psi_m(\vec{r'})|^2 |\psi_l(\vec{r})|^2}{|\vec{r} - \vec{r'}|} \tag{2.56}$$

and

$$\Theta^n_{l,m} = (N_e - \delta^{occ}_{k_n} - \sum_{j \neq n, jocc.} \delta_{\sigma_j,\sigma_n} e^{i(k_n - k_j)(m-l)a}) \tag{2.57}$$

As the correction to the energy is a real number, by taking the imaginary part, we obtain that :

$$\sum_{j \neq n, jocc.} \delta_{\sigma_j,\sigma_n} sin((k_n - k_j)(m-l)a) = 0 \tag{2.58}$$

so that it is the same to write $\Theta^n_{l,m}$ with exponential or cosine. We also notice the symmetric roles played by l and m : $I_{l,m} = I_{m,l}$.

The equation 2.55 can be rewritten as :

$$\Delta(E_{k_n}) = \frac{e^2}{N^2} \sum_{l=1}^{N} \sum_{m=1}^{N} I_{l,m} \Theta^n_{l,m} \tag{2.59}$$

We can simplify the expression 2.59 using the periodic boundary conditions. We show in **Annex 6** that :

$$\sum_{m=1}^{N} I_{l_0,m} \Theta^n_{l_0,m} \tag{2.60}$$

does not depend on the integer l_0, thanks to the **invariance by translation**. Therefore

$$\Delta(E_{k_n}) = \frac{e^2}{N} \sum_{m=1}^{N} I_{l_0,m} \Theta^n_{l_0,m} \tag{2.61}$$

for any l_0.

To compute $\Delta(E_{k_n})$, I first tried Monte-Carlo methods, namely the Metropolis algorithm. The method and algorithm I used are fully described in **Annex 7**. Actually, I realized later that it was not necessary to use such methods to have a simple estimation of the correction to the energy. However, it can turn out to be useful in the case of complicated atomic localised orbitals. As my program did not work swiftly enough, I swichted to a simpler method, which I explain below, and which worked far better in the case we chose simple localised orbitals $\psi_m(.)$, like gaussians.

We want to compute :

$$\Delta(E_{k_n}) = \frac{e^2}{N} \sum_{m=1}^{N} I_{0,m} \Theta^n_{0,m} \tag{2.62}$$

As $\Theta^n_{0,m}$ is easy to compute, we will first focus on $I_{0,m}$, which requires stochastic methods to be estimated :

$$I_{0,m} = \int \int d\vec{r} d\vec{r'} \frac{|\psi_0(\vec{r'})|^2 |\psi_m(\vec{r})|^2}{|\vec{r} - \vec{r'}|} = \int \int d\vec{r} d\vec{r'} \frac{|\chi(\vec{r'})|^2 |\chi(\vec{r} - ma\vec{e_x})|^2}{|\vec{r} - \vec{r'}|} \tag{2.63}$$

where $\chi(.)$ is the atomic orbital wave-function of the site of the lattice located at the origin of the coordinates. After changing of variables :

$$I_{0,m} = \int \int d\vec{u} d\vec{u'} \frac{|\chi(\vec{u'})|^2 |\chi(\vec{u})|^2}{|\vec{u} - \vec{u'} + ma\vec{e_x}|} \tag{2.64}$$

The dimension of $I_{0,m}$ is the inverse of a length, L^{-1}, because $d\vec{u}|\chi(\vec{u})|^2$ is a probability, i.e. a number without physical dimension. Let's notice something very important : we write the integral in the three dimensional space, because Coulomb's law of interaction isn't valid in one dimension, and the integral above would diverge a strict one dimensional lattice, anyway.

Therefore **we see the 1D lattice in the 3D space**, knowing that the movement of the electrons is mostly along the chain, i.e. mostly one-dimensional.

As $\Theta^n_{0,m}$ is also of dimension 1, $\Delta(E_{k_n})$ has the dimension of $e^2 I_{0,m} = \frac{q_e^2}{4\pi\epsilon_0 L}$, which is an energy.

Let's first assume that $\chi(.)$ has no angular dependence :

$$\chi(\vec{\rho}) = K\frac{1}{\sqrt{4\pi}}e^{-\frac{(\frac{\rho}{a})^2}{2(\frac{d}{a})^2}} \tag{2.65}$$

where K is a constant.

We switch to spherical coordinates :

$$\vec{u} = \begin{pmatrix} \rho_1 sin(\theta_1)cos(\phi_1) \\ \rho_1 sin(\theta_1)sin(\phi_1) \\ \rho_1 cos(\theta_1) \end{pmatrix}, \vec{u'} = \begin{pmatrix} \rho_2 sin(\theta_2)cos(\phi_2) \\ \rho_2 sin(\theta_2)sin(\phi_2) \\ \rho_2 cos(\theta_2) \end{pmatrix} \tag{2.66}$$

we obtain for the integrand :

$$\frac{\frac{K^4}{(4\pi)^2}e^{-\frac{(\frac{\rho_1}{a})^2}{(\frac{d}{a})^2}}e^{-\frac{(\frac{\rho_2}{a})^2}{(\frac{d}{a})^2}}\rho_1^2\rho_2^2 sin(\theta_1)sin(\theta_2)d\rho_1 d\rho_2 d\theta_1 d\theta_2 d\phi_1 d\phi_2}{\sqrt{(\rho_1 sin(\theta_1)cos(\phi_1) - \rho_2 sin(\theta_2)cos(\phi_2) - ma)^2 + (\rho_1 sin(\theta_1)sin(\phi_1) - \rho_2 sin(\theta_2)sin(\phi_2))^2 + (\rho_1 cos(\theta_1) - \rho_2 cos(\theta_2))^2)}} \tag{2.67}$$

which gives, by expanding the denominator and setting $\rho'_1 = \frac{\rho_1}{a}$, $\rho'_2 = \frac{\rho_2}{a}$:

$$\frac{1}{(4\pi)^2}\frac{K^4 a^5 e^{-\frac{\rho_1'^2}{(\frac{d}{a})^2}}e^{-\frac{\rho_2'^2}{(\frac{d}{a})^2}}\rho_1'^2\rho_2'^2 sin(\theta_1)sin(\theta_2)d\rho'_1 d\rho'_2 d\theta_1 d\theta_2 d\phi_1 d\phi_2}{\sqrt{\rho_1'^2 + \rho_2'^2 - 2\rho'_1\rho'_2(sin(\theta_1)\sin(\theta_2)cos(\phi_1 - \phi_2) + cos(\theta_1)cos(\theta_2)) + 2m(\rho'_2 sin(\theta_2)cos(\phi_2) - \rho'_1 sin(\theta_1)cos(\phi_1)) + m^2}} \tag{2.68}$$

The idea is to use the fact that the radial part of the wave functions is gaussian, as we know how to generate random normal variables. We are going to select randomly ρ'_1 and ρ'_2 according to the density of probability $f(\rho) = \frac{1}{\sqrt{\pi(\frac{d}{a})^2}}e^{-\frac{\rho^2}{(\frac{d}{a})^2}}$; a gaussian random variable with means 0 and standard deviation $\frac{d}{\sqrt{2}a}$. θ_1 and θ_2 will be selected uniformly between 0 and π according to the distribution $g(\theta) = \frac{1}{\pi}$, and ϕ_1, ϕ_2 also uniformly in the space of integration, with density of probability $h(\phi) = \frac{1}{2\pi}$.

Let denote $F_m(\rho'_1, \rho'_2, \theta_1, \theta_2, \phi_1, \phi_2)$ the following function :

$$\frac{\rho_1'^2\rho_2'^2 sin(\theta_1)sin(\theta_2)}{\sqrt{\rho_1'^2 + \rho_2'^2 - 2\rho'_1\rho'_2(sin(\theta_1)\sin(\theta_2)cos(\phi_1 - \phi_2) + cos(\theta_1)cos(\theta_2)) + 2m(\rho'_2 sin(\theta_2)cos(\phi_2) - \rho'_1 sin(\theta_1)cos(\phi_1)) + m^2}} \tag{2.69}$$

Given all these notations, we now have :

$$I_{0,m} = \frac{K^4 a^5}{(4\pi)^2}\pi(\frac{d}{a})^2\pi^2(2\pi)^2\int\int F_m(\rho'_1, \rho'_2, \theta_1, \theta_2, \phi_1, \phi_2)f(\rho'_1)d\rho'_1 f(\rho'_2)d\rho'_2 g(\theta_1)d\theta_1 g(\theta_2)d\theta_2 h(\phi_1)d\phi_1 h(\phi_2)d\phi_2 \tag{2.70}$$

Let x be the joint variable : $x = (\rho'_1, \rho'_2, \theta_1, \theta_2, \phi_1, \phi_2)$. As all these variables will be selected independently, the density of probability of x is :

$$\mu(x)d^6x = f(\rho'_1)f(\rho'_2)g(\theta_1)g(\theta_2)h(\phi_1)h(\phi_2)d\rho'_1 d\rho'_2 d\theta_1 d\theta_2 d\phi_1 d\phi_2 \tag{2.71}$$

Therefore

$$I_{0,m} = \frac{K^4 a^5 \pi^3}{4}(\frac{d}{a})^2\int F_m(x)\mu(x)d^6x \tag{2.72}$$

Let's compute K thanks to the normalisation condition :

$$\int |\chi(\vec{r})|^2 d\vec{r} = 1 \tag{2.73}$$

$$\Rightarrow \frac{K^2}{4\pi}(\int_0^\infty r^2 e^{-\frac{(\frac{r}{a})^2}{(\frac{d}{a})^2}} dr)(\int_0^\pi sin(\theta)d\theta)(\int_0^{2\pi} d\phi) = 1 \tag{2.74}$$

$$\Rightarrow K^2 a^3 \int_0^\infty u^2 e^{-\frac{u^2}{(\frac{d}{a})^2}} = K^2 a^3 \frac{\sqrt{\pi}}{2}(\frac{d}{a})^3 \tag{2.75}$$

Therefore the value of K is :

$$K = \frac{\sqrt{2}}{\pi^{\frac{1}{4}}} \frac{1}{d^{\frac{3}{2}}} \tag{2.76}$$

The equation 2.72 becomes :

$$I_{0,m} = \frac{\pi^2}{d}(\frac{a}{d})^3 \int F_m(x)\mu(x)d^6x \tag{2.77}$$

We find that $I_{0,m}$ has indeed the dimension of the inverse of a length, as all variables in the vector x have no physical dimension. Let call

$$E_\mu(F_m) = \int F_m(x)\mu(x)d^6x \tag{2.78}$$

the expectation value of F_m for the distribution of probability $\mu(.)$.

The global correction can be rewritten as :

$$\Delta(E_{k_n}) = \frac{e^2}{N}\sum_{m=1}^{N} I_{0,m}\Theta^n_{0,m} = \pi^2(\frac{a}{d})^3 \frac{q_e^2}{4\pi\epsilon_0 d}\frac{1}{N}\sum_{m=1}^{N} E_\mu(F_m)\Theta^n_{0,m} \tag{2.79}$$

The factor $\frac{q_e^2}{4\pi\epsilon_0 d}$, which is the Coulomb interaction energy for two electrons located at d one from each other, gives the order of magnitude of the terms. A very important thing is that once the integrals $I_{0,m}$ are estimated with very little deviation from their real values, we can use them for each computation of $\Delta(E_{k_n})$, having only to compute $(\Theta^n_{0,m})_{m=1..N}$ for each correction. **Therefore we only need to compute** $(I_{0,m})_{m=1..N}$ **once**.

$E_f(F_m)$ is estimated simply, by generating M times independent random variables $X_i = ((\rho'_1)_i, (\rho'_2)_i, (\theta_1)_i, (\theta_2)_i, (\phi_1)_i, (\phi_2)_i)$, each following the density of probability previously mentioned. Each vector X_i of random variables follows $x \longmapsto l(x)$ as density of probability, therefore :

$$\frac{1}{M}\sum_{i=1}^{M} F_m(X_i) \longrightarrow_{M\longrightarrow+\infty} E_\mu(F_m) = \int F_m(x)\mu(x)d^6x \tag{2.80}$$

For most of the integrals $I_{0,m}$, $M = 10000$ random selections are sufficient to esimate $I_{0,m}$ with less than 1% error.

Given that $\Theta^n_{0,m}$ is made up of two separate terms :

$$\Theta^n_{0,m} = (N_e - \delta^{occ}_{k_n} - \sum_{j\neq n, jocc.} \delta_{\sigma_j,\sigma_n} e^{i(k_n-k_j)ma}) \tag{2.81}$$

we can see the contribution to the correction of the energy only due to the term of Fock without self-interaction ; by setting $\Theta^n_{0,m} = -\sum_{j\neq n,jocc.} \delta_{\sigma_j,\sigma_n} e^{i(k_n-k_j)ma}$ in the code. We will call $\Delta(E_{k_n})^{Fockw.s.i.}$ the corresponding correction.

The correction due to Hartree's term, and Fock-self-interaction term (if there is one) only depends on n in the term $\delta^{occ}_{k_n}$:

$$\Delta(E_{k_n}) = (N_e - \delta^{occ}_{k_n})\frac{e^2}{N}\sum_{m=1}^{N} I_{0,m} = (N_e - \delta^{occ}_{k_n})\pi^2(\frac{a}{d})^3 \frac{q_e^2}{4\pi\epsilon_0 d}\frac{1}{N}\sum_{m=1}^{N} E_\mu(F_m) \tag{2.82}$$

Therefore if $N_e \gg 1$, the dependence on n of the correction $\Delta(E_{k_n})$ will become negligible, and **Hartree's effect will be to translate the energy spectrum** (computed with the Fock term) **by a constant**.
For small values of electrons in the system, Hartree's term will make a significant difference between the occupied states (such that $\delta^{occ}_{k_n} = 1$) and the empty states (such that $\delta^{occ}_{k_n} = 0$).

2.2.1 Correction of the energy spectrum due to the term of Fock only

The simulations show that the correction due to Fock's term, is always negative, as expected.

$$\Delta(E_{k_n})^{Fockw.s.i.} = -\frac{e^2}{N}\sum_{m=1}^{N} I_{0,m} \sum_{j\neq n, jocc.} \delta_{\sigma_j,\sigma_n} \cos((k_n - k_j)ma) \tag{2.83}$$

$$\Delta(E_{k_n})^{Fockw.s.i.} = -\pi^2(\frac{a}{d})^3 \frac{q_e^2}{4\pi\epsilon_0 d}\frac{1}{N}\sum_{m=1}^{N} E_\mu(F_m) \sum_{j\neq n, jocc.} \delta_{\sigma_j,\sigma_n} \cos((k_n - k_j)ma) \leq 0 \tag{2.84}$$

The following graphics show the results obtained with the method which has just been described. N is the number of atoms in the lattice, while **NB is the total number of electrons in the system** : $NB \leq 2N$. We assume that the energy levels are filled in a non-magnetic way, from the lowest energy level, each level having two electrons with opposite spins. For instance if there are 10 electrons in the system (NB=10), there will be 5 occupied states. We will see later that for numerous values of NB, there will be different ways to fill the lowest energy levels with NB electrons, and therefore different initial states, ending uo with different corrections.
nb is the number of random selections done to compute each value of $I_{0,m}$, for $m \in [1, N]$.

In blue, the energy profile computed in the tight-binding approximation :

$$E(k_n) = E_0 - t_0 - 2tcos(k_n a) \tag{2.85}$$

with $E_0 = 13eV$, $t_0 = 0.5eV$, $t = 2eV$ and $a = 10^{-10}m$, and $k_n = \frac{2\pi}{Na}m$, $m \in [-\lfloor\frac{N}{2}\rfloor, \lfloor\frac{N}{2}\rfloor]$.

In green, the energy spectrum corrected by Fock's term :

$$E(k_n)_{corrige} = E(k_n) + \Delta(E_{k_n})^{Fockw.s.i.} < E(k_n) \tag{2.86}$$

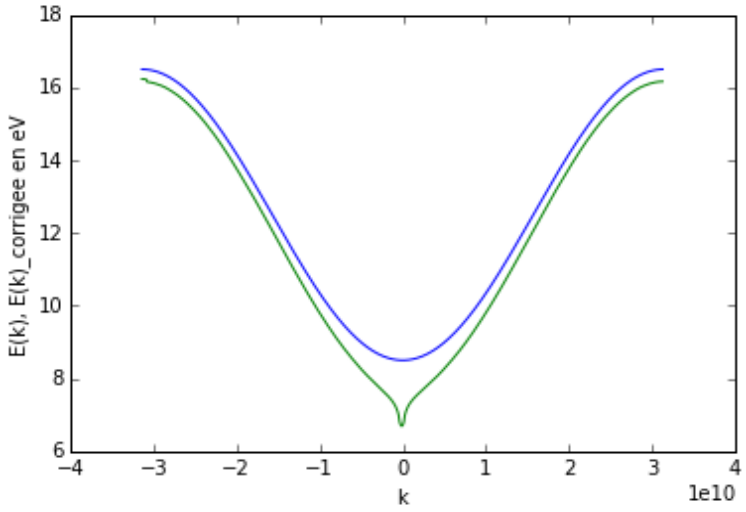

Figure 2.8: Energy computed for the one-dimensionnal lattice corrected by Fock's term, for N=500, NB=10 ($k_F = 0.03.10^{10}m^{-1}$) and nb=10000

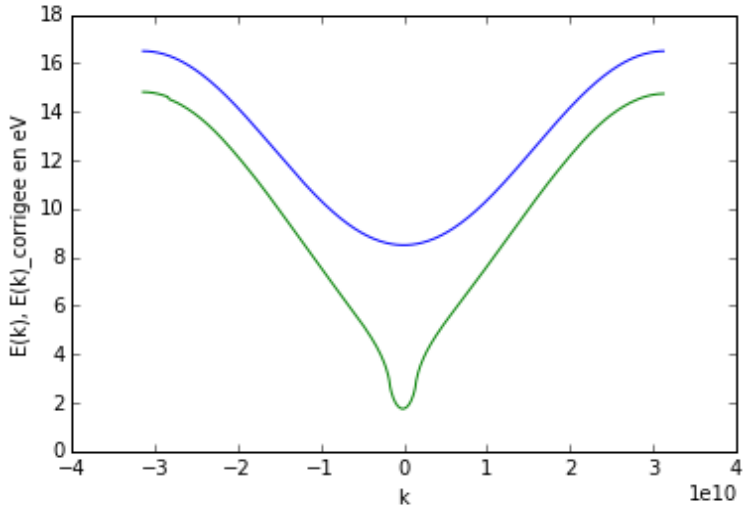

Figure 2.9: Energy computed for the one-dimensionnal lattice corrected by Fock's term, for N=500, NB=50 ($k_F = 0.16.10^{10} m^{-1}$) and nb=10000

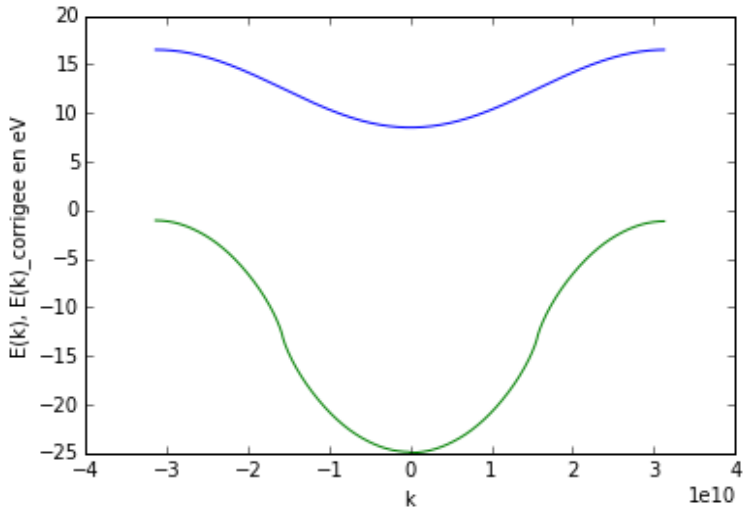

Figure 2.10: Energy computed for the one-dimensionnal lattice corrected by Fock's term, for N=500, NB=500 ($k_F = 1.57.10^{10} m^{-1}$, half-filling) and nb=10000

For a non-magnetic filling **at temperature** $T = 0K$, we fill up the states by increasing energy, with two electrons with opposite spins in each level. The modulous of the Fermi vector is given in that case by : $k_F = \frac{2\pi}{Na} p_F$, where $p_F = \frac{N^{occ}}{2} = \frac{NB}{4}$ is the number of occupied states with a positive quasi-momemtum k. Therefore :

$$k_F = \frac{\pi}{a} \frac{NB}{2N} \tag{2.87}$$

More graphs for different fillings NB can be found in **Annex 9**. We see that for a given N, the correction becomes bigger and bigger when the number of electrons in the system NB increases. Indeed, the correction to the energy, in green, is more and more negative when NB increases, N being constant.

On the contrary, at NB fixed, when the number of atoms in the lattice increases, the correction due to the term of Fock decreases, as the graphs displayed in **Annex 10** show.

The shape of the correction of the energy due to Fock's term for the one-dimensionnal lattice is very similar to that obtained for free electrons.

First, the correction of the energy due to the term of Fock is bigger for k close to 0 than in the edges of the band, which is also the case for free electrons, as we have seen in the graph 2.2.

Then, **the Fermi velocity is not defined**, being theoretically infinite ! Similarly to the case of free electrons, $k \longmapsto (\frac{dE_{corr.}}{dk})(k)$ is discontinuous at $k = k_F$ and $k = -k_F$. In the case of free electrons, the derivative of the energy goes logarithmically towards $+\infty$, which leads formally to an infinite Fermi velocity. It seems to be also the case for the one-dimensionnal lattice, as we clearly see a sudden change of concavity at $k = k_F$. However, this time the energy spectrum we obtained wasn't analytical, therefore it is difficult to be sure of the exact type of the divergence. Let's plot the derivative of the corrected energy to see the singularities at $k = k_F$ and $k = -k_F$:

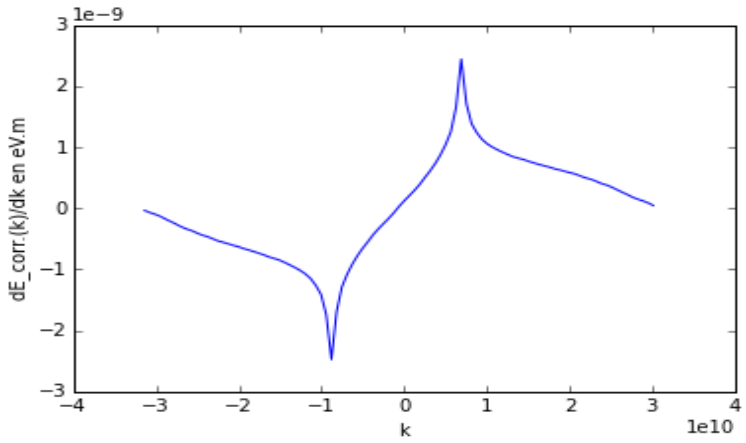

Figure 2.11: Derivative of the energy corrected by Hartree-Fock's term for $N = 100$ and $NB = 50$

Some zooms of the divergence are made in **Annex 11**, to try to proove this logarothmical divergence. However, the discretization pace in k being fixed with the number of atoms in the lattice N, it is difficult to upgrade the resolution around the peak.

Moreover, **the bandwidth of the occupied states** $\Delta E = E(k_F) - E(k = 0)$ **increases** when when take into account Hartree-Fock's term, similarly to the case of free electrons. We can also see how the bandwidth of the empty states evolves when taking interactions into account. For free electrons, this estimation wasn't possible as the bandwidth of the empty states was theoretically infinite, due to the parabolic dispersion.

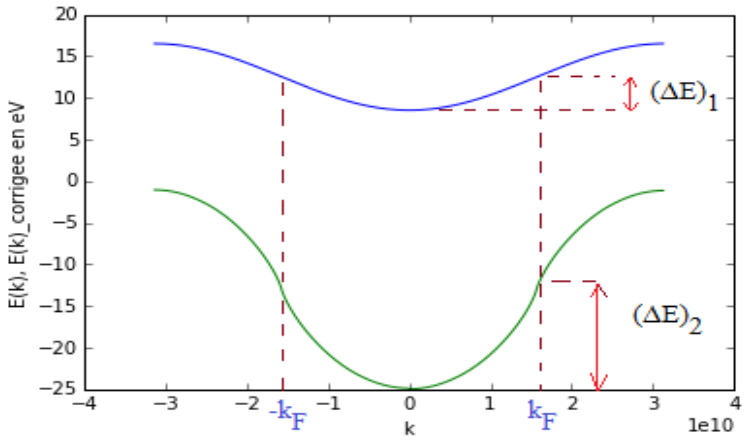

Figure 2.12: Increase of the bandwidth of the valence band for the 1D lattice by taking into account Fock's term, at half-filling : N=500, NB=500, $k_F = 1.57.10^{10} m^{-1}$)

$(\Delta E)_1$ is the bandwidth of the occupied states estimated in the tight-binding approximation, while $(\Delta E)_2$ is the same bandwidth estimated in the corrected energy spectrum, after taking Coulomb inter-

actions and Pauli principle into account. We see that $(\Delta E)_2 > (\Delta E)_1$, **for any value of the total number of electrons in the system NB**. We can understand this effect thanks to the big correction of the energy at $k = 0$, which draggs down the corrected energy spectrum. For very low fillings ($NB \leq 50$), this effect is clear and sharp, as it can be seen in the previous graph 2.9 for instance.

We must compare quantitatively the bandwidth increase in the corrected band. Let's denote $\Delta L_{occ}^{corrige}$ the bandwidth of the occupied states, computed with the corrected energy band, $\Delta L_{vide}^{corrige}$ the bandwidth of the empty states, computed with the corrected energy band, ΔL_{occ} the bandwidth of the occupied states, computed with the original energy spectrum, ΔL_{vide} the bandwidth of the occupied states, computed with the original energy band. We obtain the following evolution, for 10 computations at different filling NB, N being constant :

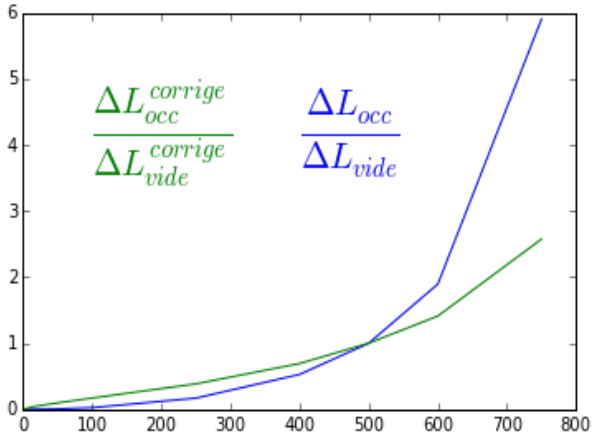

Figure 2.13: Comparison of the relative bandwidth of occupied and empty states in the corrected and non-corrected case

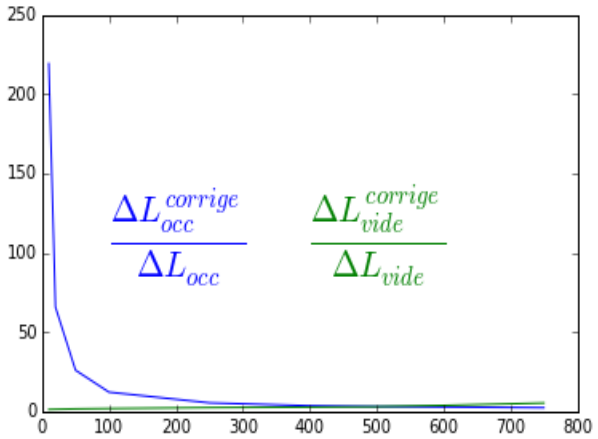

Figure 2.14: Comparison of the relative bandwidth of empty and occupied states in the corrected and non-corrected case

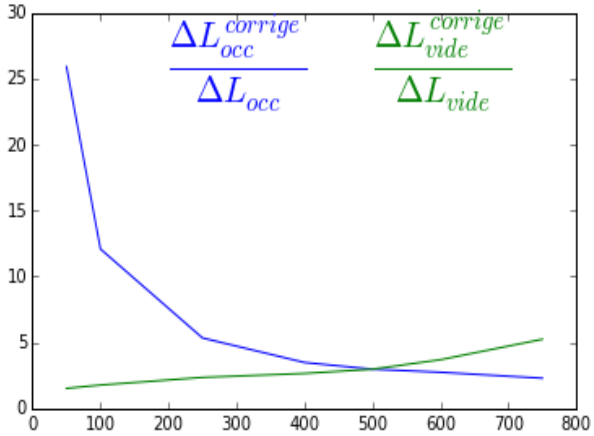

Figure 2.15: Comparison of the relative bandwidth of empty and occupied states in the corrected and non-corrected case

Conclusion : The bandwidth is much larger for small fillings in the corrected energy band, which is coherent when we look at the plots : Hartree-Fock's term draggs the band down between $-k_F$ and k_F, making a rather sharp difference between occupied and empty states (that's why there is a discontinuity of the slope at k_F), which is very clear for low fillings. It makes the bandwith much bigger than in the non-corrected case. Then, when NB increases, the trend becomes less and less visible, and there is a revearsal of this trend at the half-filling.

The total bandwidth of the corrected energy spectrum is bigger than in the non-corrected case, but also constant with NB. I have looked for a possible asymetry between electrons and holes in the corrected energy spectrum. Such an asymetry would be a different bandwidth of occupied states for a filling $NB = \alpha$ and the bandwidth of empty states for a filling $NB = 2N - \alpha$ (for the tigth-binding spectrum, there is this symmetry). I have therfore compared $\Delta L_{occ}^{corr}(\alpha)$ and $\Delta L_{vide}^{corr}(2N - \alpha)$. For small values of N, there seem to be an asymetry, but for N big enough (in the thermodynamical limit $N \longrightarrow +\infty$), this asymetry vanishes.

Some remarks :
1) We have shown that for a fixed value of NB, there can be numerous possible initial states, some of them leading to spin-polarized corrections (see **Annex 8** : spin-polarized energy corrections). For low values of N and NB, and **if NB is odd, this will necessarily be the case**, as there will be a level of energy with only one spin ! What is computed in that case thanks to my program is the correction of the energy spectrum for electrons with spin $\uparrow$, namely $k \longmapsto \Delta(E_{k,\uparrow})$, and the correction for electrons with spin $\downarrow$: $k \longmapsto \Delta(E_{k,\downarrow})$. However, as we noticed in **Annex 8**, the spin-polarization of the correction to the energy spectrum hopefully vanishes when the number of electrons increases and becomes of the same order of magnitude as the number of sites N. Indeed, the fillings we have described above aren't physical in the thermodynamical limit, when $N \longrightarrow +\infty$: both electrons with spins UP and electrons with spins DOWN see the same chemical potential, and there is no reason to favor a configuration with only spins UP or only spins DOWN in the two levels at the Fermi energy.

The code developped to estimate the spin-polarization of the correction to the energy will be useful to analyse "real" magnetic fillings, i.e. with a major part of all the electrons having the same spin. This will allow us to compute the energy associated to a ferromagnetic or an antiferromagnetic configuration, which may be lower than the energy for a non-magnetic filling at low temperature.

2) We saw that the correction of the energy computed thanks to the Fock's term seemed to become much larger than the energy itself when the number of electrons in the system increases. We should therefore check the validity of the perturbative approach, by analysing the variations of the eigen vectors $\delta\phi$ (this won't be done here). This validity is not correlated to the order of magnitude of the correction, and may remain valid for big values of corrections, as it is the case here.

2.2.2 Correction of the energy spectrum due to both terms of Hartree and Fock :

We now include Hartree's term in the correction, which makes the corrected energy spectrum translate to higher energies. The total corrections of the energy computed with Python are hopefully continuous, which is a physical result. The following graphs show how including Hartree-Fock modifies the energy band when the number of electron NB increases, at a fixed N. The first graph compares the spectrum computed in the tight-binding approximation with the corrected one, whereas the second graph displays the total correction to the energy ($k \longmapsto (E_k^{corr.} - E_k)$). More graphs, for different fillings, can be found in **Annex 13**.

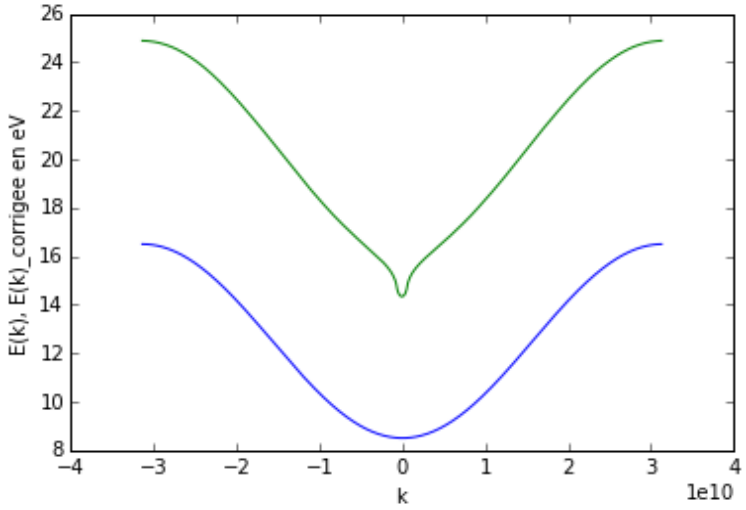

Figure 2.16: Energy computed for the one-dimensionnal lattice corrected by **Hartree-Fock's term**, for N=500, NB=20 ($k_F = 0.06.10^{10} m^{-1}$) and nb=10000

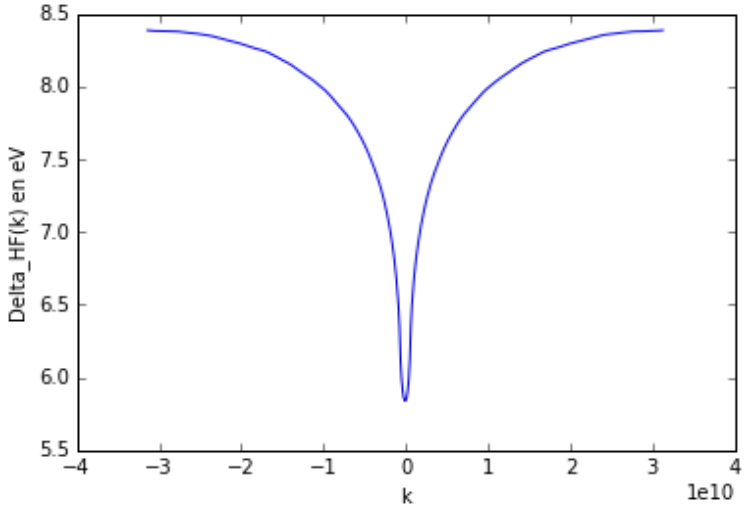

Figure 2.17: Correction of the energy by **Hartree-Fock's term** computed for the one-dimensionnal lattice , for N=500, NB=20 ($k_F = 0.06.10^{10} m^{-1}$) and nb=10000

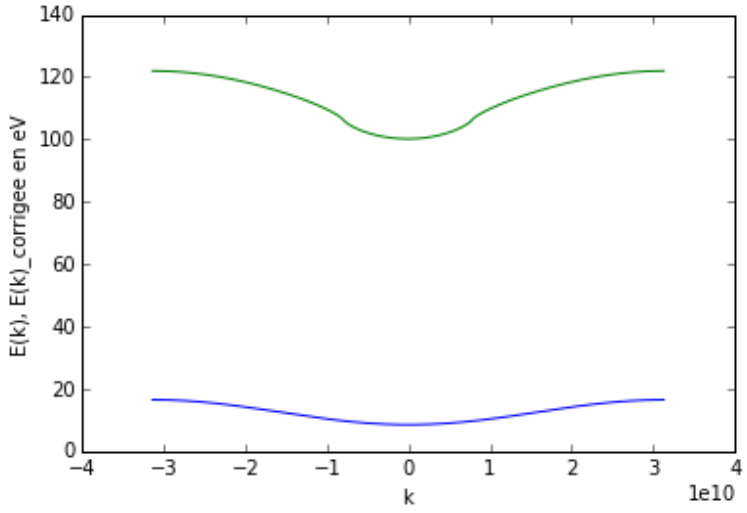

Figure 2.18: Energy computed for the one-dimensionnal lattice corrected by **Hartree-Fock's term**, for N=500, NB=250 ($k_F = 0.79.10^{10} m^{-1}$) and nb=10000

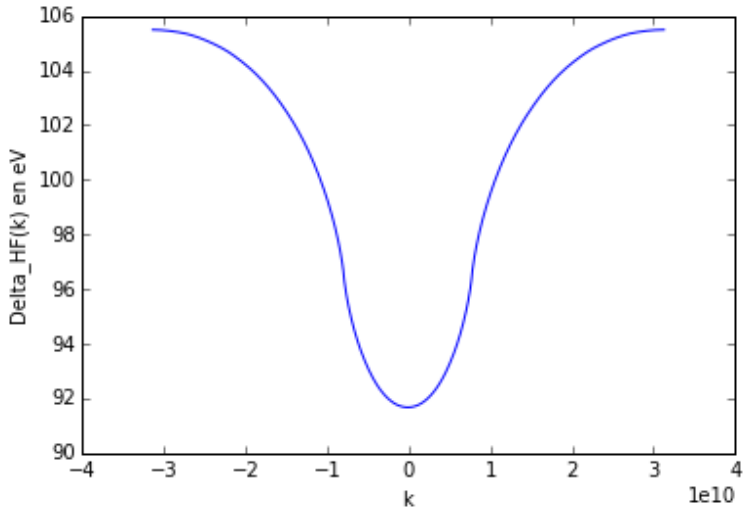

Figure 2.19: Correction of the energy by **Hartree-Fock's term** computed for the one-dimensionnal lattice , for N=500, NB=250 ($k_F = 0.79.10^{10} m^{-1}$) and nb=10000

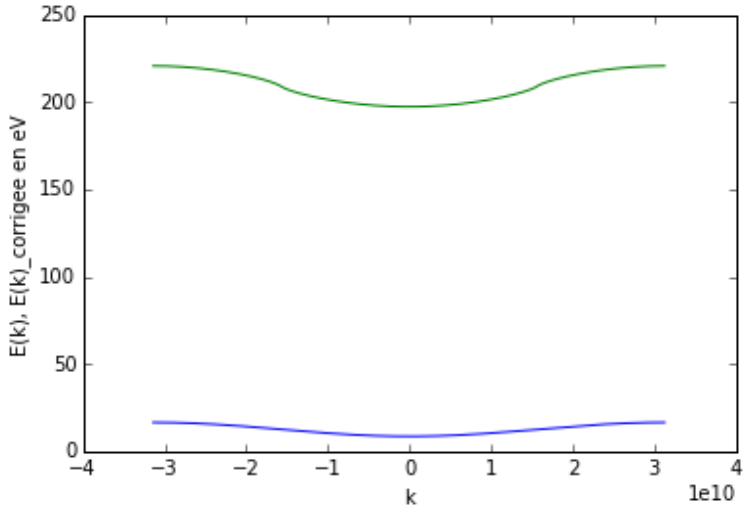

Figure 2.20: Energy computed for the one-dimensionnal lattice corrected by **Hartree-Fock's term**, for N=500, NB=500 ($k_F = 1.57.10^{10} m^{-1}$) and nb=10000

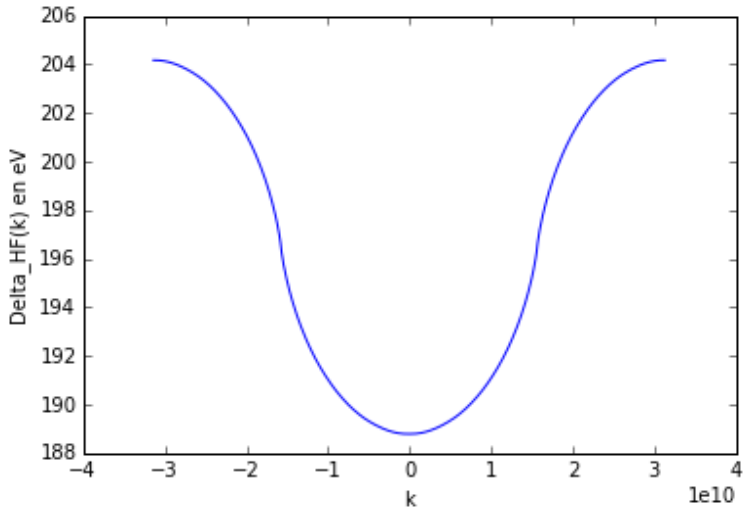

Figure 2.21: Correction of the energy by **Hartree-Fock's term** computed for the one-dimensionnal lattice , for N=500, NB=500 ($k_F = 1.57.10^{10} m^{-1}$) and nb=10000

By chance, for low fillings, i.e. small values of NB, the correction of the energy due to Hartree-Fock has the same order of magnitude as the non-corrected energy, for the arbitrary values $E_0 = 13eV$, $t = 2eV$ that we took. Both corrected and non-corrected energy spectra are therefore comparable without renormalization !

In our model, **the exchange term** (the contribution of Fock's term) **is of order 10 eV** for reasonable fillings NB. When NB increases, the contribution due to Hartree's term increases far more rapidly than Fock's term becomes more and more negative, which makes the corrected energy spectrum far more higher than the non-corrected one. To give an idea, Hartree's term reaches about 200 eV at half filling, while Fock's term is only of order 30 eV for the same value of NB ! The two separated previous parts meant to analyse separately these two contributions, which behave quite differently when NB changes.

2.2.3 How screening modulates the Hartree-Fock effect previously computed

We saw that the correction of the energy computed thanks to the Hartree-Fock was becoming much larger than the energy itself when the number of electrons in the system increases. In fact, **we have so far overestimated the effect of the repulsion between electrons**. Indeed, when there are many electrons in the system, it becomes necessary to take **screening** into account, by replacing the Coulomb potential with a Yukawa potential with an adequate screening length. Indeed, the repulsive potential between two electrons isn't a Coulomb potential anymore, because of the distributions of charges of all the other surrounding electrons. Because of the presence of other electrons, the effective potential, solution of Poisson equation, is :

$$V(\vec{r}) = \frac{q_e}{4\pi\epsilon_0}\frac{e^{-\frac{r}{\lambda}}}{r} \tag{2.88}$$

$\lambda = \lambda(NB)$ is called the screening length and depends on the total number of electrons in the system. By definition, screening becomes more and more significant when the number of electrons increases, therefore we expect $\lambda(NB)$ to decrease when NB increases. On the contrary, when $\lambda \longrightarrow +\infty$, we find the Coulomb potential again.

Screening effects make the repulsive potential decrease much more swiftly than in the case of two isolated repulsive charges. The caracteristic length of this decrease is λ : for $r \geq \lambda$, two electrons barely "see" each other in terms of potential. In a metal, this screening length is of order $1Ang$, the caracteristic size of an atom. This is why it is a good approximation to neglect electron-electron interactions in some materials, and in particular in most metals.

λ is related to the Thomas-Fermi wave-vector k_0 :

$$k_0^2 = 4\pi e^2 \frac{dn_0}{d\mu} = \frac{q_e^2}{\epsilon_0}\frac{dn_0}{d\mu} \tag{2.89}$$

where n_0 is the means number of electrons per unit volume and μ is the chemical potential. For a free electron gas, $\frac{dn_0}{d\mu} = \rho(\epsilon_F)$ is exactly the density of states at the Fermi level. I used this approximation to estimate iteratively λ, even if had some troubles to define properly a screening length in my one-dimensional problem (the quantum wave vectors have only one component $k = k_x$).

This formula comes from the Thomas-Fermi's method used to estimate screening. It is not the only method : Lindhard also proposed an alternative and more general method.

The code I developped allows to replace very easily the Coulomb potential by a screened Coulomb potential. I have computed the best value of λ to describe this 1D lattice, by an auto-coherent calculation. The initial value of λ is computed with the density of states at the Fermi level derived from the tight-binding energy spectrum. The corrected energy spectrum is then computed, and the DOS at the Fermi level changes. λ is updated, and we compute the correction of the previous energy spectrum with the new screened Coulomb potential. As $\rho(\epsilon_F) \sim \frac{1}{(\frac{d\epsilon}{dk})(k=k_F)}$, k_0 should increase at each iteration if we begin with a low screened Coulomb potential. Indeed, as we previously saw, Hartree-Fock with a potential in $\frac{1}{r}$ leads to a discontinuity in the energy spectrum, the slope becoming infinite at the Fermi wave-vector. **The goal of sreening is to smooth the energy band at** $k = k_F$, lowering the slope and making it finite. Therefore, $\lambda = \frac{1}{k_0}$ should decrease with the number of iterations and converge towards a finite value λ_{lim}.

The limit value λ_{lim} should be such that :

$$\lambda_{lim} < \lambda_c \tag{2.90}$$

where $\lambda_c = \lambda_c(NB)$ is the critical value such that : for $\theta > \lambda_c$, the screened Coulomb potential $\frac{q_e}{4\pi\epsilon_0}\frac{e^{-\frac{r}{\theta}}}{r}$ leads to a corrected energy spectrum **with a discontinuity** at the Fermi level, whereas for $\theta < \lambda_c$, the screened potential leads a continous Fermi velocity over the whole spectrum.

For instance, I found $\lambda_c \sim 5a$ for $N = 200$ and $NB = 100$. As for the optimal values of λ for a given NB, namely the limit value of the auto-coherent method, I found the following results :

$$\lambda_{lim}(NB = 40) \sim 0.87a \tag{2.91}$$

$$\lambda_{lim}(NB = 100) \sim 0.49a \tag{2.92}$$

$$\lambda_{lim}(NB = 200) \sim 0.27a \tag{2.93}$$

$$\lambda_{lim}(NB = 300) \sim 0.14a \tag{2.94}$$

As expected, the optimal value of $\lambda(NB)$ decreases when NB increases : **the effect of screening increases with the total number of electrons in the system**. The screening length found is similar to a metallic screening length, with a caracteristic length more little than the distance between two neighbouring sites. We notice that only 3 to 5 iterations were enough to reach the optimal value of lambda, whatever the initial condition λ_{in}.

The following graphs show how screening smoothes iteratively the derivative of the energy $k \longmapsto (\frac{d\epsilon}{dk})(k)$ for $N = 200$ and $NB = 202$. We show, for 3 iterations of the auto-coherent method, the corrected band structure (in green), and its derivative in the following graph.

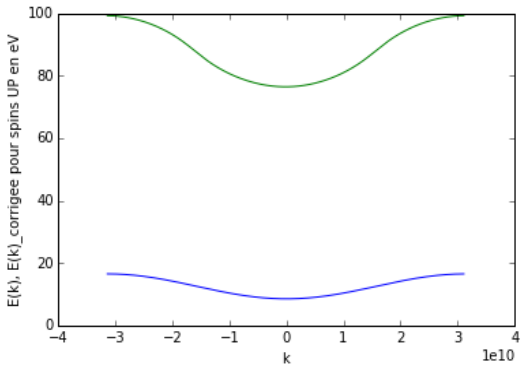

Figure 2.22: Energy band of the 1D lattice corrected with a screened Hartree-Fock potential, for N=200, NB=202, $\lambda = 5a$ (Iteration 1)

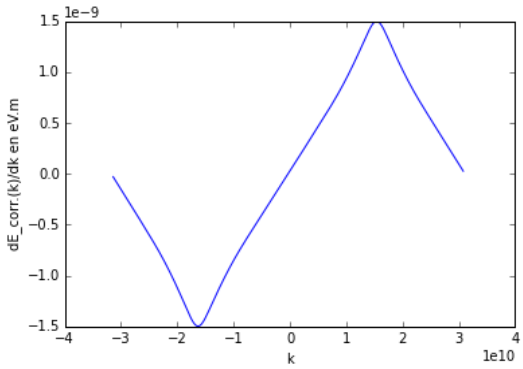

Figure 2.23: Derivative of the energy correction computed with a screened Hartree-Fock potential for the 1D lattice, for N=200, NB=202, $\lambda = 5a$ (Iteration 1)

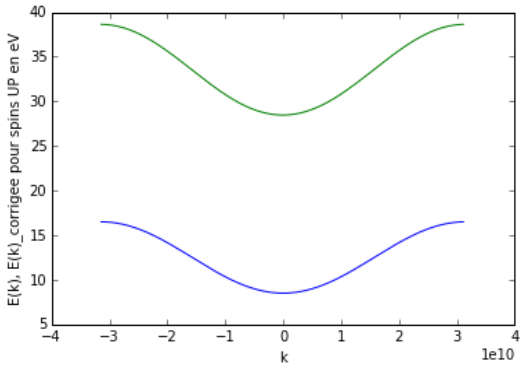

Figure 2.24: Energy band of the 1D lattice corrected with a screened Hartree-Fock potential, for N=200, NB=202, $\lambda = 0.5a$ (Iteration 2)

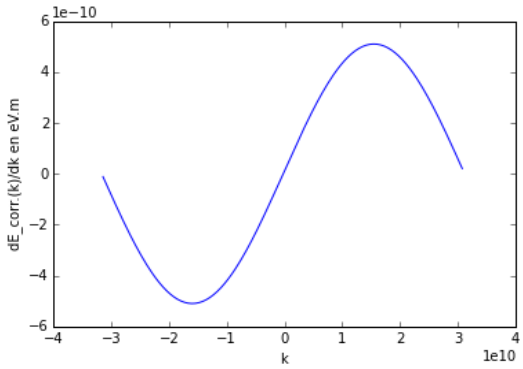

Figure 2.25: Derivative of the energy correction computed with a screened Hartree-Fock potential for the 1D lattice, for N=200, NB=202, $\lambda = 0.5a$ (Iteration 2)

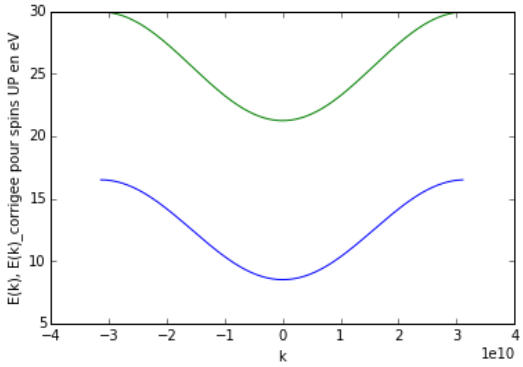

Figure 2.26: Energy band of the 1D lattice corrected with a screened Hartree-Fock potential, for N=200, NB=202, $\lambda = 0.29a$ (Iteration 3)

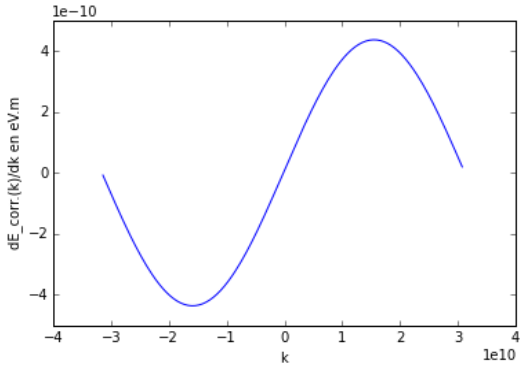

Figure 2.27: Derivative of the energy correction computed with a screened Hartree-Fock potential for the 1D lattice, for N=200, NB=202, $\lambda = 0.29a$ (Iteration 3)

Analysis of the results :

Screening Hartree-Fock enables, as we intended, to smooth the corrected energy spectrum. The limit λ_{lim} of the auto-coherent process is always smaller than λ_c, and makes therefore the Fermi velocity finite and continuous over the whole spectrum. Another effect which prooves that **a screened version of Hartree-Fock is more realistic** than Hartree-Fock without screening is that the value of the correction lowers, making the corrected energy band and the original band closer, of the same order of magnitude and much more comparable even for significant fillings.

2.2.4 Proof of a phase transition at a finite temperature in the 1D lattice, due to Hartree-Fock

The code I developped enables to estimate the spin-polarization of the correction to the energy for any polarized filling. It is therefore possible to compute the energy associated to a configuration with a major part of all the electrons having the same spin. For instance, the energy of a ferromagnetic or an antiferromagnetic configuration, with only spins UP or only spins DOWN, may be lower than the energy for a non-magnetic filling at low temperature. Indeed, we have taken interactions into account thanks to Hartree-Fock, and specially the exchange interaction. We could therefore expect that **the system orders at T=0K**, with a macroscopic magnetization leading to an equilibrium and a minimal energy. The following graphs shows the evolution of the total energy (the sum of the energies of all the electrons), when there is a fixed number of electrons in the system but a macroscopic magnetization M. That is to say, we compute the energy of each configuration ($N_{UP} = \frac{N}{2} + \frac{M}{2}, N_{DOWN} = \frac{N}{2} - \frac{M}{2}$). We use, of course, the energy corrected by Hartree-Fock.

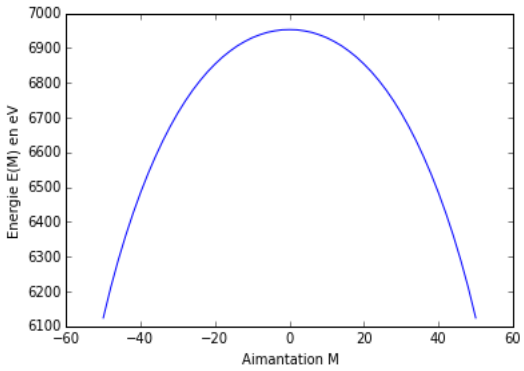

Figure 2.28: Energy of a configuration in relation to the global magnetic moment M, at T=0 K, for N=50 and NB=50 fixed, for the energy spectrum corrected by Hartree-Fock

We see that the ferromagnetic configuration, with all the spins UP, and the antiferromagnetic configuration, are the more stable at zero temperature ! This isn't that much surprising as Hartree-Fock favors the configurations with aligned spins. In fact, it can be prooven rigourously : consider a situation A with all spins aligned in the same sense UP and a situation B with all spins aligned UP except one, which is DOWN , lets call it the k^{th}. Therefore the correction to the energy of the k^{th} due to Fock's term is zero because $\forall j, \delta_{\sigma_j,\sigma_k} = 0$. In the first case the correction to the energy of the k^{th} electron was negative, because of the contribution of all the other electrons, which had same spin. Therefore the energy of the first configuration is lower : $E(A) < E(B)$. Therefore the ferromagnetic (or antiferromagnetic) state is stable at zero temperature.

When the temperature increases, the stable configuration minimizes $F = E - TS$, and not only the energy anymore. We expect the entropy to become the most important when the temperature grows sufficiently, favoring disordered configurations, with a global $M = 0$, over ordered configurations. The trend of $M \longmapsto F(M)$ at high temperature would look like the following graph, which is the energy in function of the magnetisation for the non-corrected tight-binding energy spectrum (for which $M = 0$ is the stable configuration) :

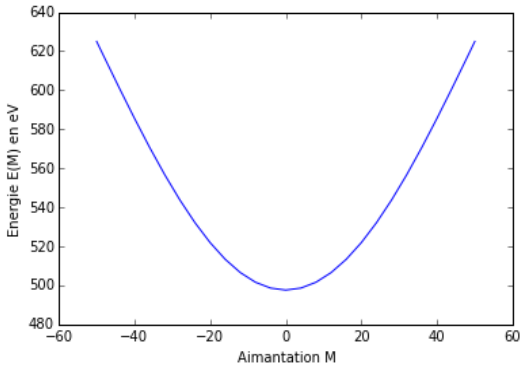

Figure 2.29: Energy of a configuration in relation to the global magnetic moment M, at T=0 K, for N=50 and NB=50 fixed, for the tigth-binding energy spectrum

To transform from the first to the second graph, when the temperature increases, implies a phase transition at a critical temperature T_c : for $T < T_c$, the stable configurations are configurations with a macroscopic magnetisation $M \neq 0$, while for $T > T_c$, the only stable configuration is $M = 0$. According to the exact type of transition, some metastables states with $M \neq 0$ can remain for $T > T_c$. Whether the magnetisation goes continuously form a macroscopic value to 0 also depends on the dynamics of the transition, a problem I haven't studied yet.

Chapter 3

Conclusion

This very interesting project could easily have been a subject for a six-month internship. We have showed that it was worth studying a one-dimensional lattice to see how the interactions modify the band structure. We also were able to estimate the screening length in that model and to detect a phase transition. We notice that this phase transition happens for a system mainly, but not strictly one-dimensional, as we have considered Coulomb interactions, and wave-functions, in 3 dimensions. This phase transition for a one-dimensional chain of atoms, that we see in a three dimensional space, doesn't contradict Mermin and Wagner's theorem, which states that there is no possible phase transition in a strictly one-dimensional system. It would be worth studying in more detail this phase transition that we have predicted, and to estimate the critical temperature or some critical exponents for instance, to see if it is a first order or second order phase transition. In two dimensions, I hadn't time to look at the energy as a function of magnetisation, but we can predict a similar ferromagnetic or antiferromagnetic behavior at zero temperature, due to Hartree-Fock's potential. As we have seen the two-dimensional lattice within a three dimensional space, this wouldn't contradict Mermin and Wagner's theorem either.

The final goal was to apply this method and the intuition we developed for one and two dimensional regular lattices, to graphene and carbon nanotubes, to derive the correction of the band structure corrected with Hartree-Fock, to study magnetic properties, and also to estimate a screening length *ab initio*. Unfortunately, I haven't results to present here, but I am still working on it and I hope to have some interesting graphs soon.

In this project, I have faced difficulties many times. I had to think which method was going to fit the best to a given problem, like estimating a complicated integral. I have learned numerous useful mathematical techniques. In also improved my skills as far as numerical tools are concerned : I coded in Python, a language I didn't know before this project. I was also introduced to GitHub, which helped me save my project iteratively, being able to go back to a previous version. My codes, my report and more graphs can be found at the adress https://github.com/rbenda/Projet3A/. I hope to continue my project on my own and presenting regularly my results to Michel Ferrero and Silke Biermann. I would like to thank both of them for their help, their kindness and their availability during the whole semester to meet either at the College de France or at the CPHT.

I am very curious about the prospects to estimate the importance of the electron-electron interactions in graphene and carbon nanotubes numerically by modifying easily in the code physical parameters like the type of nanotube (chiral, armchair, zigzag), the radius. Even if some future possible will have to be confronted to the experiments, it may encourage the development of ab initio calculations and numerical calculations based on simple but solid physical models.

Chapter 4

Annexes

4.1 Annex 1 : Density of states calulations for the two dimensional lattice

$$N_<^{2D}(E) = \int\int dm_1 dm_2 = \frac{(Na)^2}{(2\pi)^2}\int\int_{\{\vec{k}\in 1.B.Z.|E_{\vec{k}}\leq E\}} dk_x dk_y \tag{4.1}$$

$$= \frac{N^2}{(2\pi)^2}\int\int_{\{\begin{pmatrix}x\\y\end{pmatrix}\in[-\pi,\pi[^2|cos(x)+cos(y)\geq\alpha(E)\}} dxdy \tag{4.2}$$

where $\alpha(E) = \frac{E_0-t_0-E}{2t} \in [-2,2]$.

$$N_<^{2D}(E) = (\frac{N}{2\pi})^2\int_{-\pi}^{\pi}(\int_{\{z|cos(z)\geq\alpha(E)-cos(y)\}} dz)dy \tag{4.3}$$

$$N_<^{2D}(E) = (\frac{N}{2\pi})^2\int_{-\pi}^{\pi}(2\pi 1_{\alpha(E)+1\leq cos(y)} + 2Arccos(\alpha(E)-cos(y))1_{\alpha(E)-1\leq cos(y)\leq\alpha(E)+1})dy \tag{4.4}$$

$$\alpha(E)\leq 0 \Rightarrow N_<^{2D}(E) = (\frac{N}{\pi})^2[4\pi Arccos(\alpha(E)+1)+2*2\int_{Arccos(\alpha(E)+1)}^{\pi} Arccos(\alpha(E)-cos(y))dy] \tag{4.5}$$

because $y \longmapsto Arccos(\alpha(E)-cos(y))$ is an even function.

$$\alpha(E)\geq 0 \Rightarrow N_<^{2D}(E) = \frac{N^2}{(2\pi)^2}2\int_{-Arccos(\alpha(E)-1)}^{Arccos(\alpha(E)-1)} Arccos(\alpha(E)-cos(y))dy \tag{4.6}$$

Thanks to a change of variable $z = cos(y)$, we finally obtain that :

$$E\geq E_0-t_0 \Rightarrow \alpha(E)\leq 0 \Rightarrow N_<^{2D}(E) = \frac{N^2}{\pi^2}(\pi Arccos(\alpha(E)+1) + \int_{-1}^{\alpha(E)+1}\frac{Arccos(\alpha(E)-z)}{\sqrt{1-z^2}}dz) \tag{4.7}$$

$$E\leq E_0-t_0 \Rightarrow \alpha(E)\geq 0 \Rightarrow N_<^{2D}(E) = \frac{N^2}{2\pi^2}\int_{\alpha(E)-1}^{1}\frac{Arccos(\alpha(E)-z)}{\sqrt{1-z^2}}dz \tag{4.8}$$

4.2 Annex 2 : Density of states calulations for the three dimensional lattice

$$N_{3D}(E) = (\frac{N}{2\pi})^3 \int_{-\pi}^{\pi} I_x dx \tag{4.9}$$

$$\alpha(E) - cos(x) \geq 2 \longrightarrow I_x = 0 \tag{4.10}$$

$$\alpha(E) - cos(x) \leq -2 \longrightarrow I_x = (2\pi)^2 \tag{4.11}$$

$$\alpha(E) - cos(x) \in [-2,2] \Rightarrow I_x = \int\int_{cos(y)+cos(z)\geq\alpha(E+2tcos(x))} dydz = (\frac{2\pi}{N})^2 N_<^{2D}(E + 2tcos(x)) \tag{4.12}$$

To sum up these three distinctions :

$$N_<^{3D}(E) = (\frac{N}{2\pi})^3 [\int_{-\pi}^{\pi} (2\pi)^2 1_{cos(x)\geq\alpha(E)+2} dx + \int_{-\pi}^{\pi} (\frac{2\pi}{N})^2 N_<^{2D}(E + 2tcos(x)) 1_{-2\leq\alpha(E)-cos(x)\leq 2} dx] \tag{4.13}$$

$$\alpha(E) \geq -1 \Rightarrow \int_{-\pi}^{\pi} 1_{cos(x)\geq\alpha(E)+2} dx = 0 \tag{4.14}$$

$$\alpha(E) \leq -1 \Rightarrow \alpha(E) + 2 \in [-1,1] \Rightarrow \int_{-\pi}^{\pi} 1_{cos(x)\geq cos(Arccos(\alpha(E)+2))} dx = 2Arccos(\alpha(E) + 2) \tag{4.15}$$

Therefore

$$N_<^{3D}(E) = 2\frac{N^3}{2\pi} 1_{\alpha(E)\leq -1} Arccos(\alpha(E) + 2) + \frac{N}{2\pi} \int_{-\pi}^{\pi} N_<^{2D}(E + 2tcos(x)) 1_{-2\leq\alpha(E)-cos(x)\leq 2} dx \tag{4.16}$$

Let's precise the second term denoted by $T(E)$:

$$\alpha(E) \in [-1,1] \Rightarrow \forall x \in [-\pi,\pi], 1_{-2\leq\alpha(E)-cos(x)\leq 2} = 1 \tag{4.17}$$

$$\alpha(E) \leq -1 \Rightarrow \forall x \in [-\pi,\pi], 1_{-2\leq\alpha(E)-cos(x)\leq 2} =_{-2\leq\alpha(E)-cos(x)=} 1_{cos(x)\leq cos(Arccos(\alpha(E)+2))} \tag{4.18}$$

$$\alpha(E) \geq 1 \Rightarrow \forall x \in [-\pi,\pi], 1_{-2\leq\alpha(E)-cos(x)\leq 2} = 1_{\alpha(E)\leq cos(x)+2} = 1_{cos(Arccos(\alpha(E)-2))\leq cos(x)} \tag{4.19}$$

which gives for this second term :

$$\alpha(E) \in [-1,1] \Rightarrow T(E) = \frac{N}{2\pi} \int_{-\pi}^{\pi} N_<^{2D}(E + 2tcos(x)) dx \tag{4.20}$$

$$\alpha(E) \leq -1 \Rightarrow T(E) = \frac{N}{2\pi} 2 \int_{Arccos(\alpha(E)+2)}^{\pi} N_<^{2D}(E + 2tcos(x)) dx \tag{4.21}$$

$$\alpha(E) \geq 1 \Rightarrow T(E) = \frac{N}{2\pi} \int_{-Arccos(\alpha(E)-2)}^{Arccos(\alpha(E)-2)} N_<^{2D}(E + 2tcos(x)) dx \tag{4.22}$$

Therefore

$$\alpha(E) \leq -1 \Rightarrow N_<^{3D}(E) = \frac{N^3}{\pi} Arccos(\alpha(E) + 2) + \frac{N}{\pi} \int_{Arccos(\alpha(E)+2)}^{\pi} N_<^{2D}(E + 2tcos(x)) dx \tag{4.23}$$

$$\alpha(E) \in [-1,1] \Rightarrow N_<^{3D}(E) = \frac{N}{\pi} \int_0^{\pi} N_<^{2D}(E + 2tcos(x)) dx \tag{4.24}$$

$$= \frac{N}{\pi} (\int_0^{Arccos(\alpha(E))} N_<^{2D}(E + 2tcos(x)) dx + \int_{Arccos(\alpha(E))}^{\pi} N_<^{2D}(E + 2tcos(x)) dx) \tag{4.25}$$

$$\alpha(E) \geq 1 \Rightarrow N_<^{3D}(E) = \frac{N}{\pi} \int_0^{Arccos(\alpha(E)-2)} N_<^{2D}(E + 2tcos(x)) dx \tag{4.26}$$

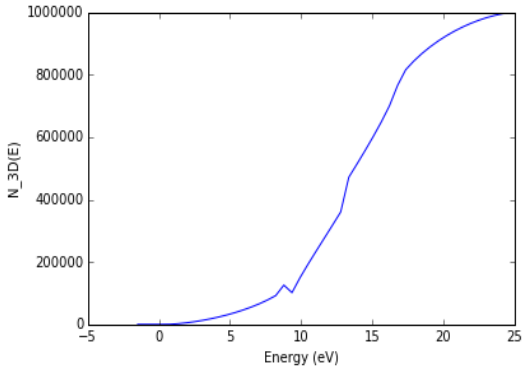

Figure 4.1: Number of energy states in a three dimensional lattice

4.3 Annex 3 : Exact formula for the density of states in a three dimensionnal lattice

$\forall E \geq E_0 - t_0 + 2t$,

$$D^{3D}(E) = \frac{N}{\pi} \int_{Arccos(\frac{E_0 - t_0 + 4t - E}{2t})}^{\pi} D^{2D}(E + 2tcos(x))dx \tag{4.27}$$

$\forall E \leq E_0 - t_0 - 2t$

$$D^{3D}(E) = \frac{N}{\pi} \int_{0}^{Arccos(\frac{E_0 - t_0 - 4t - E}{2t})} D^{2D}(E + 2tcos(x))dx \tag{4.28}$$

For $E \in]E_0 - t_0 - 2t, E_0 - t_0 + 2t[$, if we take formally the derivative of :

$$\int_{0}^{Arccos(\alpha(E))^-} N_<^{2D}(E + 2tcos(x))dx; \int_{Arccos(\alpha(E))^+}^{\pi} N_<^{2D}(E + 2tcos(x))dx \tag{4.29}$$

we obtain :

$$D^{3D}(E) = \frac{N}{\pi}[\int_{0}^{Arccos(\frac{E_0 - t_0 - E}{2t})} D^{2D}(E + 2tcos(x))dx + \int_{Arccos(\frac{E_0 - t_0 - E}{2t})}^{\pi} D^{2D}(E + 2tcos(x))dx] \tag{4.30}$$

$$+ \frac{N}{2\pi t} \frac{lim_{E \longrightarrow (E_0 - t_0))^+} N_<^{2D}(E) - lim_{E \longrightarrow (E_0 - t_0))^-} N_<^{2D}(E)}{\sqrt{1 - \alpha(E)^2}} \tag{4.31}$$

The problem is that $N_<^{2D}(E + 2tcos(x))$ is not continuous at $x = Arccos(\alpha(E))$ because $N_<^{2D}(.)$ is not continuous at $E_0 - t_0$. We cut the integral because D^{2D} goes towards $+\infty$ at $E_0 - t_0$.

Formally, we obtain :

$$E \in]E_0 - t_0 - 2t, E_0 - t_0 + 2t[\Rightarrow D^{3D}(E) = \frac{N}{\pi} \int_{0}^{\pi} D^{2D}(E + 2tcos(x))dx + \frac{N}{2\pi t} \frac{lim_{E \longrightarrow (E_0 - t_0))^-} N_<^{2D}(E)}{\sqrt{1 - \alpha(E)^2}} \tag{4.32}$$

having used the expression 1.13 for the limits of $N^{2D}(E)$.

The previous expressions of $D^{3D}(E)$ give the following trend :

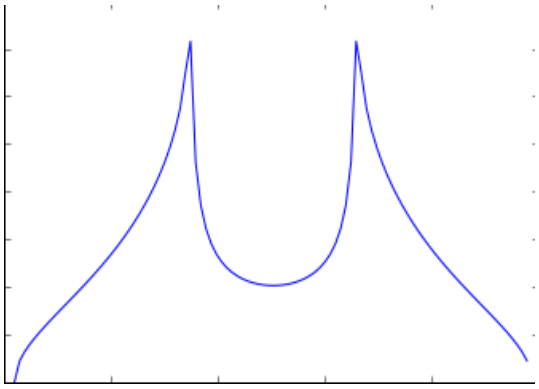

Figure 4.2: Density of states in a three dimensional lattice

The analytical expressions we found, related to the density of states for a two dimensionnal lattice, seem correct for $E < E_0 - t_0 - 2t$ and $E > E_0 - t_0 + 2t$, but not in-between.
This time, contrary to the one and two dimensionnal lattice, the density is continuous.

4.4 Annex 4 : Details of the computation of the energy correction due to Hartree-Fock for free electrons

In the case $\vec{k} = k\vec{e_z}$, 2.15 becomes :

$$\Delta(\vec{k}) = \frac{4\pi e^2}{(2\pi)^3} 2\pi \int_0^{k_F} \int_0^{\pi} \int_0^{2\pi} \frac{r'^2 sin(\theta')}{k^2 + r'^2 - 2r'kcos(\theta')} dr' d\theta' d\phi' = \frac{4\pi e^2}{(2\pi)^3} 2\pi \int_0^{k_F} r^2 (\int_0^{\pi} \frac{sin(\theta)}{k^2 + r^2 - 2rkcos(\theta)} d\theta) dr \tag{4.33}$$

$$\Delta(\vec{k}) = \frac{4\pi e^2}{(2\pi)^3} \int_0^{k_F} \int_0^{\pi} r^2 \frac{1}{2rk} [ln|k^2 + r^2 - 2rkcos(\theta)|]_0^{\pi} dr' = \frac{4\pi e^2}{(2\pi)^3} \frac{2\pi}{k} \int_0^{k_F} r \ln|\frac{k+r}{k-r}| dr \tag{4.34}$$

Now, we notice that :

$$\frac{d}{dr}((k^2 - r^2) \ln|\frac{k+r}{k-r}|) = -2r \ln|\frac{k+r}{k-r}| + 2k \tag{4.35}$$

therefore

$$\frac{d}{dr}(-\frac{1}{2}[(k^2 - r^2) \ln|\frac{k+r}{k-r}| - 2kr]) = r \ln|\frac{k+r}{k-r}| \tag{4.36}$$

Using this primitive in 4.34, we finally find :

$$\Delta(\vec{k}) = \frac{4\pi e^2}{(2\pi)^3} (-\frac{\pi}{k} k_F^2 ((\frac{k}{k_F})^2 - 1) ln|\frac{1 + \frac{k}{k_F}}{1 - \frac{k}{k_F}}| + 2\pi k_F) \tag{4.37}$$

$$\Longrightarrow \Delta(\vec{k}) = \frac{2e^2}{\pi} k_F (\frac{1}{2} + \frac{1 - (\frac{k}{k_F})^2}{4\frac{k}{k_F}} ln|\frac{1 + \frac{k}{k_F}}{1 - \frac{k}{k_F}}|) =^{def} \frac{2e^2}{\pi} k_F G(x) \tag{4.38}$$

where $x = \frac{k}{k_F}$ and

$$G(x) = \frac{1}{2} + \frac{1 - x^2}{4x} \ln|\frac{1+x}{1-x}| \tag{4.39}$$

At a fixed k, the correction is bigger when k_F decreases (that is to say the total number of particle decreases), remaining greater than k :

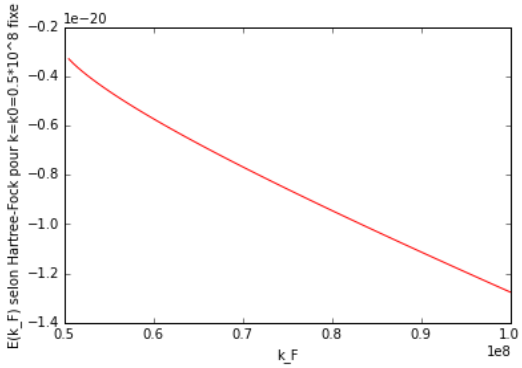

Figure 4.3: Hartree-Fock energy at $k = k_0$ fixed and variable k_F

4.5 Annex 5 : Computation of the energy correction for free electrons using Monte-Carlo techniques

The computation of the integral $\Delta(\vec{k})$ with a Monte-Carlo method gives the following result :

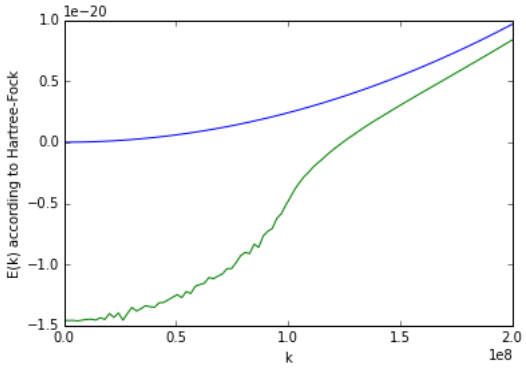

Figure 4.4: Correction the energy of free electrons estimated by Hartree-Fock's term for $k_F = 10^8 m^{-1}$, computed with a Monte-Carlo approach : n=1000000

The method consists to use random variables K_1, K_2, K_3 uniform over the intervals $[k_x - k_F, k_x + k_F]$, $[k_y - k_F, k_y + k_F]$ and $[k_z - k_F, k_z + k_F]$ respectively. Thus (K_1, K_2, K_3) is a uniform random variable over the cube centered in $\vec{k}$ and of side length k_F. The volume of this cube is therefore $(2k_F)^3$. Let's denote the integrand $f(\vec{k'}) = \frac{1}{|\vec{k'} - \vec{k}|^2}$ and n the number of such independent random variables $\vec{K}^i =^{def} (K_1^i, K_2^i, K_3^i)$. Monte-Carlo techniques imply that

$$V_n =^{def} \frac{1}{n} \sum_{i=1}^{n} 1_{\vec{K}^i \in B(\vec{k}, k_F)} f(\vec{K}^i) \longrightarrow^{p.s}_{n \longrightarrow \infty} E(1_{\vec{K} \in B(\vec{k}, k_F)} f(\vec{K})) \tag{4.40}$$

where :

$$E(1_{\vec{K} \in B(\vec{k}, k_F)} f(\vec{K})) = \frac{1}{(2k_F)^3} \int_{-d}^{d} \int_{-d}^{d} \int_{-d}^{d} 1_{\begin{pmatrix} x \\ y \\ z \end{pmatrix} \in B(\vec{k}, k_F)} f(x, y, z) dx dy dz \tag{4.41}$$

because the density of the uniform random variable $\vec{K}$ is constant and equal to $\frac{1}{(2k_F)^3}$.

Therefore

$$\int\int\int_{\vec{k'} \in B(\vec{k}, k_F)} f(\vec{k'}) = \int\int\int_{\vec{k'} \in B(\vec{k}, k_F)} \frac{1}{|\vec{k'} - \vec{k}|^2} = (2k_F)^3 lim_{n \longrightarrow \infty} V_n \tag{4.42}$$

The results we obtain are shown above in the plot 4.5. The plot of the energy corrected by Hartree-Fock's term and estimated thanks to a Monte-Carlo approach is smoother for $k > k_F$ than for $k < k_F$. Indeed when $\vec{k}$ becomes greater than k_F in norm, there isn't singularity anymore in the integral, as $|\vec{k'} - \vec{k}| > 0$ for every $\vec{k'} \in B(\vec{k}, k_F)$.

Let's now compare these results with the exact expression of this triple integral, found by Ashcroft and Mermin :

$$\Delta(\vec{k}) = \frac{2e^2}{\pi} k_F G(\frac{k}{k_F}) \tag{4.43}$$

where $G(.)$ is the following function :

$$G(x) = \frac{1}{2} + \frac{1 - x^2}{4x} \ln |\frac{1 + x}{1 - x}| \tag{4.44}$$

The graph of the function $k \longmapsto G(\frac{k}{k_F})$ is given below (k_F being fixed at $10^8 m^{-1}$) :

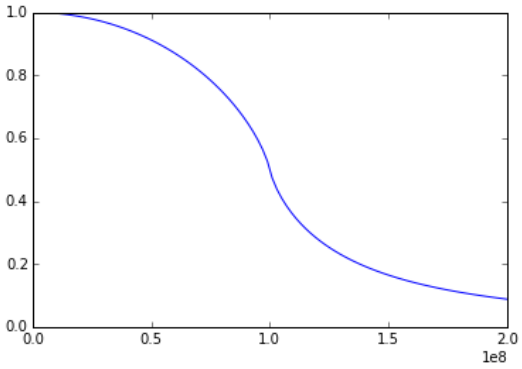

Figure 4.5: Function G

4.6 Annex 6 : Remarks and simplifications of the expression of the energy correction by Hartree-Fock for a 1D lattice

A little calculation, using that $k_n = \frac{2\pi}{Na} p_n$ (p_n being an integer) for a one-dimensionnal lattice, gives the following :

$$l = m \Rightarrow \Theta^n_{l,m} = N_e - N^{occ} = \frac{N_e}{2} \tag{4.45}$$

if (k_n, σ_n) is not an occupied state.

If $l \neq m$ and all the N possible states are occupied, each by two electrons with opposite spins, :

$$\Theta^n_{l,m} = N_e - \delta^{occ}_{k_n} + 1 \approx N_e = 2N^{occ} \tag{4.46}$$

because

$$\sum_{j=1,jocc.}^{N} e^{i\frac{2\pi}{N}(n-j)(m-l)} = e^{i\frac{2\pi}{N}n(m-l)} \sum_{j=1,jocc.}^{N} (e^{i\frac{2\pi}{N}(l-m))})^j = 0 \tag{4.47}$$

in this specific case.

Invariance by translation

We can simplify the expression 2.59 using the periodic boundary conditions. Let l_0 be an integer in $[1, N]$. Let's prove that

$$\sum_{m=1}^{N} I_{l_0,m} \Theta^n_{l_0,m} \tag{4.48}$$

does not depend on the integer l_0.

$$I_{l_0+1,m} = \int d\vec{r} \int d\vec{r'} \frac{|\psi_m(\vec{r'})|^2 |\psi_{l_0+1}(\vec{r})|^2}{|\vec{r} - \vec{r'}|} = \int d\vec{r} \int d\vec{r'} \frac{|\chi(\vec{r'} - ma\vec{e_x})|^2 |\chi(\vec{r} - (l_0+1)a\vec{e_x})|^2}{|\vec{r} - \vec{r'}|} \tag{4.49}$$

where $\chi(.)$ is the atomic orbital of the site at the origin of the lattice.

Thanks to the new variable $\vec{u} = \vec{r} - a\vec{e_x}$:

$$I_{l_0+1,m} = \int d\vec{u} \int d\vec{r'} \frac{|\chi(\vec{r'} - ma\vec{e_x})|^2 |\chi(\vec{u} - l_0 a\vec{e_x})|^2}{|\vec{u} - (\vec{r'} - a\vec{e_x})|} \tag{4.50}$$

and $\vec{v} = \vec{r'} - a\vec{e_x}$:

$$I_{l_0+1,m} = \int d\vec{u} \int d\vec{v} \frac{|\chi(\vec{v} - (m-1)a\vec{e_x})|^2 |\chi(\vec{u} - l_0 a\vec{e_x})|^2}{|\vec{u} - \vec{v}|} = \int d\vec{u} \int d\vec{v} \frac{|\psi_{m-1}(\vec{v})|^2 |\psi_{l_0}(\vec{u})|^2}{|\vec{u} - \vec{v}|} \tag{4.51}$$

We have proven that

$$I_{l_0+1,m} = I_{l_0,m-1} \tag{4.52}$$

Moreover

$$\Theta^n_{l_0+1,m} = (N^{occ} - \delta^{occ}_{k_n} - \sum_{j\neq n, jocc.} \delta_{\sigma_j,\sigma_n} e^{i(k_n-k_j)(m-l_0-1)a}) = \Theta^n_{l_0,m-1} \tag{4.53}$$

Therefore :

$$\sum_{m=1}^{N} I_{l_0+1,m}\Theta^n_{l_0+1,m} = \sum_{m=1}^{N} I_{l_0,m-1}\Theta^n_{l_0,m-1} \tag{4.54}$$

The Periodic Boundary Conditions give :

$$I_{l_0,0} = \int d\vec{r} \int d\vec{r'} \frac{|\psi_0(\vec{r'})|^2 |\psi_{l_0}(\vec{r})|^2}{|\vec{r}-\vec{r'}|} = \int d\vec{r} \int d\vec{r'} \frac{|\psi_N(\vec{r'})|^2 |\psi_{l_0}(\vec{r})|^2}{|\vec{r}-\vec{r'}|} = I_{l_0,N} \tag{4.55}$$

because the N^{th} atom of the lattice also is the atom labelled by 0 in the PBC approximation.

$$\Theta^n_{l_0,N} = (N_e - \delta^{occ}_{k_n} - \sum_{j\neq n, jocc.} \delta_{\sigma_j,\sigma_n} e^{i(k_n-k_j)(N-l_0)a}) = (N_e - \delta^{occ}_{k_n} - \sum_{j=1, j\neq n, jocc.} \delta_{\sigma_j,\sigma_n} e^{-i(k_n-k_j)l_0 a}) \tag{4.56}$$

because $(k_n - k_j)Na = \frac{2\pi(p_n-p_j)}{Na} Na = 2\pi(p_n - p_j)$ where p_n and p_j are integers.

In the end, 4.54 becomes :

$$\sum_{m=1}^{N} I_{l_0+1,m}\Theta^n_{l_0+1,m} = \sum_{m=1}^{N} I_{l_0,m}\Theta^n_{l_0,m} \tag{4.57}$$

4.7 Annex 7 : Implementation of the Metropolis algorithm to estimate the integrals involved in the energy correction for a 1D lattice

My first idea was to find a simple way to compute the integrals $I_{l,m}$, as we need them to estimate the global correction to the energy. I used Monte-Carlo methods. Nevertheless, because of the divergence of the integrand at some points, the convergence speed wasn't good enough. M. Ferrero then told me about **Metropolis algorithm**.

We write the correction due to Hartree-Fock's term in the following way :

$$\Delta(E_{k_n}) = e^2 \sum_{m=1}^{N} \int d\vec{r} \int d\vec{r'} \frac{(N_e - \delta_{k_n}^{occ} - \sum_{j \neq n, jocc.} \delta_{\sigma_j,\sigma_n} e^{i(k_n - k_j)ma})}{|\vec{r} - \vec{r'}|} \frac{|\psi_0(\vec{r})|^2 |\psi_m(\vec{r'})|^2}{N} \tag{4.58}$$

Let denote

$$\pi(m, \vec{r}, \vec{r'}) = \frac{|\psi_0(\vec{r})|^2 |\psi_m(\vec{r'})|^2}{N} > 0 \tag{4.59}$$

and

$$F(m, \vec{r}, \vec{r'}) = \frac{\Theta_{0,m}^{1D}}{|\vec{r} - \vec{r'}|} = \frac{(N_e - \delta_{k_n}^{occ} - \sum_{j \neq n, jocc.} \delta_{\sigma_j,\sigma_n} e^{i(k_n - k_j)ma})}{|\vec{r} - \vec{r'}|} \tag{4.60}$$

We notice that $\pi(.)$ is a density of probability :

$$\int \int d\vec{r} d\vec{r'} \sum_m \pi(m, \vec{r}, \vec{r'}) = 1 \tag{4.61}$$

Indeed, $\psi_m(.)$ is an atomic orbital and is therefore normalised :

$$\int d\vec{r'} |\psi_m(\vec{r'})|^2 = 1 \tag{4.62}$$

We want to compute

$$\frac{\Delta(E_{k_n})}{e^2} = \sum_m \int \int d\vec{r} d\vec{r'} F(m, \vec{r}, \vec{r'}) \pi(m, \vec{r}, \vec{r'}) \tag{4.63}$$

We use the **ergodic theorem** : if $(X_n)_{n \geq 0}$ is a recurrent, irreductible and positive Markov chain ; $\pi(.)$ being its unique invariant probability measure :

$$\frac{1}{M} \sum_{i=1}^{M} F(X_i) \longrightarrow_{M \longrightarrow \infty} E_\pi(F) = \sum_m \int \int d\vec{r} d\vec{r'} F(m, \vec{r}, \vec{r'}) \pi(m, \vec{r}, \vec{r'}) \tag{4.64}$$

Let's give a hint to understand this theorem. When computing the means of the values of $F(.)$ over the Markov chain, we are somehow counting the number of points of the Markov chain close to x (given by the density $\pi(x) = lim_{n \longrightarrow +\infty} P(X_n = x)$), and multiplying it by the value of F there : $\pi(x)F(x)$. Then we sum over the contributions x. The closest the distribution of the points of the Markov chain is to the density $\pi(.)$, the better the approximation of the integral with the mean value is.

We see that the points x that will count the most to compute the integral are those with higher values of $\pi(x)$ (where the points of the Markov chain concentrate the more). In our case $\pi(m, \vec{r}, \vec{r'})$ is maximal for $\vec{r'}$ close to $ma\vec{e_x}$. Therefore the Markov chain will have with high probability a lot of points in the neighbouring of such values of $\vec{r'}$. This algorithm thus enables to focus on the points where the integrand becomes very big or even diverges. Such regions are much better explored than with a classic Monte-Carlo algorithm, where the random variables X_i are uniform over the whole space of integration.

Our goal is therfore to generate a Markov chain whose invariant probability measure is π, and the means of the values of $F(.)$ along the trajectory will give us an approximation of the correction to the energy.

Construction of the Markov chain :

Let $W_{x\longrightarrow y}$ be the probability of transition from x to y :

$$W_{x\longrightarrow y} = P(X_{n+1} = y | X_n = x) \tag{4.65}$$

if $y \neq x$.
If $x = y$: $W_{x\longrightarrow x} = 1 - \sum_{y\neq x} W_{x\longrightarrow y}$.

We decompose $W_{x\longrightarrow y}$ as :

$$W_{x\longrightarrow y} = T_{x\longrightarrow y} A_{x\longrightarrow y} \tag{4.66}$$

where $A_{x\longrightarrow y}$ is the acceptation rate and $T_{x\longrightarrow y}$ the transition rate.

The transition matrix $T_{x\longrightarrow y}$ over the space of possible states E has to be irreductible and to satisfy :

$$\forall (x,y) \in E^2, T_{x\longrightarrow y} > 0 \Rightarrow T_{y\longrightarrow x} > 0 \tag{4.67}$$

As an acceptation rate, we can use :

$$A_{x\longrightarrow y} = h(\frac{\pi(y) T_{y\longrightarrow x}}{\pi(x) T_{x\longrightarrow y}}) \tag{4.68}$$

where $h :]0; +\infty[\longrightarrow]0, 1]$ is increasing and such that $h(u) = u h(\frac{1}{u})$. For instance, $h(u) = inf(1, u)$ or $h(u) = \frac{u}{1+u}$ are possible functions. **We choose** $h(u) = inf(1, u)$ **in the following calculations**. We also take a symetric transition rate : $T_{y\longrightarrow x} = T_{x\longrightarrow y}$, to simplify the previous expression.

The algorithm is the following :
Given X_n, we first choose Y according to the transition law $T_{X_n\longrightarrow Y}$.
We then choose a uniform random number U_{n+1} in $[0, 1]$:
If $U_{n+1} < A_{X_n\longrightarrow Y}$, then $X_{n+1} = Y$.
Otherwise : $X_{n+1} = X_n$.

The state Y is accepted with probability $A_{X_n\longrightarrow Y}$, hence the name of "acceptation rate".

The theorem of Metropolis implies that the transition matrix $W_{x\longrightarrow y}$ is irreductible and reversible for the measure π :

$$\forall (x,y) \in E^2, \pi(y) W_{y\longrightarrow x} = \pi(x) W_{x\longrightarrow y} \tag{4.69}$$

Therefore $\pi(.)$ is its unique invariant measure.

As a transition rate, I choose :

$$T_{x\longrightarrow y} = P(X_{n+1} = y = (m', \vec{r_1}, \vec{r_1'}) | X_n = x = (m, \vec{r}, \vec{r'})) \tag{4.70}$$

such that :
- given $m = X_n[1]$, $l' = X_{n+1}[1]$ equals $m + 1$ with probability $\frac{1}{2}$ and $m - 1$ with probability $\frac{1}{2}$
- given $\vec{r}$, $\vec{r_1}$ is choosen uniformly in a cube centered in $\vec{r}$ and of tunable side length θ.
- given $\vec{r'}$, $\vec{r_1'}$ is choosen uniformly in a cube centered in $\vec{r'}$ and of tunable side length θ.

Thus we have $T_{x\longrightarrow y} = T_{y\longrightarrow x}$.

For a one-dimensional lattice, the equation 4.58 can be rewritten in the following way, if we take gaussian functions as localised orbitals ($\psi_l(r) = \chi(r - la)$ where $\chi(.)$ is the wave function of an atomic orbital) :

$$e^2 K \sum_{m=1}^{N} \int\int \frac{(N_e - \delta_{k_n}^{occ} - \sum_{j\neq n, jocc.} \delta_{\sigma_j,\sigma_n} e^{i(k_n - k_j)ma})}{\sqrt{(x_1 - x_2)^2 + (y_1 - y_2)^2 + (z_1 - z_2)^2}} \frac{e^{-2(\frac{x_1^2 + y_1^2 + z_1^2}{\delta^2})} e^{-2(\frac{(x_2 - ma)^2 + y_2^2 + z_2^2}{\delta^2})}}{N} d\vec{r_1} d\vec{r_2} \tag{4.71}$$

where K is a constant coming from the integration on the angular part of the atomic orbital wave function. So far we take a constant angular function to simplify the calculations.

Other type of functions, like lorentzians, are possible and also satisfy the **non-overlapping assumption** we used. After changing the origins of the two space integrations :

$$\frac{\Delta(E_{k_n})}{e^2} = a^5 K \sum_{m=1}^{N} \int\int \frac{(N_e - \delta_{k_n}^{occ} - \sum_{j\neq n, jocc.} \delta_{\sigma_j,\sigma_n} e^{i(k_n - k_j)ma})}{\sqrt{(x_1 - x_2 - m)^2 + (y_1 - y_2)^2 + (z_1 - z_2)^2}} \frac{e^{-2(\frac{x_1^2+y_1^2+z_1^2}{(\frac{\delta}{a})^2})} e^{-2(\frac{x_2^2+y_2^2+z_2^2}{(\frac{\delta}{a})^2})}}{N} d\vec{r_1} d\vec{r_2} \tag{4.72}$$

where K is a constant with the good dimension (as e^2 is an energy times a length, the product Ka^5 is the inverse of a length.

In a two-dimensional lattice, we have a similar expression for $\frac{\Delta(E_{(k_n)_x,(k_n)_y})}{e^2}$:

$$a^5 K' \sum_{l_1,p_1} \sum_{l_2,p_2} \int\int \frac{(N_e - \delta_{k_n}^{occ} - \sum_{j\neq n, jocc.} \delta_{\sigma_j,\sigma_n} e^{i(\vec{k_n} - \vec{k_j})(R_{\vec{l_1},p_1} - R_{\vec{l_2},p_2})})}{\sqrt{(x_1 - x_2 + l_2 - l_1)^2 + (y_1 - y_2 + p_2 - p_1)^2 + (z_1 - z_2)^2}} \frac{e^{-2(\frac{x_1^2+y_1^2+z_1^2}{(\frac{\delta}{a})^2})} e^{-2(\frac{x_2^2+y_2^2+z_2^2}{(\frac{\delta}{a})^2})}}{N^4} d\vec{r_1} d\vec{r_2} \tag{4.73}$$

However after numerous tests, I noted that this algorithm was converging very slowly. Other problem : even with 1000000 random selections (1000000 points in the Markov chain), the estimation of the integral doesn't seem to converge... How to know the number of random selections to do ?

We finally decided to use a simpler method, which worked far better in the case we chose gaussian localised orbitals $\psi_m(.)$.

4.8 Annex 8 : Spin-polarized energy corrections

In theory, there are different possible ways of filling up the energy levels, for a given number of electrons NB, which can lead to different correction spectra. We will illustrate this important fact with the simple case of 8 electrons in the system. Of course, when the number of electrons in the system becomes huge, the following situations won't be physical... (at the thermodynamic limit, there isn't any reason to break the symmetry of the filling : in a non-magnetic solid, electrons with spins up and down will see the same chemical potential).

We start from an initial state which is a Slater determinant of single-electron states computed in the tight binding approximation, each of these occupied states having an energy $E_0 - t_0 - 2tcos(k_n a)$, where k_n is the corresponding quasi-momemtum. Our approach is a perturbative approach : we assume that the correction to the energy $E(k_n)$ of a single-electron state due to Fock's term is small enough to be estimated by the means value $< \psi_{k_n} | H^{Fock} | \psi_{k_n} >$ of the perturbation in the eigen state ψ_{k_n} computed in the tight-binding approximation. We haven't taken into account the possible variation $\delta\psi$ of the state itself.

In fact, the single-electron state to be considered is (k_n, σ_n). Indeed, because of Pauli principle, computing the correction to the energy implies to compare the spin σ_n to the spins σ_j of all other electrons in the occupied states k_j (except the state k_n itself in case it is occupied). Electrons contribute to the correction of the energy only for spins σ_j parallel to σ_n.

Let's look for an example that gives a spin-polarized energy correction, that is to say

$$\Delta(E_{k_n,\sigma_n=\uparrow}) \neq \Delta(E_{k_n,\sigma_n=\downarrow}) \tag{4.74}$$

for some values of k_n. We consider 8 electrons in the system. At **zero temperature**, we fill up the energy levels by increasing energy. Therefore we know that 6 of these electrons are in the three lowest energy levels, but we don't know the precise states of the other two electrons at the Fermi energy.

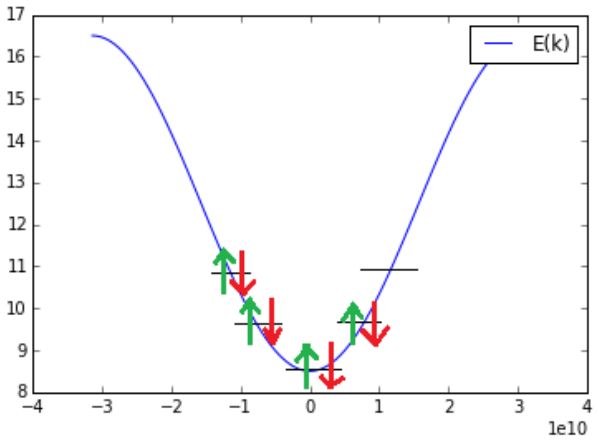

Figure 4.6: $NB = 8$ electrons, situation 1

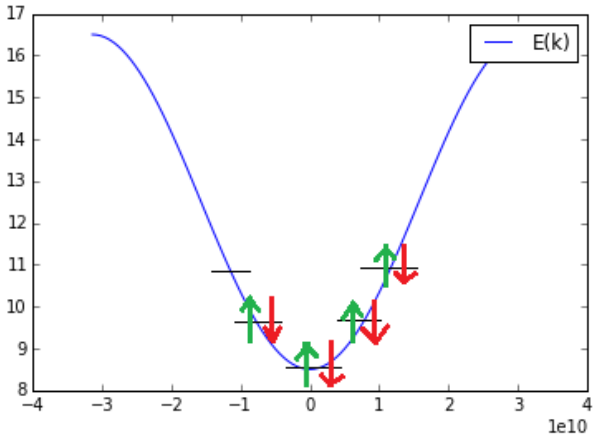

Figure 4.7: $NB = 8$ electrons, situation 2

These two first situations don't lead to a spin-polarized energy correction :

$$\forall k_n, \Delta(E_{k_n,\sigma_n=\uparrow}) = \Delta(E_{k_n,\sigma_n=\downarrow}) \tag{4.75}$$

Indeed, each occupied state contains two electrons with opposite spins so that $\{j \neq n, jocc.|\delta_{\sigma_n=\uparrow,\sigma_j} = 1\} = \{j \neq n, jocc.|\delta_{\sigma_n=\downarrow,\sigma_j} = 1\}$ for all n, which leads to the same correction for both states of spin.

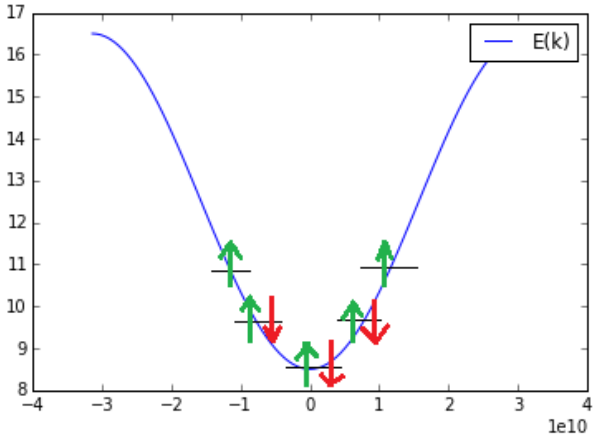

Figure 4.8: $NB = 8$ electrons, situation 3

For the situation above, there is a dependence of the correction of the energy on spin. Let's analyse it in further detail in this simple example. The three full states are $k_{-1} = -\frac{2\pi}{Na}$, $k_0 = 0$ and $k_1 = \frac{2\pi}{Na}$. The two states at the Fermi energy, each with one electron with spin up, are associated to the quasi-momemta $k_{-2} = -\frac{4\pi}{Na}$ and $k_2 = \frac{4\pi}{Na}$.

For any state k_n different from k_2 and k_{-2}, the corrections are different for the states $(k_n, \sigma_n = \uparrow)$ and $(k_n, \sigma_n = \downarrow)$:

$$\Delta E_{k_n=\frac{2\pi}{Na}n,\uparrow} = -\frac{e^2}{N}\sum_{m=1}^{N} I_{0,m}[\sum_{j\in\{-1,0,1\},j\neq n} \cos((k_n - k_j)ma) + \cos((k_n - \frac{4\pi}{Na})ma) + \cos((k_n + \frac{4\pi}{Na})ma)] \tag{4.76}$$

$$\Delta E_{k_n=\frac{2\pi}{Na}n,\downarrow} = -\frac{e^2}{N}\sum_{m=1}^{N} I_{0,m}\sum_{j\in\{-1,0,1\},j\neq n} \cos((k_n - k_j)ma) \tag{4.77}$$

as there are no electrons with spin $\downarrow$ in the states k_{-2} and k_2.

This magnetic filling thus leads to a difference of energy :

$$\Delta E_{k_n=\frac{2\pi}{Na}n,\uparrow} - \Delta E_{k_n=\frac{2\pi}{Na}n,\downarrow} = -\frac{e^2}{N}\sum_{m=1}^{N} I_{0,m}[\cos((k_n - \frac{4\pi}{Na})ma) + \cos((k_n + \frac{4\pi}{Na})ma)] = -2\frac{e^2}{N}\sum_{m=1}^{N} I_{0,m}\cos(\frac{2\pi n}{N}m)\cos(\frac{4\pi}{N}m \tag{4.78}$$

For the two states k_{-2} and k_2, there is no difference of the correction due to the spin :

$$\Delta E_{\frac{4\pi}{Na},\uparrow} = \Delta E_{\frac{4\pi}{Na},\downarrow}, \Delta E_{-\frac{4\pi}{Na},\uparrow} = \Delta E_{-\frac{4\pi}{Na},\downarrow} \tag{4.79}$$

(notice that $(k_2 = \frac{4\pi}{Na}, \downarrow)$ and $(k_{-2} = \frac{-4\pi}{Na}, \downarrow)$ are empty states)

The polarized correction to the band structure computed with Python for some similar filling at the energy level gives the following :

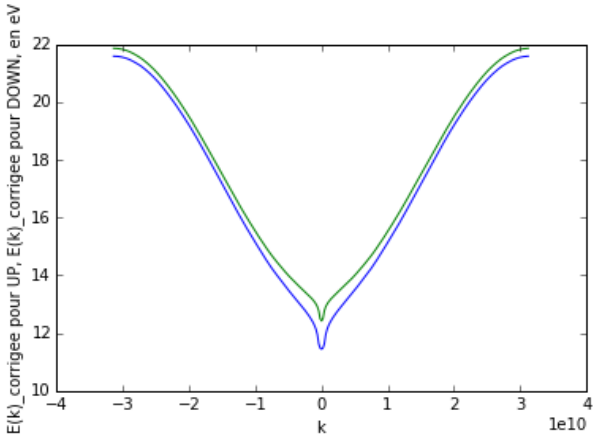

Figure 4.9: Spin-polarized correction to the energy computed with Hartree-Fock for $N = 300$ and $NB = 8$

In green, the band corresponding to the spins DOWN. In blue, to the the spins UP. This spin-polarized energy spectrum reminds us of the energy spectrum of some ferromagnets like iron, whose energy band for spins DOWN is above the energy band for spins UP.

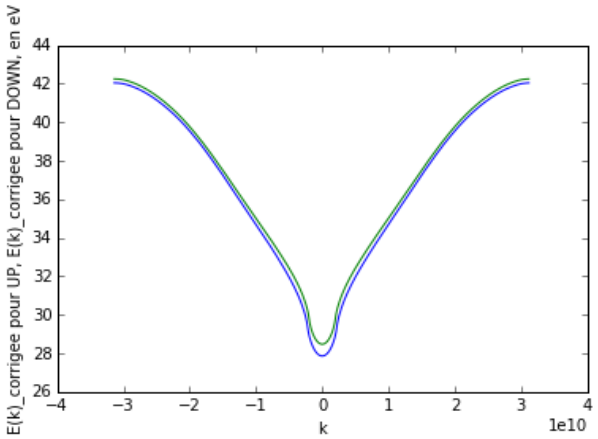

Figure 4.10: Spin-polarized correction to the energy computed with Hartree-Fock for $N = 300$ and $NB = 40$

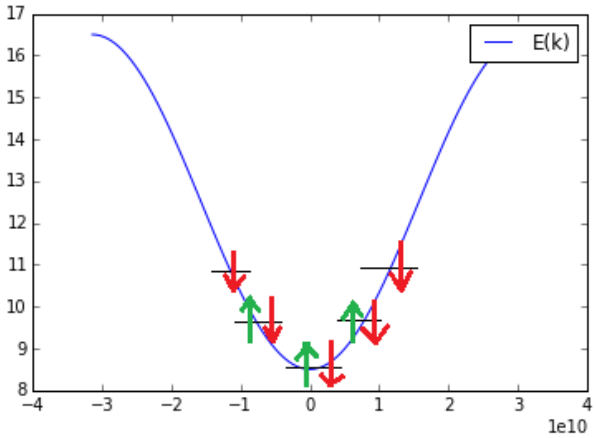

Figure 4.11: $NB = 8$ electrons, situation 4

For the situation 4, we have for $n \neq 2$ and $n \neq -2$:

$$\Delta E_{k_n=\frac{2\pi}{Na}n,\uparrow} = -\frac{e^2}{N}\sum_{m=1}^{N} I_{0,m} \sum_{j\in\{-1,0,1\},j\neq n} \cos((k_n - k_j)ma) \tag{4.80}$$

$$\Delta E_{k_n=\frac{2\pi}{Na}n,\downarrow} = -\frac{e^2}{N}\sum_{m=1}^{N} I_{0,m}[\sum_{j\in\{-1,0,1\},j\neq n} \cos((k_n - k_j)ma) + \cos((k_n - \frac{4\pi}{Na})ma) + \cos((k_n + \frac{4\pi}{Na})ma)] \tag{4.81}$$

This magnetic situation lifts the degeneracy of spin by the energy :

$$\Delta E_{k_n=\frac{2\pi}{Na}n,\uparrow} - \Delta E_{k_n=\frac{2\pi}{Na}n,\downarrow} = +\frac{e^2}{N}\sum_{m=1}^{N} I_{0,m}[\cos((k_n - \frac{4\pi}{Na})ma) + \cos((k_n + \frac{4\pi}{Na})ma)] = 2\frac{e^2}{N}\sum_{m=1}^{N} I_{0,m}\cos(\frac{2\pi n}{N}m)\cos(\frac{4\pi}{N}m) \tag{4.82}$$

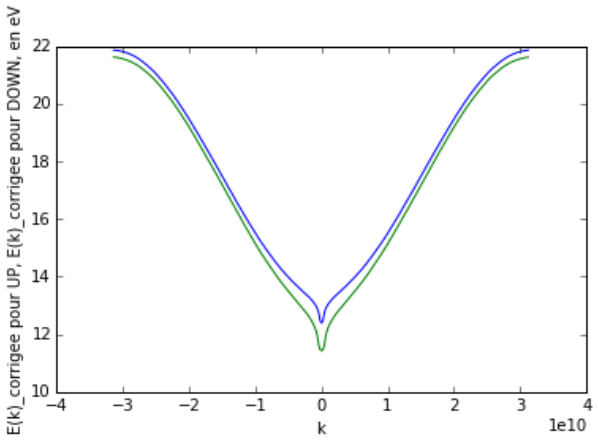

Figure 4.12: Spin-polarized correction to the energy computed with Hartree-Fock for $N = 300$ and $NB = 8$

In green, the band corresponding to the spins DOWN. In blue, to the the spins UP.

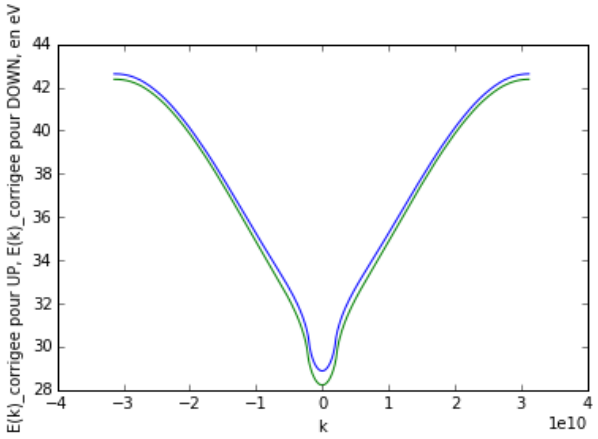

Figure 4.13: Spin-polarized correction to the energy computed with Hartree-Fock for $N = 300$ and $NB = 40$

The effect becomes weaker and weaker for bigger values of NB, when the number of electrons in the system increases, as the following graph shows :

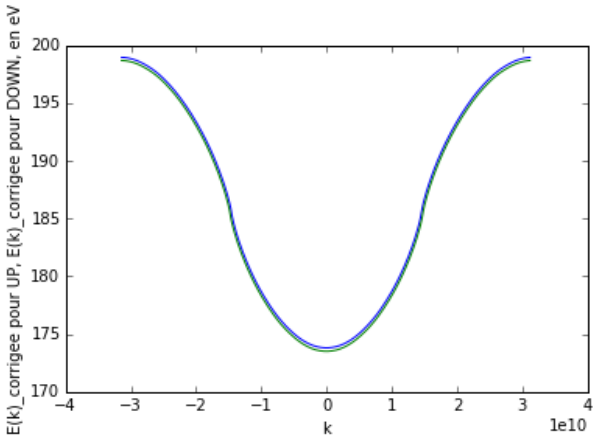

Figure 4.14: Spin-polarized correction to the energy computed with Hartree-Fock for $N = 300$ and $NB = 280$

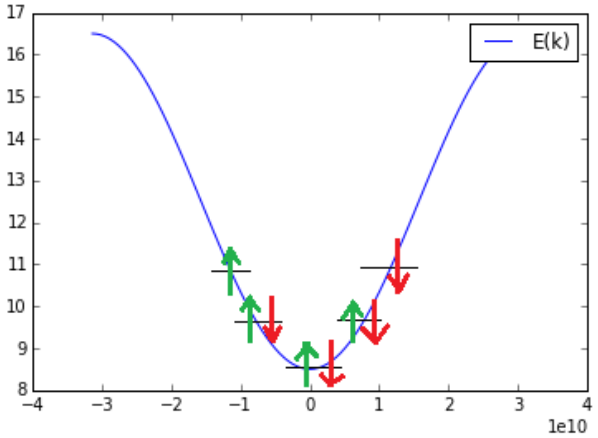

Figure 4.15: $NB = 8$ electrons, situation 5

For this last possible situation, every level of energy becomes spin-polarized. For $n \neq 2$ and $n \neq -2$:

$$\Delta E_{k_n=\frac{2\pi}{Na}n,\uparrow} = -\frac{e^2}{N}\sum_{m=1}^{N} I_{0,m}[\sum_{j\in\{-1,0,1\},j\neq n} \cos((k_n-k_j)ma) + \cos((k_n+\frac{4\pi}{Na})ma)] \tag{4.83}$$

$$\Delta E_{k_n=\frac{2\pi}{Na}n,\downarrow} = -\frac{e^2}{N}\sum_{m=1}^{N} I_{0,m}[\sum_{j\in\{-1,0,1\},j\neq n} \cos((k_n-k_j)ma) + \cos((k_n-\frac{4\pi}{Na})ma)] \tag{4.84}$$

which leads to :

$$\Delta E_{k_n=\frac{2\pi}{Na}n,\uparrow} - \Delta E_{k_n=\frac{2\pi}{Na}n,\downarrow} = +\frac{e^2}{N}\sum_{m=1}^{N} I_{0,m}[\cos((k_n-\frac{4\pi}{Na})ma) - \cos((k_n+\frac{4\pi}{Na})ma)] = 2\frac{e^2}{N}\sum_{m=1}^{N} I_{0,m}\sin(\frac{2\pi n}{N}m)\sin(\frac{4\pi}{N}m) \tag{4.85}$$

This time,

$$\Delta E_{k_2=\frac{4\pi}{Na},\uparrow} = -\frac{e^2}{N}\sum_{m=1}^{N} I_{0,m}[\sum_{j\in\{-1,0,1\},j\neq n} \cos((k_n-k_j)ma) + \cos((k_n+\frac{4\pi}{Na})ma)] \tag{4.86}$$

$$\Delta E_{k_2=\frac{4\pi}{Na},\downarrow} = -\frac{e^2}{N}\sum_{m=1}^{N} I_{0,m}\sum_{j\in\{-1,0,1\},j\neq n} \cos((k_n-k_j)ma) \tag{4.87}$$

because k_{-2} is occupied, bbut only with an electron with spin $\uparrow$.

Therefore

$$\Delta E_{k_2=\frac{4\pi}{Na},\uparrow} - \Delta E_{k_2=\frac{4\pi}{Na},\downarrow} = -\frac{e^2}{N}\sum_{m=1}^{N} I_{0,m}\cos((k_n+\frac{4\pi}{Na})ma) \tag{4.88}$$

$(k_n = \frac{4\pi}{Na},\uparrow)$ is an empty state, while $(k_n = \frac{4\pi}{Na},\downarrow)$ is occupied.

Similarly,

$$\Delta E_{k_{-2}=-\frac{4\pi}{Na},\uparrow} = -\frac{e^2}{N}\sum_{m=1}^{N} I_{0,m}\sum_{j\in\{-1,0,1\},j\neq n} \cos((k_n-k_j)ma) \tag{4.89}$$

and

$$\Delta E_{k_{-2}=-\frac{4\pi}{Na},\downarrow} = -\frac{e^2}{N}\sum_{m=1}^{N} I_{0,m}[\sum_{j\in\{-1,0,1\},j\neq n} \cos((k_n-k_j)ma) + \cos((k_n-\frac{4\pi}{Na})ma)] \tag{4.90}$$

Therefore

$$\Delta E_{k_{-2}=-\frac{4\pi}{Na},\uparrow} - \Delta E_{k_{-2}=-\frac{4\pi}{Na},\downarrow} = +\frac{e^2}{N}\sum_{m=1}^{N} I_{0,m}\cos((k_n-\frac{4\pi}{Na})ma) \tag{4.91}$$

$(k_{-2} = -\frac{4\pi}{Na},\uparrow)$ is an occupied state, while $(k_{-2} = -\frac{4\pi}{Na},\downarrow)$ is empty.

In that case, this "magnetic" filling at the Fermi level shifts the two bands (one for spins UP, one for spins DOWN) horizontally, and not vertically :

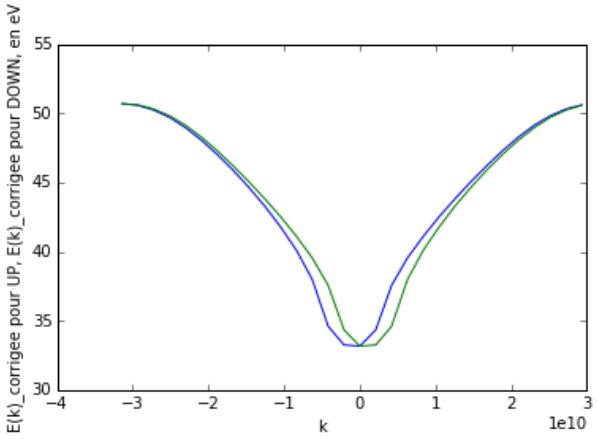

Figure 4.16: Spin-polarized correction to the energy computed with Hartree-Fock for $N = 30$ and $NB = 8$

We have shown that for a fixed value of NB, there can be numerous possible initial states, some of them leadind to spin-polarized corrections. **If NB is odd, this will necessarily be the case** (as there will be a level of energy with only one spin)! What should be computed in that case is the correction of the energy spectrum for electrons with spin $\uparrow$, namely $k \longmapsto \Delta(E_{k,\uparrow})$, and the correction for electrons with spin $\downarrow$: $k \longmapsto \Delta(E_{k,\downarrow})$.
Ä

However, as we noticed, the spin-polarization of the correction to the energy spectrum hopefully vanishes when the number of electrons increases and becomes of the same order of magnitude as the number of sites N. Indeed, the fillings we have described above aren't physical in the thermodynamical limit, when $N \longrightarrow +\infty$: both electrons with spins UP and electrons with spins DOWN see the same chemical potential, and there is no reason to favor a configuration with only spins UP or only spins DOWN in the two levels at the Fermi energy. However, the code developped to estimate the spin-polarization of the correction to the energy will be useful to analyse "real" magnetic fillings, i.e. with a macroscopic part of all the electrons having the same spin. This will allow us to compute the energy associated to a ferromagnetic or an antiferromagnetic configuration, which may be lower than the energy for a non-magnetic filling at low temperature.

4.9 Annex 9 : Graphs of the energy corrected by Fock's term only, for different fillings

In blue, the original, non-corrected energy spectrum (computed in the tight-binding approximation). In green, the energy band corrected by taking into account Fock's term.

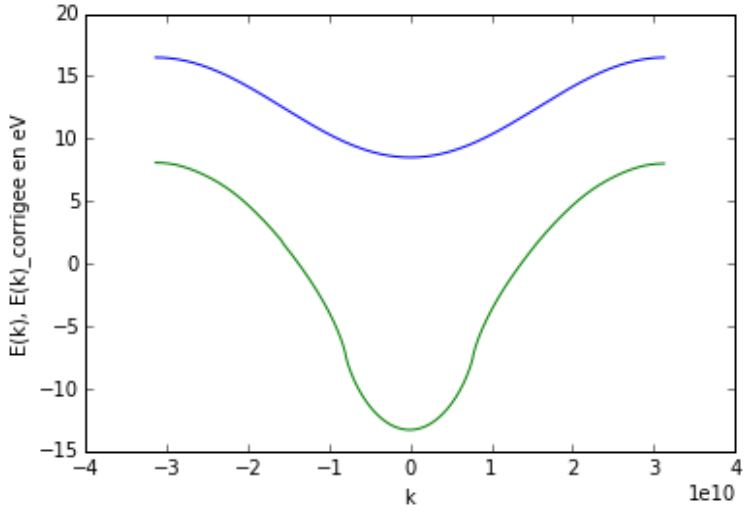

Figure 4.17: Energy computed for the one-dimensionnal lattice corrected by Fock's term, for N=500, NB=250 ($k_F = 0.79.10^{10} m^{-1}$) and nb=10000

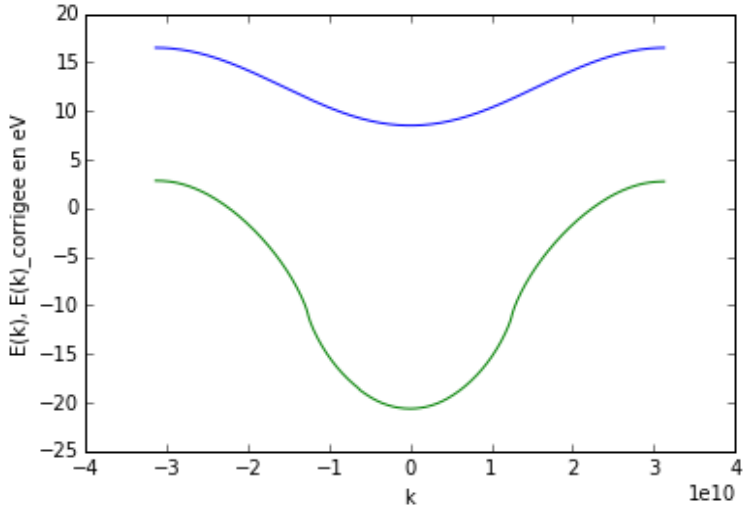

Figure 4.18: Energy computed for the one-dimensionnal lattice corrected by Fock's term, for N=500, NB=400 ($k_F = 1.26.10^{10} m^{-1}$) and nb=10000

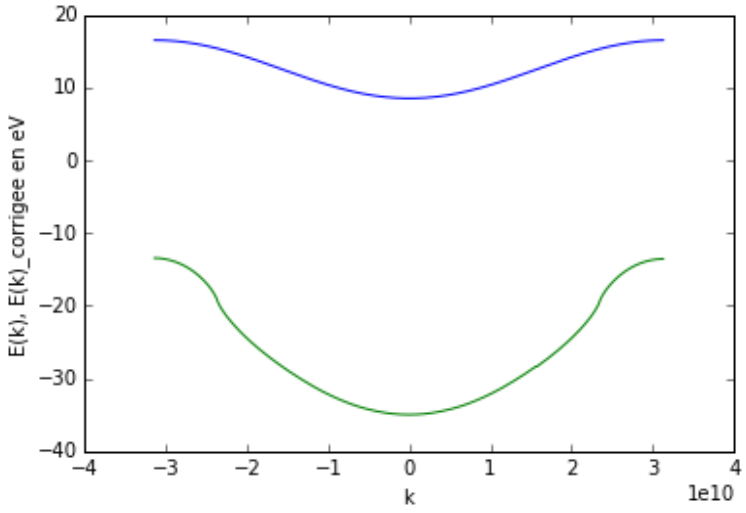

Figure 4.19: Energy computed for the one-dimensionnal lattice corrected by Fock's term, for N=500, NB=750 ($k_F = 2.4.10^{10} m^{-1}$) and nb=10000

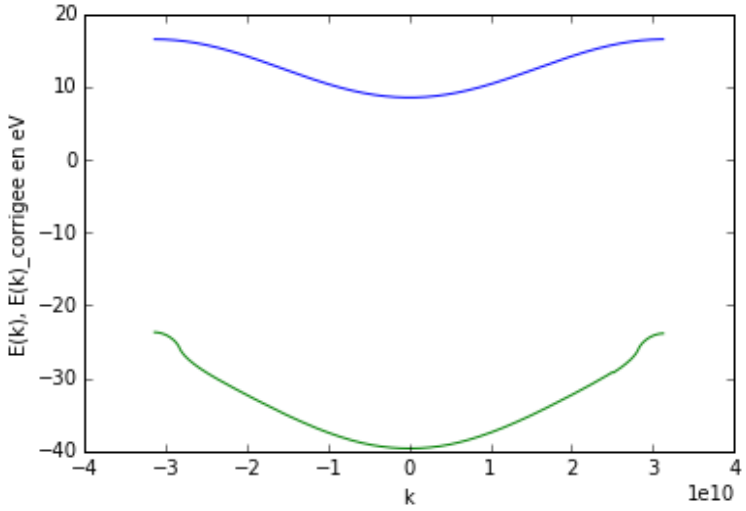

Figure 4.20: Energy computed for the one-dimensionnal lattice corrected by Fock's term, for N=500, NB=900 ($k_F = 2.8.10^{10} m^{-1}$) and nb=10000

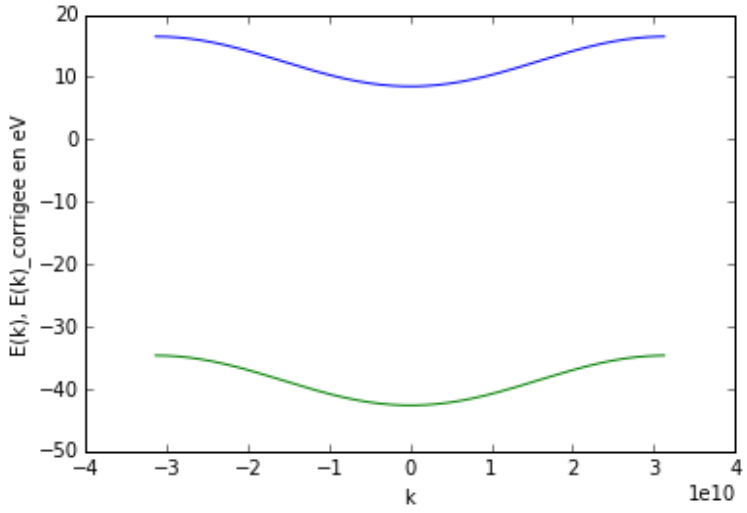

Figure 4.21: Energy computed for the one-dimensionnal lattice corrected by Fock's term, for N=500, NB=1000 ($k_F = \frac{\pi}{a} = 3.14.10^{10} m^{-1}$) and nb=10000

4.10 Annex 10 : The correction to the energy due to Fock's term for a fixed filling NB lowers when N increases

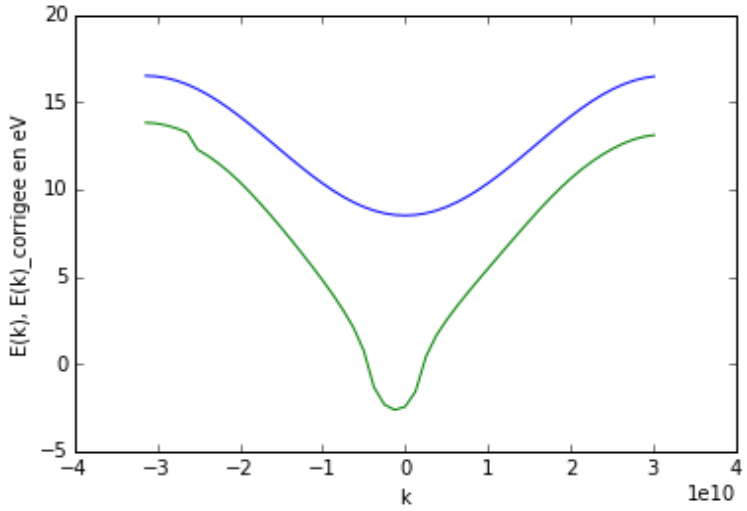

Figure 4.22: Energy computed for the one-dimensionnal lattice corrected by Fock's term, for N=50, NB=10 ($k_F = 0.3.10^{10} m^{-1}$) and nb=10000

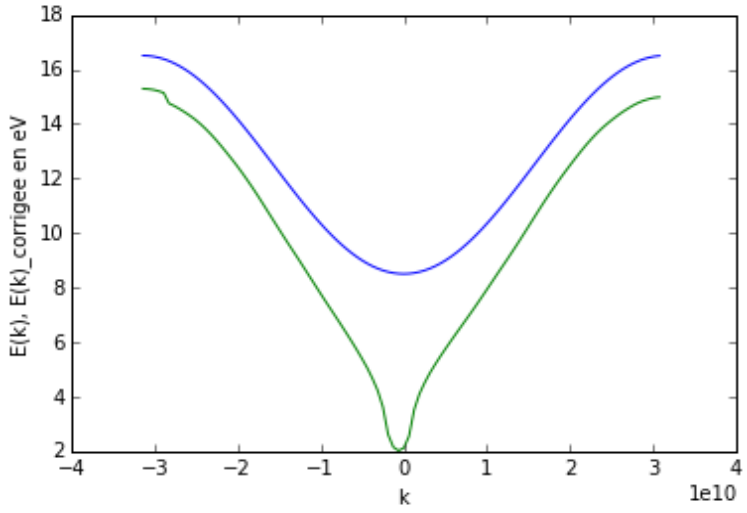

Figure 4.23: Energy computed for the one-dimensionnal lattice corrected by Fock's term, for N=100, NB=10 ($k_F = 0.15.10^{10} m^{-1}$) and nb=10000

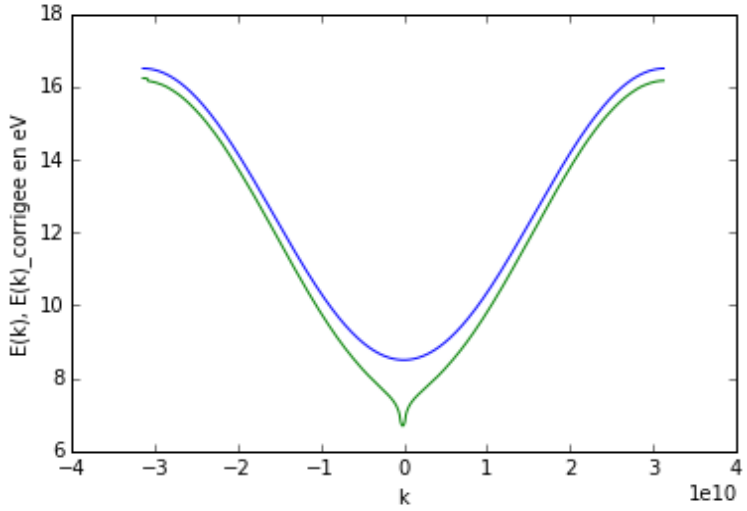

Figure 4.24: Energy computed for the one-dimensionnal lattice corrected by Fock's term, for N=500, NB=10 ($k_F = 0.03.10^{10} m^{-1}$) and nb=10000

4.11 Annex 11 : Anaysis of the divergence of the Fermi velocity caused by Hartree-Fock correction for the 1D lattice

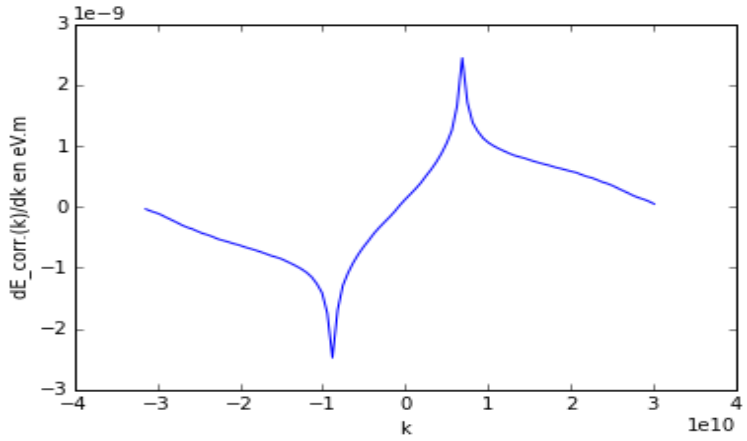

Figure 4.25: Derivative of the energy corrected by Hartree-Fock's term for $N = 100$ and $NB = 50$

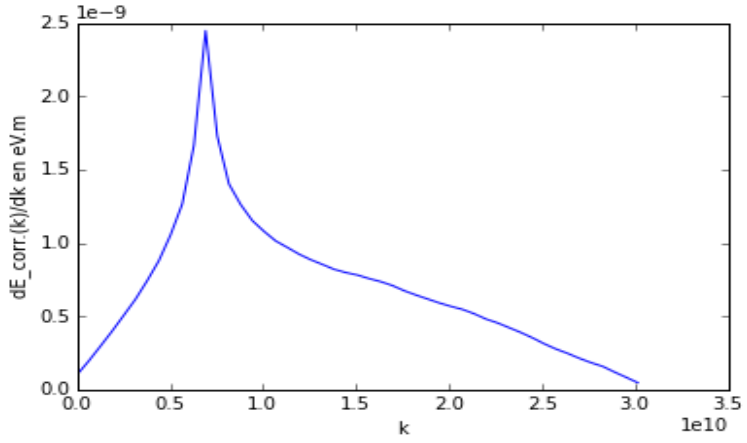

Figure 4.26: Zoom 1 on the derivative of the energy corrected by Hartree-Fock's term for $N = 100$ and $NB = 50$

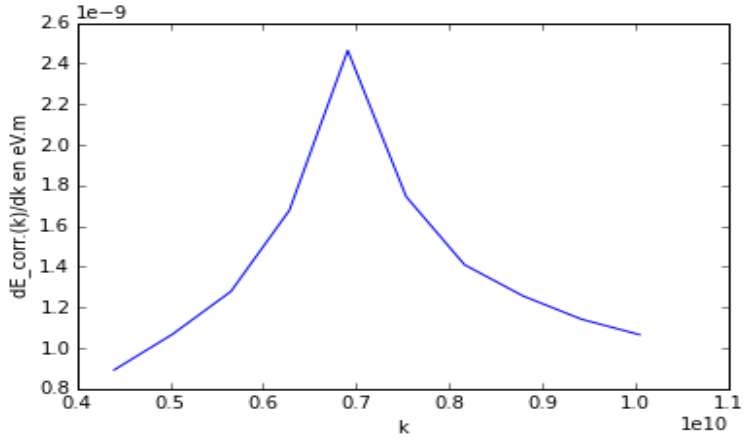

Figure 4.27: Zoom 2 on the derivative of the energy corrected by Hartree-Fock's term for $N = 100$ and $NB = 50$

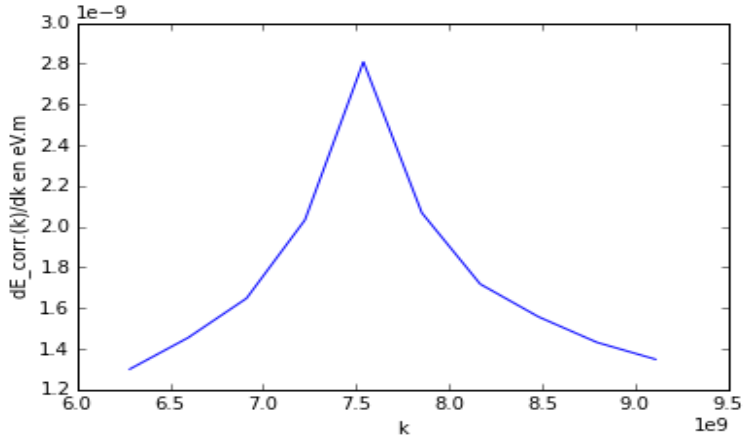

Figure 4.28: Zoom on the derivative of the energy corrected by Hartree-Fock's term for $N = 200$ and $NB = 100$

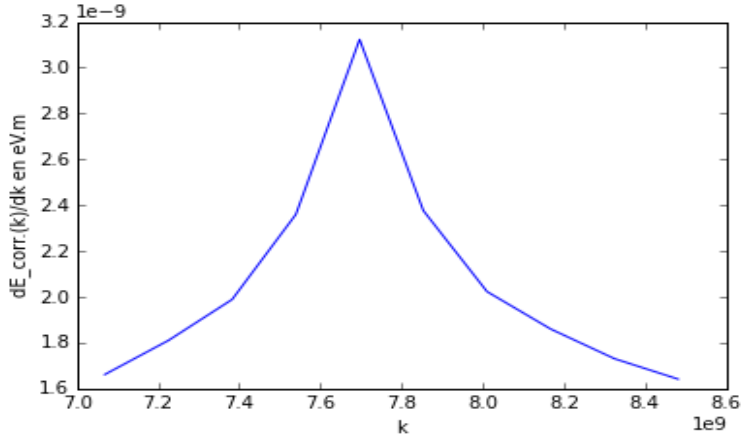

Figure 4.29: Zoom on the derivative of the energy corrected by Hartree-Fock's term for $N = 400$ and $NB = 200$

We can see the peak slowly rising when we increase N and the number of electrons NB in the system, keeping the same proportion (so that k_F is constant).

4.12 Annex 12: Non solved problem : finding a model to estimate ab initio the coupling constant t

Let's say that our method works to estimate the corrections both for one-dimensionnal and two-dimensionnal lattices. It would be useful to compare the bandwidth we obtain with **the coupling constant** t between two neighbouring atoms. This coupling depends on which type of localised atomic orbital we choose.

$$t =< \psi_l|V_{l+1}|\psi_{l+1} >= \sum_{i=1,i\neq l}^{N} < \psi_l|V_{at}(\vec{r}-\vec{R_i})|\psi_{l+1} > \tag{4.92}$$

An idea would be to find a relation between the electronic density $n(\vec{r})$ (computed in an auto-coherent way thanks to the one-electron wave-functions solution of Hartree-Fock equations), and the effective atomic potential $V_{at}(\vec{r})$. As the coupling t involves this potential, this would be a way to estimate the former for a given form of atomic orbitals. Using an explicit form of Hohenberg-Kohn's theorem may be a way to estimate $V_{at}(r)$ iteratively ?

4.13 Annex 13 : More graphs of the correction of the energy spectrum by Hartree-Fock's term, for the 1D lattice

In blue, the original, non-corrected energy spectrum (computed in the tight-binding approximation). In green, the corrected energy band for several fillings (at a fixed $N = 500$), after taking into account both Hartree and Fock's term.

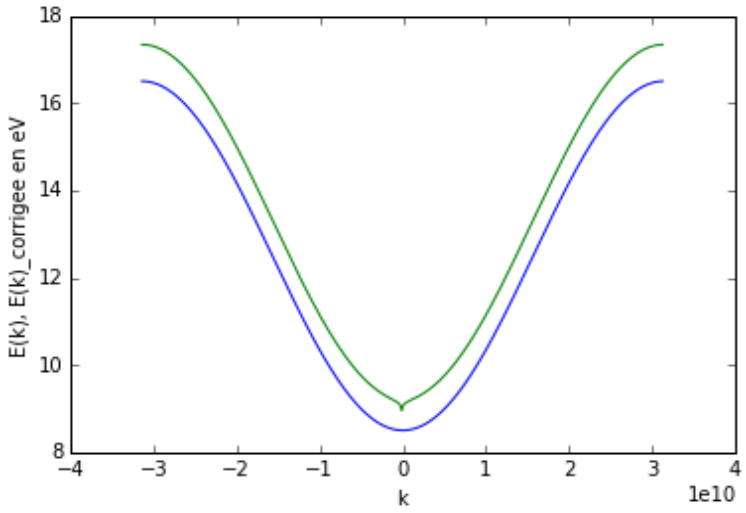

Figure 4.30: Energy computed for the one-dimensionnal lattice corrected by **Hartree-Fock's term**, for N=500, NB=2 ($k_F = 0.006.10^{10} m^{-1}$) and nb=10000

The following graph is the difference between the two energy bands above (the corrected and non-corrected energy spectra).

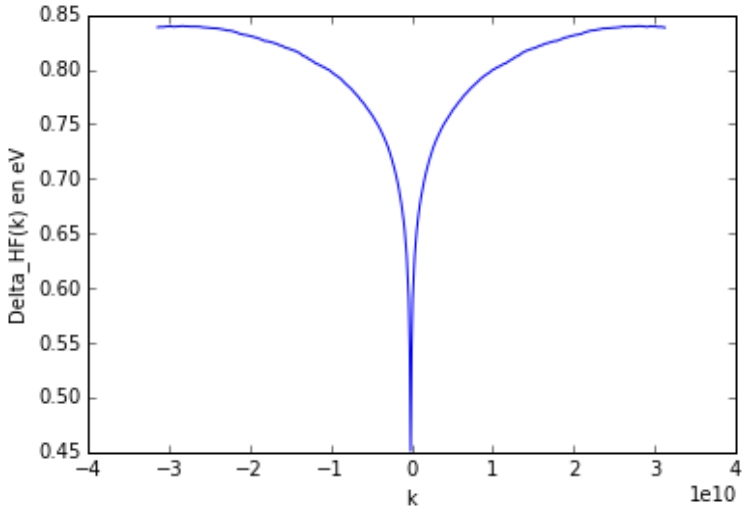

Figure 4.31: Correction of the energy by **Hartree-Fock's term** computed for the one-dimensionnal lattice , for N=500, NB=2 ($k_F = 0.006.10^{10} m^{-1}$) and nb=10000

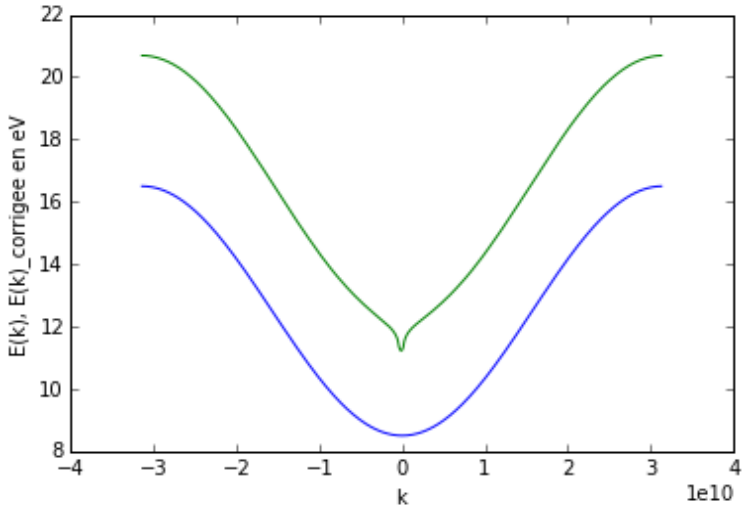

Figure 4.32: Energy computed for the one-dimensionnal lattice corrected by **Hartree-Fock's term**, for N=500, NB=10 ($k_F = 0.03.10^{10} m^{-1}$) and nb=10000

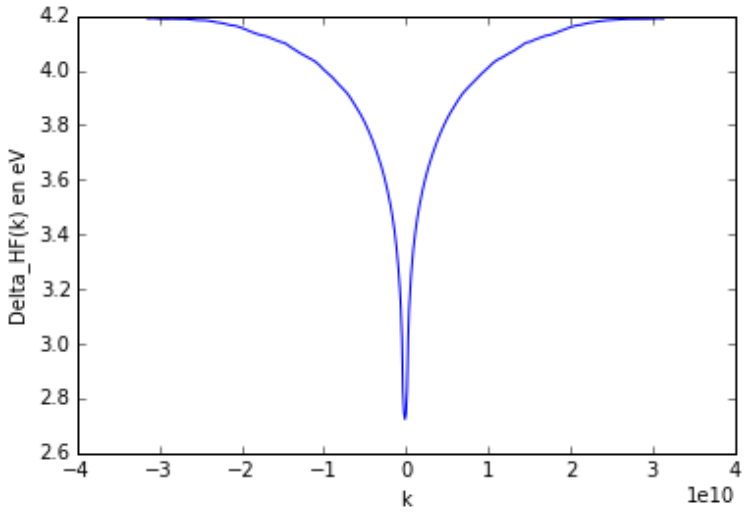

Figure 4.33: Correction of the energy by **Hartree-Fock's term** computed for the one-dimensionnal lattice , for N=500, NB=10 ($k_F = 0.03.10^{10} m^{-1}$) and nb=10000

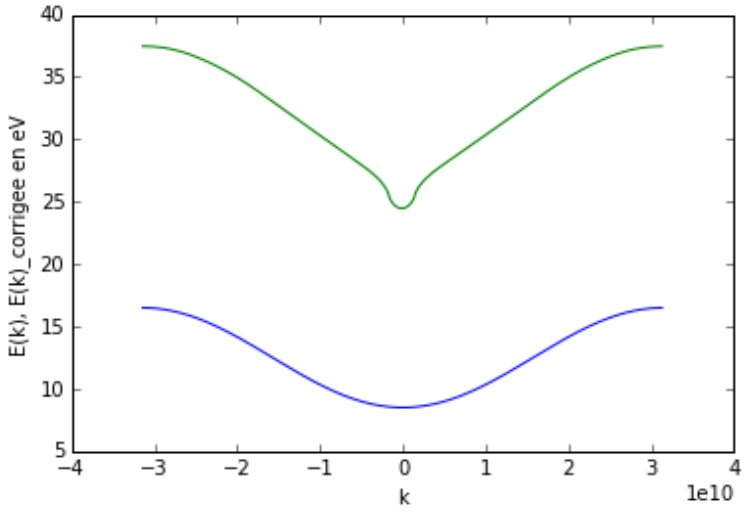

Figure 4.34: Energy computed for the one-dimensionnal lattice corrected by **Hartree-Fock's term**, for N=500, NB=50 ($k_F = 0.16.10^{10} m^{-1}$) and nb=10000

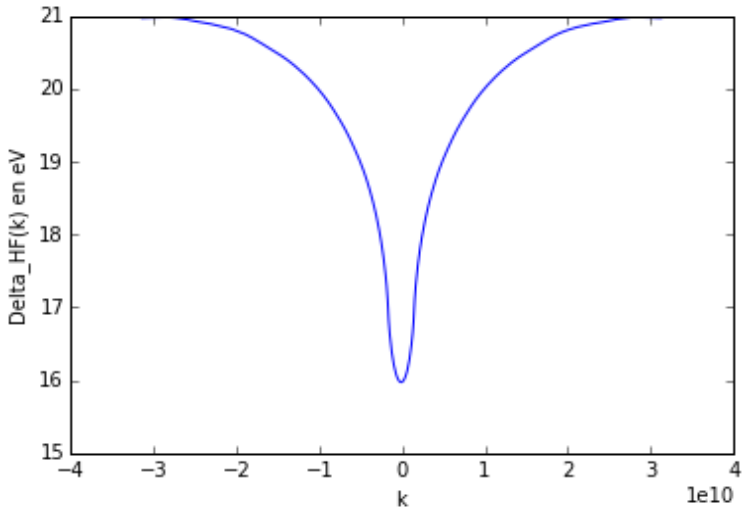

Figure 4.35: Correction of the energy by **Hartree-Fock's term** computed for the one-dimensionnal lattice , for N=500, NB=50 ($k_F = 0.16.10^{10} m^{-1}$) and nb=10000

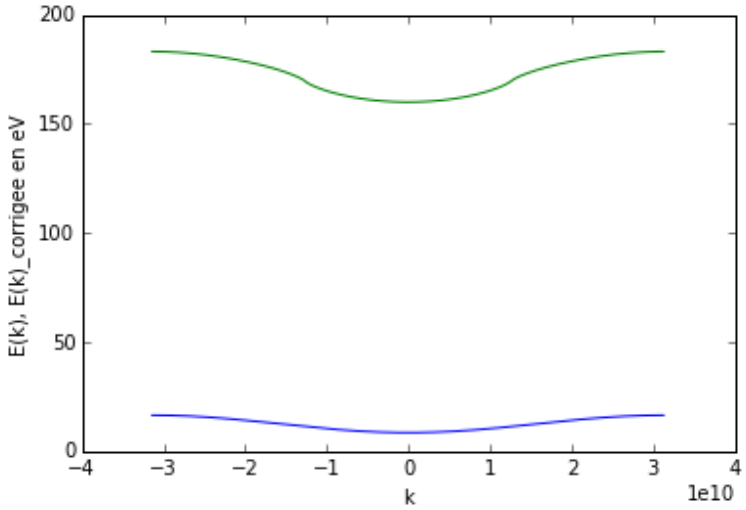

Figure 4.36: Energy computed for the one-dimensionnal lattice corrected by **Hartree-Fock's term**, for N=500, NB=400 ($k_F = 1.26.10^{10} m^{-1}$) and nb=10000

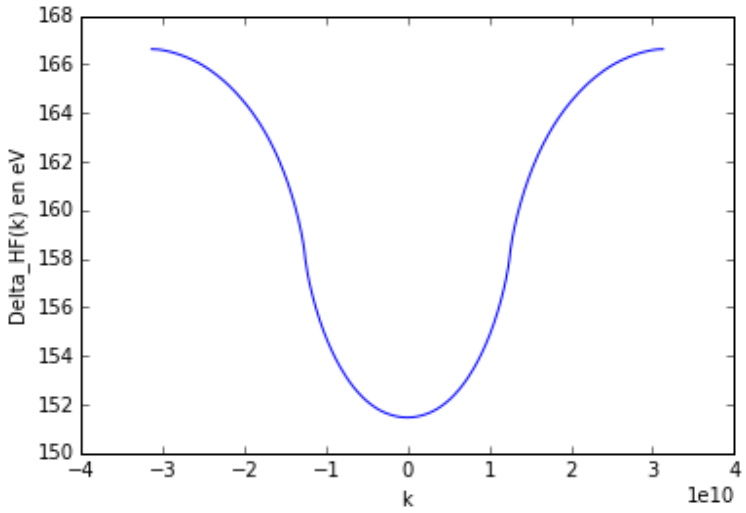

Figure 4.37: Correction of the energy by **Hartree-Fock's term** computed for the one-dimensionnal lattice , for N=500, NB=400 ($k_F = 1.26.10^{10} m^{-1}$) and nb=10000

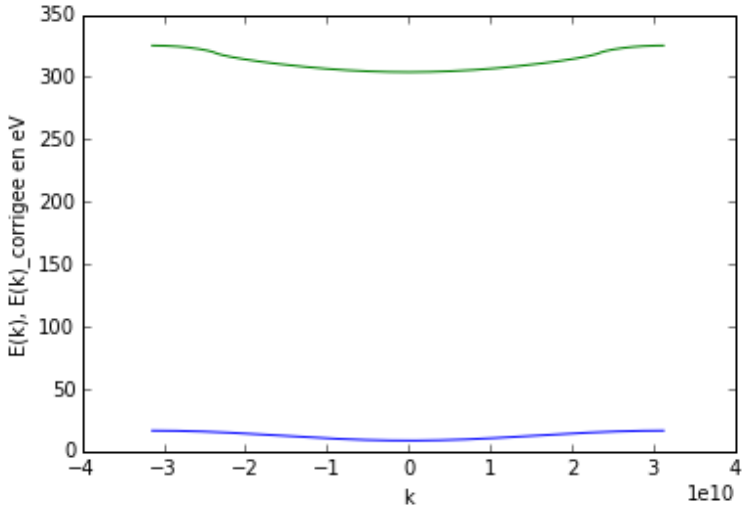

Figure 4.38: Energy computed for the one-dimensionnal lattice corrected by **Hartree-Fock's term**, for N=500, NB=750 ($k_F = 2.4.10^{10} m^{-1}$) and nb=10000

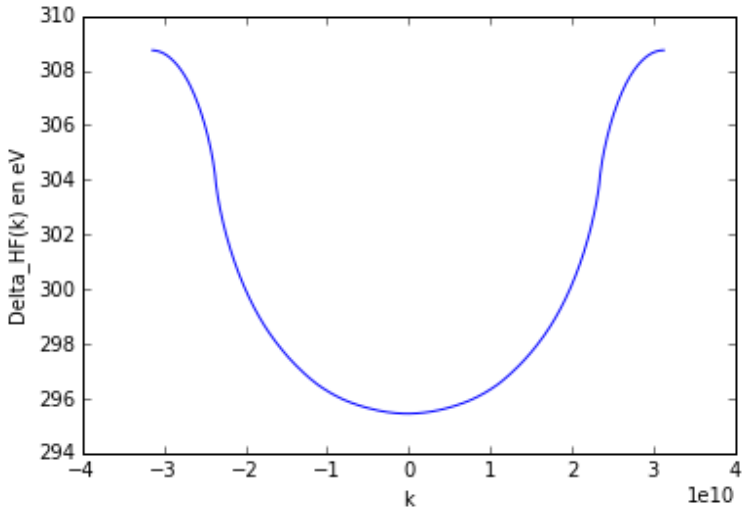

Figure 4.39: Correction of the energy by **Hartree-Fock's term** computed for the one-dimensionnal lattice , for N=500, NB=750 ($k_F = 2.4.10^{10} m^{-1}$) and nb=10000

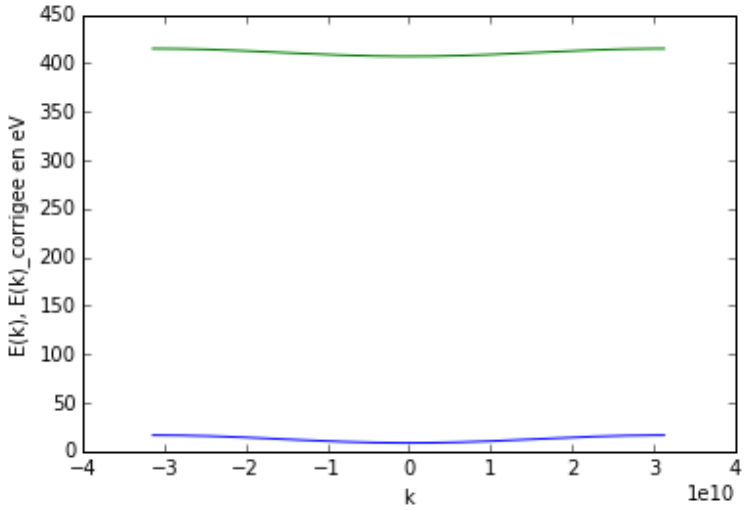

Figure 4.40: Energy computed for the one-dimensionnal lattice corrected by **Hartree-Fock's term**, for N=500, NB=1000 ($k_F = \frac{\pi}{a} = 3.14.10^{10} m^{-1}$) and nb=10000

4.14 Annex 14 : Analysis of the form of the energy correction in the case of several orbitals per atom involved in the hybridisation

So far, we have only considered one possible state per atom ; one possible wave-function. **The underlying assumption was that only one level per atom was contributing to the hybridasation**, leading to an electron delocalised over the whole chain. For instance, the Bloch wave-function that we have being using as eigen vectors could be linear combinations of $1s$ orbitals, with coefficients e^{ikma}. However, to be more realistic, we should have considered the possible hybridisation of $1s$ and $2p$ orbitals of neighbouring atoms, for instance (this may happen is their respective energy level are close enough one to each other), which is equivalent to take two possible states into account in a given site of the lattice.

Let χ_1 and χ_2 be the two possible orbitals of a localized wave function. The extensive calculations from the very beginning of Hartree-Fock's term happen to be difficult and long. However, we are tempted to generalize the expression of the correction in the following way :

$$\Delta E_{k_n,\sigma_n,\chi_1} = \frac{e^2}{N} \sum_{m=1}^{N} [I_{0,m}(N^e - \delta^{occ}_{k_n,\sigma_n,\chi_1}) - \sum_{j \neq n, k_j occ.} \delta_{\sigma_n,\sigma_j}(I^{1,1}_{0,m}\delta^{occ}_{k_j,\sigma_j,\chi_1} + I^{1,2}_{0,m}\delta^{occ}_{k_j,\sigma_j,\chi_2}) - I^{1,2}_{0,0}\delta^{occ}_{k_n,\sigma_n,\chi_2}] \tag{4.93}$$

where

$$I^{i,j}_{0,m} = \int\int \frac{|\chi^i_1(\vec{r}|^2 |\chi^i_2(\vec{r}|^2}{|\vec{r} - \vec{r'} - ma\vec{e_x}} \tag{4.94}$$

There are now inter and intra atomic exchange terms, due to the possible overlapping of the two orbitals of a given atom, and because of the inter-atomis contribution of the Coulomb interaction between an electron having k_n, with spin UP and in the state $\chi_1(.)$ and an electron having a quasi-momentum k_j, with spin UP and in the state $\chi_2(.)$.

This ends up with a spin-polarized and **orbital-polarized** energy correction !

4.15 Annex 15 : Similar calculations for a two-dimensional lattice

In two dimensions, we can perform similar calculations as for the 1D lattice in terms of Hartree-Fock correction and screening length. These calculations aren't fully detailed. The final result we obtain to estimate the correction is :

$$\Delta(E_{(k_n)_x,(k_n)_y}) = \frac{e^2}{N^4}\sum_{l_1,p_1}\sum_{l_2,p_2} I_{l_1,p_1,l_2,p_2}\Theta^n_{l_1,p_1,l_2,p_2} \tag{4.95}$$

We proove the invariance by translation like in one dimension, therefore :

$$\Delta(E_{(k_n)_x,(k_n)_y}) = \frac{e^2}{N^2}\sum_{l_1,p_1} I_{l_1,p_1,0,0}\Theta^n_{l_1,p_1,0,0} \tag{4.96}$$

where

$$I_{l_1,p_1,0,0} = \frac{K^4a^5}{(4\pi)^2}\pi(\frac{d}{a})^2\pi^2(2\pi)^2\int\int F_{l_1,p_1}(\rho'_1,\rho'_2,\theta_1,\theta_2,\phi_1,\phi_2)f(\rho'_1)d\rho'_1 f(\rho'_2)d\rho'_2 g(\theta_1)d\theta_1 g(\theta_2)d\theta_2 h(\phi_1)d\phi_1 h(\phi_2)d\phi_2 \tag{4.97}$$

$F_{l_1,p_1}(\rho'_1,\rho'_2,\theta_1,\theta_2,\phi_1,\phi_2)$ is the generalisation of the function $F_m(.)$ that we used in one dimension :

$$\frac{\rho'^2_1\rho'^2_2 sin(\theta_1)sin(\theta_2)}{\sqrt{(\rho'_1 sin(\theta_1)cos(\phi_1) - \rho'_2 sin(\theta_2)cos(\phi_2) - l_1)^2 + (\rho'_1 sin(\theta_1)sin(\phi_1) - \rho'_2 sin(\theta_2)sin(\phi_2) - p_1)^2 + (\rho'_1 cos(\theta_1) - \rho'_2 cos(\theta_2))^2}} \tag{4.98}$$

With the same notations as for the one-dimensionnal case, the correction can be rewritten as :

$$\Delta(E_{(k_n)_x,(k_n)_y}) = \frac{e^2}{N^2}\sum_{l_1,p_1} I_{l_1,p_1,0,0}\Theta^n_{l_1,p_1,0,0} = \pi^2(\frac{a}{d})^3\frac{q_e^2}{4\pi\epsilon_0 d}\frac{1}{N^2}\sum_{l_1,p_1} E_\mu(F_{l_1,p_1})\Theta^n_{l_1,p_1,0,0} \tag{4.99}$$

where

$$\Theta^n_{l_1,p_1,0,0} = N_e - \delta^{(k_n)_x,(k_n)_y}_{occ} - \sum_{j\neq n,jocc.}\delta_{\sigma_j,\sigma_n}cos[((k_n)_x - (k_j)_x)l_1a + ((k_n)_y - (k_j)_y)p_1a] \tag{4.100}$$

$$\Theta^n_{l_1,p_1,0,0} = N_e - \delta^{\vec{k_n}}_{occ} - \sum_{j\neq n,jocc.}\delta_{\sigma_j,\sigma_n}cos((\vec{k_n} - \vec{k_j}).(l_1a\vec{e_x} + p_1a\vec{e_y})) \tag{4.101}$$

The following graphs are some results of the correction of the energy computed in the tight-binding approximation, in two dimensions. The lattice is a square of size N which repeats periodically. There are N^2 possible states, and $2N^2$ electrons at most in the system.

We denote α_1 the number of differents values of $(k_n)_x$ for all occupied states, and α_2 the number of differents values of $(k_n)_y$ ($\alpha_1 \leq N$ and $\alpha_2 \leq N$). There are $\alpha_1\alpha_2$ occupied states, and $2\alpha_1\alpha_2$ in the system (we only treat non-magnetic fillings). The occupied states are such that :

$$(k_n)_x = -\frac{\pi}{a} + i_1\frac{2\pi}{Na}, i_1 \in [\frac{N-\alpha_1}{2}, \frac{N+\alpha_1}{2}] \tag{4.102}$$

and

$$(k_n)_y = -\frac{\pi}{a} + i_1\frac{2\pi}{Na}, i_1 \in [\frac{N-\alpha_2}{2}, \frac{N+\alpha_2}{2}] \tag{4.103}$$

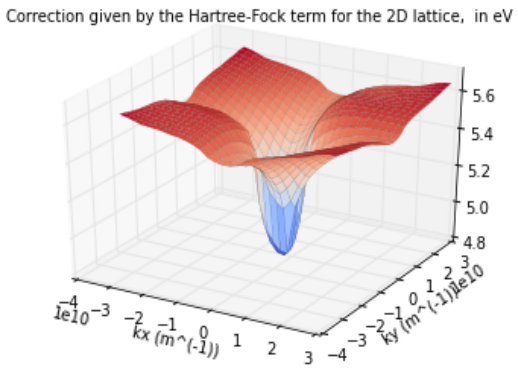

Figure 4.41: Correction to the energy due to Hartree Fock's term computed for the two-dimensionnal lattice, for N=30, $\alpha_1 = 5$, $\alpha_2 = 5$, NB=50 and nb=1000

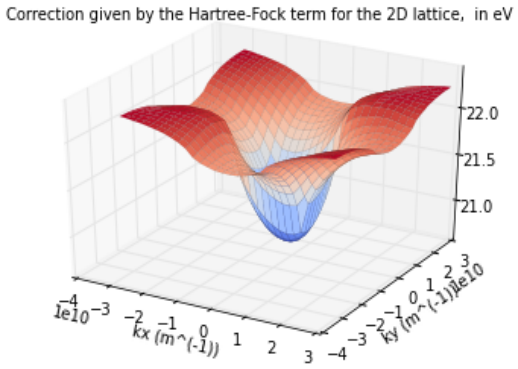

Figure 4.42: Correction to the energy due to Hartree Fock's term computed for the two-dimensionnal lattice, for N=30, $\alpha_1 = 10$, $\alpha_2 = 10$, NB=200 and nb=1000

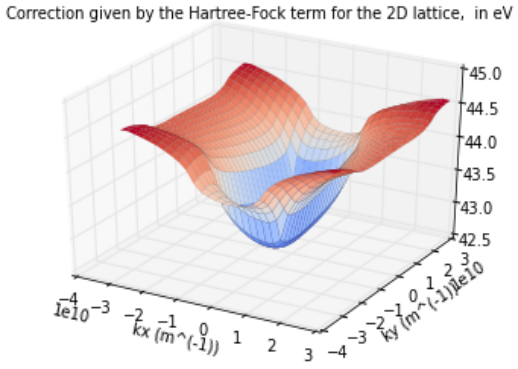

Figure 4.43: Correction to the energy due to Hartree Fock's term computed for the two-dimensionnal lattice, for N=30, $\alpha_1 = 10$, $\alpha_2 = 20$, NB=400 and nb=1000

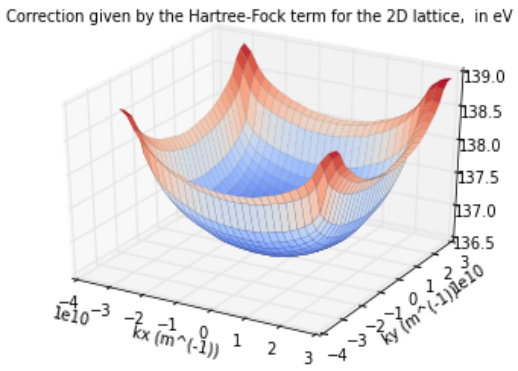

Figure 4.44: Correction to the energy due to Hartree Fock's term computed for the two-dimensionnal lattice, for N=30, $\alpha_1 = 25$, $\alpha_2 = 25$, NB=1250 and nb=1000

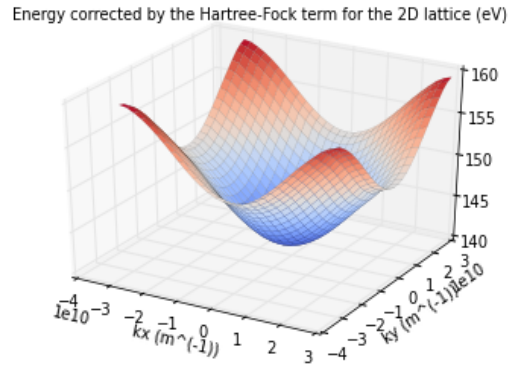

Figure 4.45: Energy spectrum corrected by Hartree Fock's term for the two-dimensionnal lattice, for N=30, $\alpha_1 = 25$, $\alpha_2 = 25$, NB=1250 and nb=1000

The correction is constant when all the states are occupied.

Remarks on the energy correction for the 2D lattice compared with the 1D lattice

In two dimensions, the main features commented and studied in 1D remain. However, we notive that Fock's term, of order **1 eV**, is now much lower than Hartree's term, even for small fillings. Hartree's term order of magnitude is **10 eV** for low filings, and **100 eV** for macroscopic fillings. The corrected energy spectrum in two dimensions mainly reflects Hartree's term. The Fock's term has the same effect as in one dimension, namely to dragg the energy band down for $\vec{k}$ close to 0, and produces a discontinuity that we can guess in the graphs. Nevertheless, this distortion can't be seen in the energy spectrum, and has barely no effect on the total bandwidth.